

**Resource Characterization and Quantification of Natural Gas-Hydrate and
Associated Free-Gas Accumulations in the Prudhoe Bay – Kuparuk River
Area on the North Slope of Alaska**

**June 2004 Quarterly Technical Report
Seventh Quarterly Report: April 2004 – June 2004
Cooperative Agreement Award Number DE-FC-01NT41332**

Submitted to the
United States Department of Energy
National Energy Technology Laboratory
ADD Document Control

by
BP Exploration (Alaska), Inc.
Robert Hunter (Principal Investigator)
P.O. Box 196612
Anchorage, Alaska 99519-6612
Email: hunterrb@bp.com
robert.hunter@asrcenergy.com
Tel: (907)-339-6377

with
University of Alaska Fairbanks
Shirish Patil (Principal Investigator)
425 Duckering Building
P.O. Box 755880
Fairbanks, Alaska 99775-5880

and
Arizona Board of Regents
University of Arizona, Tucson
Robert Casavant (Principal Investigator)
Dept. Mining and Geological Engineering
Rm. 245, Mines and Metallurgy Bldg. #12
1235 E. North Campus Dr., POB 210012
Tucson, AZ 85721-0012

in collaboration with
United States Geological Survey
Tim Collett (Principal Investigator)
Denver Federal Center
Box 25046, MS939
Denver, CO 80225

September 28, 2004

DISCLAIMER

This report was prepared as an account of work sponsored by an agency of the United States Government. Neither the United States Government nor any agency thereof, nor any of their employees, makes any warranty, express or implied, or assumes any legal liability or responsibility for the accuracy, completeness, or usefulness of any information, apparatus, product, or process disclosed, or represents that its use would not infringe privately owned rights. Reference herein to any specific commercial product, process, or service by trade name, trademark, manufacturer, or otherwise does not necessarily constitute or imply its endorsement, recommendation, or favoring by the United States Government or any agency thereof. The views and opinions of authors expressed herein do not necessarily state or reflect those of the United States Government or any agency thereof or of BP Exploration (Alaska) Inc.

ABSTRACT

This cooperative project between BP Exploration (Alaska), Inc. (BPXA) and the U.S. Department of Energy (DOE) facilitates a high level of collaboration between industry, government, and university researchers. The mutually beneficial research activities would not otherwise have been independently conducted by industry. Project results will help identify technical and economic factors that must be understood for government and industry to make informed decisions regarding the resource potential of gas hydrate accumulations on the Alaska North Slope (ANS).

One of the important contributors to this effort is the U.S. Geological Survey, which has led ANS gas hydrate research for three decades. Dr. Timothy Collett of the USGS continues to promote the importance of this area to gas hydrate research and potential development. Shirish Patil of the University of Alaska Fairbanks (UAF) School of Mining and Engineering is leading reservoir and petroleum engineering research and supporting laboratory studies. Dr. Robert Casavant leads the reservoir and fluid characterization efforts at the University of Arizona (UA) with Dr. Roy Johnson and Dr. Mary Poulton.

Gas hydrates are present in many arctic regions and offshore areas around the world. In the U.S., notable deposits of gas hydrate occur in the offshore Atlantic, Gulf of Mexico (GOM), offshore Pacific, offshore Alaska, and also onshore Alaska regions beneath permafrost. Collett (1998) estimates that up to 590 TCF of in-place ANS gas resources may be trapped in clathrate hydrates. Of that total, an estimated 44 to 100 TCF of in-place gas hydrate resources may occur beneath existing ANS production infrastructure within the Eileen and Tarn trends, respectively (Collett, 1993). However, much like conventional oil and gas resources, economic production of gas from potential gas hydrate resources will require a unique combination of factors, including all of the required petroleum system components (e.g., source, trap, seal, charge, reservoir, etc.), adequate industry infrastructure, industry access to acreage, familiar production technology, and favorable economics. In addition, industry must be able to estimate ultimate recovery potential, production rates, operating costs, and potential profitability within reasonable risk limits. Currently, the most likely areas for a favorable combination of these factors are the ANS and the Gulf of Mexico.

In this project, ANS gas hydrate and associated free gas-bearing reservoirs are being studied to determine reservoir extent, stratigraphy, structure, continuity, quality, variability, and geophysical and petrophysical property distribution. The objective of Phase 1 (Oct. 2002 – Oct. 2004) is the characterization of reservoirs and fluids, leading to estimates of recoverable reserve and commercial potential, and the definition of procedures for gas hydrate drilling, data acquisition, completion, and production. If justified by prior phase results, phases 2 (Nov. 2004 – Dec. 2005) and 3 (Jan. 2006 – Dec. 2006) will integrate well, core, log, and production test data from additional wells. Ultimately, the program could lead to development of an ANS gas hydrate pilot project and determine whether or not gas hydrates can become a part of the overall ANS gas resource portfolio.

Interim results from this project have identified potential shallow gas hydrate prospects within reservoir sands of the Sagavanirktok formation in the Milne Point Unit (MPU) area. Areas where gas hydrate may exist in association with movable free gas or possibly movable water have the most potential for production of hydrate-sourced natural gas, based on a preliminary understanding of the geology and potential production behavior investigated within reservoir model scenarios. However, these potential prospects remain largely unproven and require confirmation, delineation, and further data acquisition to mitigate uncertainties.

The shallow gas hydrate-bearing reservoirs of the Tertiary Sagavanirktok formation are part of a complex fluvial-deltaic system complicated by structural compartmentalization within the Eileen trend. Stacked sequences of fluvial, deltaic, and nearshore marine sands are interbedded with both terrestrial and marine shales. Facies changes, intraformational unconformities, and high-angle normal faults disrupt reservoir continuity. Phase 1 work related to volumetric assessment includes detailed well-log analyses and description of reservoir facies and fluids as integrated with the 3D seismic data. In conjunction with structural analyses, the identification and mapping of net pay in discrete sand bodies improves understanding of resource quality, quantity, distribution, and continuity. This work helps refine volume estimates, reservoir models, and recovery factors, production forecasts, and economic analyses.

Interpretations of gas hydrate and associated free-gas resources within the study area correlate with gas hydrates that were originally cored and tested in the 1972 NW Eileen State #2 well and also penetrated by other wells targeting deeper reservoirs within the ANS development area. Geophysical attributes of gas hydrate occurrence are also under investigation. Seismic modeling of shallow (<950 ms) velocity fields suggests both amplitude and waveform variations may help locate gas hydrate-bearing reservoirs. Permafrost can also complicate seismic identification of gas hydrates due to its similar acoustic properties. Identification of gas hydrate prospects within the MPU 3D seismic volume are based on seismic interpretation and modeling, gas hydrate-similar waveform classes, and fault-seal geometries integrated with well log-derived properties. Fault blocks with significant in-place volumes within identified gas hydrate-bearing reservoirs can be further delineated and/or production tested if the project proceeds into phases 2 and 3.

Understanding the nature of fluid flow and permeability is critical to assessing the productivity of gas hydrates. As part of this project, UAF has developed a new method for measuring gas-water relative permeability for laboratory synthesized gas hydrate within porous media. This work provides input to reservoir modeling and fluid flow. Although laboratory methods may

differ from natural methods required to form gas hydrate, the experiment design allows gas hydrate to form in porous media over relatively long periods of time and allows measurement of effective permeability and relative permeability for different saturation values. Although some dissociation of gas hydrate occurs due to differential pressure across the core, the low temperature decreases the rate of gas dissociation. Considerable additional experimental and theoretical work remains to develop an analytical or generalized model to predict relative permeability for gas hydrate reservoir simulation. The experimental data obtained from this work will allow identification of gas hydrate stability zones, determination of flow behavior, and development of techniques for safe production of natural gas from gas hydrates.

The project team has adapted a commercial simulator (CMG-STAR3) to model gas hydrate dissociation due to depressurization of an adjacent free gas accumulation in an MPU-area ANS gas hydrate prospect containing an estimated 23 BCF gas in-place. Preliminary results also demonstrate the potential of the depressurization production method by dissociation of gas hydrate adjacent to free gas. Modeling indicates that as gas is produced at rates from 8 to 25 MMscfd per well, the free gas zone depressurizes and the adjacent gas hydrate accumulation begins to release significant additional gas. Preliminary results also demonstrate the potential for depressurization of a partially-saturated gas hydrate-bearing reservoir through production of movable connate waters from a reservoir containing both gas hydrate and movable water at fractional saturations.

Work is proceeding in the areas described above as well as on a number of other tasks as described below. Phase 1 of the project is currently scheduled for completion by November 2004. The Phase 2 progression or project termination decision is scheduled for the next quarter.

TABLE OF CONTENTS

1.0	LIST OF TABLES AND FIGURES	1
2.0	INTRODUCTION	3
2.1	Project Open Items	3
2.2	Project Status Assessment and Forecast	3
2.3	Project Research Collaborations	3
2.4	Project Performance Variance	5
3.0	EXECUTIVE SUMMARY	6
4.0	EXPERIMENTAL.....	7
4.1	TASK 5.0, Logging and Seismic Technology Advances – USGS, BPXA	7
4.2	TASK 6.0, Reservoir and Fluids Characterization	7
4.2.1	Subtask 6.1: Reservoir and Fluid Characterization and Visualization	7
4.2.2	Subtask 6.2: Seismic Attributes and Calibration	7
4.2.3	Subtask 6.3: Petrophysical and Neural Network Attribute Analyses	7
4.3	TASK 7.0: Laboratory Studies for Drilling, Completion, and Production Support	7
4.3.1	Subtask 7.1: Characterize Gas Hydrate Equilibrium	7
4.3.2	Subtask 7.2: Measure Gas-Water Relative Permeabilities	7
4.4	TASK 8.0: Evaluate Drilling Fluids and Assess Formation Damage – UAF	8
4.5	TASKS 11.0 and 13.0: Reservoir Modeling and Project Commerciality and Progression Assessment – UAF, BP, Ryder Scott Co.	8
5.0	RESULTS AND DISCUSSION	8
5.1	TASK 1.0: Research Management Plan – BPXA and Project Team	8
5.2	TASK 2.0: Provide Technical Data and Expertise – BPXA, USGS	8
5.3	TASK 3.0: Wells of Opportunity, Data Acquisition – BPXA.....	8
5.4	TASK 4.0: Research Collaboration Link – BP, USGS, Project team.....	8
5.5	TASK 5.0: Logging and Seismic Technology Advances – USGS, BP	9
5.6	TASK 6.0: Reservoir and Fluids Characterization – UA	9
5.6.1	Subtask 6.1: Reservoir and Fluid Characterization and Visualization – UA.....	10
5.6.1.1	Products and Interim Findings	10
5.6.1.2	Volumetrics Interim Findings	11
5.6.1.2.1	Discussion of Volumetrics Methodologies and Comparisons	12
5.6.1.3	Miscellaneous Project Activities.....	13
5.6.1.4	Research Publications and Presentations	14
5.6.1.5	Work In-Progress	14
5.6.1.6	Continuing Needs and Future Work	15
5.6.2	Subtask 6.2: Seismic Attribute Characterization and Fault Analysis – UA	15
5.6.2.1	Products.....	15
5.6.2.2	Work in Progress.....	20
5.6.2.3	Future Work	23
5.6.3	Subtask 6.3: Petrophysical and Neural Network Attribute Analysis – UA	25
5.6.3.1	Products.....	25
5.6.3.2	Work in Progress.....	27
5.6.3.3	Future Work	28
5.7	TASK 7.0: Lab Studies for Drilling, Completion, and Production Support – UAF	29
5.7.1	Subtask 7.1: Characterize Gas Hydrate Equilibrium	29
5.7.2	Subtask 7.2: Relative Permeability Studies	29

5.7.2.1	Experiment Setup and Apparatus	29
5.7.2.2	Experimental Procedure	29
5.7.2.2.1	Hydrate Formation in Core Holder	30
5.7.2.2.2	Single Phase Flooding.....	30
5.7.2.2.3	The Displacement Experiment.....	31
5.7.2.3	Experimental Results	31
5.7.2.3.1	Gas Hydrate Formation Analysis	32
5.7.2.3.2	Permeability Discussion.....	32
5.7.2.3.3	Quarterly Results.....	33
5.7.2.3.4	Conclusion	39
5.7.2.3.5	Future Work	39
5.8	TASK 8.0: Evaluation of Drilling Fluid and Assess Formation Damage	40
5.8.1	Subtask 8.1: Design Integrated Mud System for Effective Drilling, Completion and Production Operation.....	40
5.8.1.1.1	Task 8 Objectives.....	40
5.8.2	Task 8.2, Assess Formation Damage: Testing, Analysis and Interpretation	40
5.8.2.1	Background, Experiment Approach and Design	40
5.8.2.2	Accomplishments and Challenges	41
5.8.2.3	Future Work	43
5.9	TASK 9.0: Design Cement Program	44
5.10	TASK 10.0: Study Coring Technology	44
5.11	TASKS 11.0 and 13.0: Reservoir Modeling and Project Commerciality and Progression Assessment – UAF, BP, LBNL, Ryder Scott	44
5.11.1	UAF Reservoir Model Accomplishments.....	44
5.11.1.1	UAF Reservoir Modeling Future Plans	49
5.11.2	Ryder-Scott Company Reservoir Model Accomplishments	49
5.11.2.1	Production Test Screening Studies	49
5.11.2.2	Simplified Screening model development and testing.....	54
5.12	TASK 12.0: Select Drilling Location and Candidate – BP, UA, USGS	58
6.0	CONCLUSION.....	59
7.0	PROJECT AND RELATED REFERENCES	59
7.1	General Project References	59
7.2	Task 7, Gas Hydrate Phase Behavior and Relative Permeability References	62
7.3	Task 8, Drilling Fluid Evaluation and Formation Damage References	63
7.4	Task 10, Coring Technology References	66
7.5	Task 11, 13: Reservoir and Economic Modeling References	67
7.6	Short Courses	69
8.0	LIST OF ACRONYMS AND ABBREVIATIONS	69
9.0	APPENDICES	70
9.1	APPENDIX A: Project Task Schedules and Milestones	70
9.1.1	U.S. Department of Energy Milestone Log	70
9.1.2	U.S. Department of Energy Milestone Plan.....	71

1.0 LIST OF TABLES AND FIGURES

Table 1: Summary of well log-based volumetric calculations and methodologies at University of Arizona	Page 12
Table 2: Fault activity for three stratigraphic intervals (28-30, 30-34, 34-E)	Page 22
Table 3: Basic data for gas-brine (2%) relative permeability measurements at 7 % hydrate saturation for Anadarko field sample	Page 37
Figure 1: MPU area shaded relief map illustrating shallow fault zones and NW-trending hingeline	Page 16
Figure 2: West to east seismic cross section (in milliseconds) of the wavelet processed Milne Point Survey	Page 17
Figure 3: Fault throw (ft) calculated for all seismically interpreted faults in the MPU, along three stratigraphic intervals	Page 18
Figure 4: Fault growth for the stratigraphic interval between horizons 28 and 30.....	Page 19
Figure 5: Fault growth for the stratigraphic interval between horizons 30 and 34.....	Page 20
Figure 6: Fault growth for the stratigraphic interval between horizons 34 and E.....	Page 21
Figure 7: Fault growth for the stratigraphic interval between horizons 28 and 34, representing most of stratigraphic interval within the Gas Hydrate Stability Zone	Page 23
Figure 8: Fault seal potential calculated for horizon 34 (Unit C gas hydrate) using three different methods.....	Page 24
Figure 9: Well logs for wells WSak-25 and MPA-01, including sonic (DT), deep resistivity (Res) and gamma ray (GR).....	Page 25
Figure 10: Results of supervised waveform classification along the Unit C gas-hydrate interval	Page 26
Figure 11: Results of supervised waveform classification along the Unit D gas-hydrate interval	Page 27
Figure 12: Results of supervised waveform classification along the Unit E gas-hydrate interval	Page 28
Figure 13: The experimental set-up picture constructed for forming gas hydrates and measuring relative permeability	Page 29
Figure 14: Schematic of laboratory apparatus for measuring relative permeability	Page 31
Figure 15: Volume change in methane cylinder confirms gas hydrate dissociation	Page 32
Figure 16: Pressure decline confirms gas hydrate formation.....	Page 32
Figure 17: Effective permeability for various gas hydrate saturation values.....	Page 33
Figure 18: Relative permeability curves for various hydrate saturation values	Page 33
Figure 19: Possible gas hydrate zonation in the sample	Page 34

Figure 20: Ratio of effective permeability to gas and water for different hydrate saturation values for the Oklahoma 100 mesh sand samples	Page 35
Figure 21: Ratio of effective permeability to gas and water for different hydrate saturation values for the Anadarko field samples	Page 36
Figure 22: Gas relative permeability data at different hydrate saturation for Oklahoma 100 mesh sand sample	Page 36
Figure 23: Water relative permeability data at different hydrate saturation values for Oklahoma 100 mesh sand sample	Page 37
Figure 24: Brine (2%) relative permeability data at different hydrate saturation for Anadarko field sample	Page 38
Figure 25: Gas relative permeability data at different hydrate saturation for Anadarko field samples	Page 38
Figure 26: Gas-brine (2%) relative permeability data for Anadarko field sample Hydrate saturation (S_h) = 7 %	Page 39
Figure 27: Modified Layout for assessing formation damage due to static, dynamic filtration and by leak-off tests	Page 43
Figure 28: Hypothetical geologic model	Page 45
Figure 29: Temperature distribution after 3 years, depressurization case	Page 45
Figure 30: Cumulative gas produced vs. time (at low permeability, 15md)	Page 46
Figure 31: Location of injection, production wells, and initial distribution of water Saturation	Page 46
Figure 32: Temperature distribution after 3 years, depressurization and injection at 40°C	Page 47
Figure 33: Gas hydrate-saturation profiles in the bottom gas hydrate-bearing layer during hot water injection after 9 months (Injection rate 20m ³ /day, water temperature = 40°C)	Page 47
Figure 34: Cumulative gas produced vs. time (Hot water injection rate 20m ³ /day)	Page 48
Figure 35: Comparison of all production schemes at 300 md reservoir permeability	Page 48
Figure 36: Gas Rate from screening model of free gas depressurization case	Page 51
Figure 37: Milne Point Area Saturation in Reservoir Model	Page 52
Figure 38: Milne Point Area Temperature in Reservoir Model	Page 52
Figure 39: Milne Point Area Pressure in Reservoir Model	Page 53
Figure 40: Sensitivity to conductive heat flux constant. Red base case is matched value from Mallik Simulation (provided by Collett)	Page 53
Figure 41: 15 year time series showing temperature depression around dissociation locations (Blue is cold, green is warm)	Page 55

Figure 42: 15 year time series showing ternary saturation (Dark blue is water, green is gas hydrate, red is free gas)	Page 56
Figure 43: ProCast Data Entry Panel reflecting Hydrate terms	Page 57
Figure 44: Three Sample reservoirs in ProCast reflecting different gas hydrate dissociation descriptions	Page 58

2.0 INTRODUCTION

This project is helping to solve the technical and economic issues to enable government and industry to make informed decisions regarding potential future commercialization of unconventional gas-hydrate resources. The project is characterizing and quantifying in-place and recoverable ANS gas-hydrate and associated free-gas resources, initially using Eileen trend area well and seismic data in the Milne Point Unit (MPU) and publicly-available well data in the Prudhoe Bay Unit (PBU) and Kuparuk River Unit (KRU) areas. The project is also investigating gas hydrate phase equilibrium and relative permeability within porous media. Additional laboratory investigations include design of best practices for drilling, completion, and production operations within and near gas hydrate-bearing reservoirs.

Successful determination of the resource potential of gas hydrate and associated free gas resources could significantly increase current developable gas reserves available for ANS reservoir energy support, enhanced oil recovery, fuel gas, and commercial sales within and beyond current infrastructure. Proving technical production feasibility and commerciality of this unconventional gas resource could lead to greater energy independence for the U.S., providing for future gas needs through an abundant, safe, secure, and stable domestic resource.

2.1 Project Open Items

Contracts updated in September 2004 fully obligate Phase 1 project funding, allow Phase 1 time extension for the full 2-year Phase 1 research program through end-October 2004, and pre-fund \$195,000 of potential Phase 2 activities. Phase 1 interim results, reservoir-fluid characterization, reservoir modeling, and economic modeling will contribute to a Phase 2 progression decision during third quarter 2004. An incremental Phase 1 funding request of \$500,000 was initiated in June 2004 to accomplish unanticipated well-of-opportunity data acquisition, reservoir characterization, and reservoir modeling tasks in support of the Phase 2 progression or termination decision. As of the writing of this report, the DOE contracting officer completed the contract amendment 5 and the amendment was received and signed by BPXA.

2.2 Project Status Assessment and Forecast

Project technical accomplishments from April 2004 through end-June 2004 are presented by associated project task. The attached milestone forms (Appendix A) present project tasks 1 through 13 with task duration and completion timelines.

2.3 Project Research Collaborations

Progress towards completing project objectives significantly benefits from DOE awareness, support, and/or funding of the following associated collaborations, projects, and proposals. Section 5.4 provides additional detail on collaborative research accomplishments during the reporting period.

1. **Reservoir Model studies (Ryder Scott Co., UAF, LBNL):** The LBNL TOUGH2 EOSHYDR2 Beta-test reservoir model for BPXA team testing and use was originally scheduled for release by January 2004. The TOUGHfX reservoir model was delivered in early July 2004 following training at the NETL facility in June 2004. This research includes reservoir model code calibration to data collected during the 2002 Mallik gas hydrate test program. Interim reservoir characterizations of MPU gas hydrate prospects are in-progress by Ryder Scott Company (RS) in collaboration with UAF and USGS. RS is providing industry-standard reservoir modeling using CMG STARS for evaluation of gas hydrate prospects, input into the Phase 2 progression decision, and optimization of potential future development and delineation plans.
2. **DE-FC26-01NT41248:** UAF/PNNL/BPXA studies to determine effectiveness of CO₂ as an enhanced recovery mechanism for gas dissociation from methane hydrate. Recent project status presentation updates and funding indicate a strong level of DOE support for this associated project. UAF seconded a graduate student to PNNL to assist with this research. PNNL and BPXA presented project research updates to Jim Slutz (DOE) in January in Anchorage. A project update is planned for the AAPG Hedberg research conference in September.
3. **UAF/Argonne National Lab project:** This associated project was approved for funding by the Arctic Energy and Technology Development Lab (AETDL), forwarded to NETL for review, and has been funded as of the writing of this report. The project is designed to determine the efficacy of Ceramicrete cold temperature cement to future gas hydrate drilling and completion operations. Evaluating the stability and use of a cold temperature cement will greatly enhance the ability to maintain the low temperatures of the gas hydrate stability field during drilling and completion operations, helping to ensure safer and more cost-effective operations.
4. **Precision Combustion, Inc. (PCI) – DOE collaborative research project:** Potential synergies from this DOE-supported research project with our gas hydrate research program were recognized in December 2003 by Edie Allison (DOE). Dialog and correspondence with Precision Combustion researchers indicate some significant potential synergies, particularly regarding potential in-situ reservoir heating. Successful modeling and lab work could potentially proceed into field application of gas hydrate thermal recovery enhancement testing if this project progresses into phases 2 and/or 3. BPXA provided a letter in April 2004 in support of progression of PCI's project into phase 2: prototype tool design and possible surface testing. DOE awarded Phase 2 to PCI during this quarter.
5. **UAF/McMillan-McGee/PNNL proposal:** This proposal was highly ranked during 2003 presentations to AETDL, but not forwarded to NETL for funding. The proposal also received letters of support from BPXA and Conoco-Phillips viscous oil development teams. The project would investigate the potential for in-situ electromagnetic (EM) heating as an enhanced recovery method for both viscous oil and gas hydrate production. In addition to depressurization of an adjacent free gas, this technology might thermally enhance gas dissociation from gas hydrate-bearing reservoirs and perhaps counteract any endothermic cooling reaction, thus providing greater flow assurance during gas production. A brief, independent assessment and first-principles numerical modeling of the EM methodology is being considered to determine whether or not to proceed with further proposals of this nature in support of potential Phase 2-3 operations procedures.

6. **Japan gas hydrate research:** Progress toward completing the objectives of this project remain aligned with gas hydrate research by Japan Oil, Gas, and Metals National Corporation (JOGMEC), formerly Japan National Oil Corporation (JNOC). JOGMEC remains interested in research collaboration, particularly if the project proceeds into Phase 2 operations.
7. **India gas hydrate research:** India's Institute of Oil and Gas Production Technology (IOGPT) indicated an interest in participating with our research program in correspondence with DOE during September 2003. BPXA has not initiated contact with IOGPT.
8. **Korea gas hydrate research:** Korea is developing a gas hydrate research program. They have discussed potential participation in future Alaska gas hydrate research with USGS. BPXA has not initiated contact with Korea.
9. **U.S. Department of Interior, USGS, BLM, State of Alaska DGGS:** An additional collaborative research project under the Department of Interior (DOI) is providing significant benefits to this project. The BLM, USGS, and the State of Alaska recognize that gas hydrates are potentially a large untapped onshore energy resource on the North Slope region of Alaska. To develop a complete regional understanding of this potential energy resource, the BLM, USGS and State of Alaska Division of Geological and Geophysical Surveys (DGGS) have entered into an Assistance Agreement to assess regional gas hydrate energy resource potential in northern Alaska. This agreement combines the resource assessment responsibilities of the USGS and the DGGS with the surface management and permitting responsibilities of the BLM. As interest in the resource potential of Alaska gas hydrates continue to grow, information generated from this agreement will help guide these agencies to promote responsible development of this potential arctic energy resource. The DOI project is working with the BPXA – DOE project to assess the regional recoverable resource potential of onshore natural gas hydrate and associated free-gas accumulations in northern Alaska, initially within and eventually beyond current industry infrastructure.
10. **Drilling fluids evaluation:** Halliburton Energy Services and Baroid recently agreed to provide drilling fluid samples in support of Task 8.0. Also, a recently formed company in Europe, "Worldwide Gas Hydrates", has developed a potassium formate-based brine (VapornetTMGHF-164), which might provide an environmentally-safe and cost-effective gas hydrate stimulation fluid, to help initiate and maintain gas dissociation from gas hydrates during production. This fluid may be evaluated for possible application in phases 2 and/or 3 operations and production testing. UAF may request access to this fluid for formation damage studies, Task 8.2.

2.4 Project Performance Variance

Release of shallow portions of PBU seismic data under confidentiality constraints to the project is not currently feasible. BPXA has consistently recognized that contribution (under confidentiality constraints) of PBU seismic data to the project is dependent upon industry partner approval. Future plans include presentation of project results to industry partners to help facilitate understanding of and potential future participation in the research.

3.0 EXECUTIVE SUMMARY

This Quarterly report encompasses project work from April 1, 2004 through June 30, 2004. Sections 4 and 5 provide a detailed project activities report.

- Updated Phase 1 research program tasks, timelines, deliverables, and budget
 - Anticipate Phase 2 progression decision by end-summer 2004
 - Phase 1 research will continue through end-October 2004
 - Phase 2 may continue through end-December 2005, pending BPXA decision
 - Phase 3 may continue through end-December 2006, pending BPXA decision
- Continued gas hydrate research collaborations/discussions with many associated projects
- Coordinated, compiled, and completed project weekly, technical, and financial reports
- Planned and implemented input to 2004 conferences, meetings, and presentations
- Reviewed and coordinated approval of UA and UAF presentation materials and theses
- Completed 9 abstracts for presentation at September 2004 AAPG Hedberg Conference
 - Conference provides a major opportunity to present Phase 1 study results
- Prepared project summary and submitted to Spring 2004 DOE Fire and Ice Newsletter
- Analyzed seismic attributes for direct gas-gas hydrate indicator study of 21 prospects
 - Developed volumetrics and uncertainty analysis methods for prospect evaluation
- Confirmed geomorphologic trends correlate with certain fault zones and structural trends
- Studied USGS gas hydrate zone thickness in relation to fault proximity in the MPU
 - Analyzed faults to study syndepositional and sealing natures vs. gas hydrate zones
- Studied coals and potential relationship to gas hydrate and free gas-bearing reservoirs
- Completed well log-based MPU gas in-place volumetrics for 12 stratigraphic sequences
 - Identified in-place potential: 0.8 – 1.5 TCF gas hydrate and 0.8 – 1.6 TCF free gas
- Completed supervised waveform classification of gas hydrate-bearing Units C, D and E
 - Correlated and discovered link of fault seal potential to waveform classification
 - Linked structure and possibly syntectonic deposition with gas hydrate distribution
- Classified fluid saturations and estimated confidence levels with log-based expert system
 - Used neural network to predict gas hydrate, gas, coal, sand, and water saturation
- Studied gas hydrate relative and effective permeability dynamics with unique experiments
 - Discovered possible gas hydrate zonation in the experiment porous media samples
 - Showed effective permeability tends to decline as gas hydrate saturation increases
 - Saw water relative permeabilities decrease with increasing gas hydrate saturation
 - Nucleation of gas hydrates during formation may result in pore structure change
- Designed experimental apparatus for evaluation of formation damage and mud systems
- Continued industry-standard gas hydrate reservoir modeling with CMG Stars and ProCast
 - Incorporated Milne Point gas hydrate/free gas prospect into CMG Stars model
 - Planned reservoir model evaluation/development scenarios and scope-of-work
 - Developed analytical models to simulate gas hydrate depressurization production
 - Incorporated CMG STARS simulation work from University of Calgary and UAF
 - Evaluated permeability, spacing, production, and gas hydrate saturation variations
 - Incorporated beta release of a moving gas hydrate dissociation front into ProCast
 - Began to incorporate and understand an ice component and its effects in CMG Stars
 - Evaluated saturation, pressure, and temperature changes in 15 year production life
 - Evaluated sensitivity to conductive heat flux constant and thermal recovery history
 - Evaluated gas hydrate dissociation dynamics over 15 year production history

4.0 EXPERIMENTAL

During the reporting time period from April through June 2003, primary experimental activities consisted of experiment apparatus design, setup, and execution at UAF as well as reservoir and fluid characterization studies using 3D seismic and well data at UA and USGS.

4.1 TASK 5.0, Logging and Seismic Technology Advances – USGS, BPXA

The U.S. Geological Survey (USGS) continues to analyze seismic attributes within the Milne 3D dataset to investigate the potential for direct detection of pore fluids associated with gas hydrate-bearing reservoirs. Research confirms that seismic velocity, amplitudes, and wavelet character respond to fluid and reservoir changes within the gas hydrate-bearing reservoir system. Multiple possible gas-gas hydrate-bearing prospects have been identified within prospect fairways.

4.2 TASK 6.0, Reservoir and Fluids Characterization

The University of Arizona (UA) continued resource characterization studies revealing shallow sand reservoir stratigraphic heterogeneity and structural compartmentalization. Progress continues on geologic/geophysical project tasks. Full integration of well and seismic data interpretations remains incomplete. Section 5.6 provides additional details, results, and recommendations.

4.2.1 Subtask 6.1: Reservoir and Fluid Characterization and Visualization

Continued to refine well log-based bulk volume calculations in MPU area gas hydrate prospects.

4.2.2 Subtask 6.2: Seismic Attributes and Calibration

Completed supervised waveform classification of gas hydrate units C, D, and E within MPU. Correlated fault seal potential and waveform classification to determine possible effects on gas hydrate distribution and trapping mechanism.

4.2.3 Subtask 6.3: Petrophysical and Neural Network Attribute Analyses

Completed multiple iterations of the log-based expert system and algorithms to classify fluid saturation, estimate confidence, and detect coal occurrence. Evaluated and compared results to manual interpretations. Determined velocity and resistivity response for water saturated zones. Trained a neural network to predict gas hydrate, free gas, coal, clean sand, and water saturation components within reservoir sands from well log signatures.

4.3 TASK 7.0: Laboratory Studies for Drilling, Completion, and Production Support

The University of Alaska Fairbanks (UAF) conducted several experiments for gas hydrate relative permeability studies. Section 4.7 provides additional details, results, and recommendations.

4.3.1 Subtask 7.1: Characterize Gas Hydrate Equilibrium

No further work accomplished during reporting period.

4.3.2 Subtask 7.2: Measure Gas-Water Relative Permeabilities

A conventional experimental apparatus for measuring relative permeability was successfully used for studying gas hydrates within porous media. Several experiments were performed,

effective permeability was measured, and relative permeability was calculated for various gas hydrate saturations.

4.4 TASK 8.0: Evaluate Drilling Fluids and Assess Formation Damage – UAF

Erected the experimental apparatus and refined standard testing procedures. Section 4.8 provides additional details, results, and recommendations.

4.5 TASKS 11.0 and 13.0: Reservoir Modeling and Project Commerciality and Progression Assessment – UAF, BP, Ryder Scott Co.

Continued to adapt reservoir simulator, CGM STARS, to analyze MPU-area gas hydrate-bearing reservoirs. Section 4.11 provides additional details, results, and recommendations.

5.0 RESULTS AND DISCUSSION

Project technical accomplishments from April 2004 through June 2004 are presented in chronological order by associated project task.

5.1 TASK 1.0: Research Management Plan – BPXA and Project Team

Task schedules are presented in the attached milestones forms (Appendix A). Project expenditures are reported separately on financial forms 269A and 272.

- Coordinated, compiled, and completed project technical and financial reports
- Participated in weekly project teleconference discussions with DOE project manager
- Reviewed, processed, and ensured budget consistency of subcontractor invoices
- Coordinated additional reservoir modeling work with UAF and Ryder Scott Company
 - Decided to proceed using industry-standard, commercially-available CMG STARS
- Completed project manager transition to ASRC Energy Services
- Updated internal Authority for Expenditure (AFE) categories, amounts, and approvals
- Initiated planning for potential phase 2 project scope-of-work and ideas in preparation for Phase 2 progression or project termination decision
- Updated project tasks, timeline, deliverables, and budget for 2-year Phase 1 research
 - Phase 1 research will continue through end-October 2004
 - Phase 2 may continue through end-December 2005, pending BPXA decision
 - Phase 3 may continue through end-December 2006, pending BPXA decision

5.2 TASK 2.0: Provide Technical Data and Expertise – BPXA, USGS

- Reviewed and coordinated approval of UA and UAF presentation materials and theses
- Discussed and reviewed interpretation of Eileen-West End gas hydrates and saturations
- Helped plan reservoir model evaluation and development scenarios and scope-of-work

5.3 TASK 3.0: Wells of Opportunity, Data Acquisition – BPXA

- Monitored drilling schedules and communicated with operations groups

5.4 TASK 4.0: Research Collaboration Link – BP, USGS, Project team

- Coordinated reservoir modeling plans and actions with UAF and Ryder Scott Co.
 - Communicated with University of Calgary regarding their 2003 independent study of gas hydrate reservoir systems using CMG STARS reservoir model.

- University adapted reaction terms in STARS to simulate gas hydrates
 - Study documented in Hong (2003) thesis and in 2004 JPT publication
- Coordinated UAF representation at NETL training for TOUGHfX
 - Reviewed training course notes and manual
 - Generated questions for team review and model evaluation/comparison
- Reviewed contracts and data sharing agreements to confirm USGS data needs
 - Requested UA copy VSP, Checkshot, and NWEileen 3D survey (truncated at 950 ms and MPU boundary) for USGS project work
- Provided BP Canada with project update to ensure coordination with industry activity
- Contacted McGee/McMillan in Calgary to discuss potential field/downhole application of electromagnetic heating methods for enhancing dissociation of gas from gas hydrate
- Met with Pacific Northwest National Lab: discussed research results and synergies
- Prepared and presented interim research results to AAPG Annual Meeting, Dallas
 - Provided gas hydrate subcommittee project update for planning and discussion
- Prepared and presented interim research results to Alaska Geological Society Conference
- Prepared and presented interim research results to CSPG Annual Meeting, Calgary
- Prepared, reviewed, coordinated, and submitted 9 project abstracts for AAPG Hedberg
 - 1 project overview abstract, 3 UAF Abstracts, and 5 UA abstracts
- Prepared project input for DOE Fire and Ice Newsletter; coordinated BPXA approval
- Continued contact with Precision Combustion, study potential in-situ thermal stimulation
 - Coordinated providing BPXA support letter to PCI Phase 2 advance
- Submitted project research summary to BP Helios awards for corporate recognition
- Initiated contact with Shell researchers to discuss gas hydrate reservoir model methods
 - Informal reply forwarded within Shell; no formal followup

5.5 TASK 5.0: Logging and Seismic Technology Advances – USGS, BP

United States Geological Survey

USGS Principle Investigator: Timothy Collett

USGS Participating Scientists: David Taylor, Warren Agena, Myung Lee, Tanya Inks (IS)

- Provided input to potential wireline logging data acquisition plans
- Applied seismic model and attribute analyses for direct gas-gas hydrate indicator study
 - Applied developed synthetic models illustrating seismic attribute response to fluid (gas hydrate – free gas – water) and reservoir changes to MPU gas hydrate seismic interpretation and prospect development
 - Continued interpretation of 14 potential MPU area gas hydrate prospects and 7 associated free gas prospects within play fairways.
 - Developed interim volumetrics and uncertainty analysis methods for evaluation of 14 specific MPU gas hydrate prospects and 7 associated free gas prospects for input into Phase 2 progression or termination decision.

5.6 TASK 6.0: Reservoir and Fluids Characterization – UA

University of Arizona

UA Principle Investigator: Robert Casavant

UA Co-Principle Investigator: Roy Johnson, Mary Poulton

UA Participating Scientists: Karl Glass, Ken Mallon

UA Graduate Students: Casey Hagbo, Bo Zhao, Andrew Hennes, Justin Manuel, Scott Geauner
UA Undergraduate Student Assistant: Greg Gandler

This section represents a listing of gas hydrate research activities that were completed or are in progress as of June 30, 2004 at the University of Arizona (UA). Progress in the UA geological and geophysical reservoir characterization of the gas hydrate and free gas resources in the MPU area and southward into the northern KRU and western Eileen block of PBU has involved the continued investigation and characterization of:

- Variation in fault throws and inferred fault seal potential across the MPU
- Lateral and vertical variations in the timing and influence of fault reactivation on deposition of the reservoir units within the Sagavanirktok and Gubik Formations
- Variations in seismic amplitude responses associated with gas hydrate-prone intervals via supervised waveform classifications and the role of faulting on compartmentalization and migration of hydrocarbons in the MPU area
- Facies-related contributions to gas emplacement
- The base of the ice-bearing permafrost and gas hydrate stability fields based on available empirical, wireline log and temperature log data
- Linkages between fault morphology, distribution and gas hydrate/free-gas resource

The results of a comparative well log-based volumetric study across the MPU are also discussed. A separate draft report with full tables and maps is on file at UA. The final report will be made available in September 2003 when the major student contributors have returned from summer break.

5.6.1 Subtask 6.1: Reservoir and Fluid Characterization and Visualization – UA

5.6.1.1 Products and Interim Findings

- Reviewed small amount of requested digital, raster, and hardcopy mudlog data.
 - Interpreted coal-bearing zones and qualitative coal gas from the mudlogs and entered with digital total gas background into UA database.
 - Displayed data on UA Petra log displays for petrophysical analysis.
 - Petrophysical analysis helped identify coal zones.
 - Trained and high-graded UA log-based fluid prediction expert system and neural network algorithms using coal-bearing zone interpretations.
- Discussed re-converting data files and map files for transfer to LandMark (especially StratWorks and ZMap-Plus) with Petra technical support. Grid conversion will be tested before end of Phase 1.
- Confirmed spatial correlation between shoreline and some river trends with certain fault zones and structure. Results will be presented at AAPG Hedberg conference.
- Studied USGS gas hydrate zone thickness in relation to fault proximity in the MPU
 - Study confirms a fair degree of correlation (Gandler & Casavant, 2004) suggesting that these faults were syndepositional, and if sealing, continue to play a role in gas hydrate distribution.
 - Analyzed spatial relationships with fault orientation, morphology, complexity, and fault throws from Hennes (2004) in Gandler study (report in preparation).

- Recent thesis by Hennes (2004), based from seismic data, confirmed this in a very detailed manner.
- Completed preliminary study of coal occurrence and investigated lateral and vertical spatial relationships between reservoir-quality sands containing coal beds and the distribution of gas hydrate/free-gas occurrence.
 - Incorporated changes in background gas from available mudlog information.
 - Investigated possible indirect linkage to the types of reservoir sands associated with coal occurrences, proximity of the facies to faulting, and updip charging of reservoir sands.
 - Plan to present findings at the AAPG Hedberg Gas Hydrate Research Conference.
- Integrated log-based net shale and sand unit thicknesses, sand/shale ratios, and crossplots with seismic data interpretations of fault throws
 - Determined the sealing/non-sealing nature of faults (Hennes et al., 2004).
 - Used this data to assess sand body continuity (Geauner, Casavant et al., 2004 and Manual, Casavant, 2004 in preparation).
- Completed most of the research on the predicted significance of the "NW-trending hingelines" (minimal dip slip/fracture zones/strike-slip component, below seismic resolution) as probable fluid barriers and influence on dip slip variations along NNE fault zones (Figure 1).

5.6.1.2 Volumetrics Interim Findings

- Completed well log-based MPU gas in-place volumetric calculations (Table 1).
 - Calculations using both the UA automated fluid predictor by Glass and manual assessment by the rest of the team are a very iterative exercise.
 - Assessments of total gas hydrate and free-gas volumes incorporate revisions of the UA fluid identification expert system and include mudlog, cuttings, and core logs, as well as additional portions of the gas-bearing Cascade well logs
 - Volumetric assessments include total background gas records digitized by USGS.
 - Created a second set of logs for gas hydrate, free gas, ice, petroleum, and coal-bearing zones and input into the UA database and Petra displays.
 - Updated earlier comparative volumetric analysis/chart (based on an earlier and preliminary automated fluid predictor) with a newer fluid predictor and confidence levels.
 - Adjusted net gas-hydrate and free-gas pay for reinterpretations of the depth of the base of the ice stability zone (also known as the "base ice-bearing permafrost" BIBPF) and the base of the gas hydrate stability zone (BHSZ).
 - Noted and confirmed variations in thickness or depth of the BHSZ based on communications with USGS and BPXA
 - Determined gas expansion factor and unit porosity for 12 stratigraphic sequences
 - Totaled these factors and input into volumetric calculations
 - Compared volumetric calculations/methodologies in varied MPU frameworks and completed interim volumetrics for all onshore gas hydrate and free-gas resources within the MPU boundary (Table 1). Final volumetrics will require minor editing of some map grids.

Table 1: Summary of well log-based volumetric calculations and methodologies at University of Arizona

Assessment Method	Gas Hydrate In-Place	Free Gas In-Place	Total Gas In-Place
USGS Lithostrat	1.46 – 2.73 TCF	Not Determined	1.46 – 2.73 TCF
UA Waveform Class.	0.77 – 1.31 TCF	Not Determined	0.77 – 1.31 TCF
UA Lithostrat.	Not Determined	Not Determined	Not Determined
UA Sequence Strat. 1	1.03 – 1.22 TCF	0.77 – 1.31 TCF	1.8 – 2.53 TCF
UA Sequence Strat. 2	1.28 – 1.51 TCF	1.6 TCF	2.88 – 3.11 TCF

5.6.1.2.1 Discussion of Volumetrics Methodologies and Comparisons

The UA lithostratigraphic-based method was not used for bulk volumetrics. The UA sequence stratigraphic method #1 used maximum and minimum UA manual log analysis. The UA sequence stratigraphic method 2 used the automatic fluid predictor and confidence model, expert system #2, at a 25% confidence level.

The UA maximum values reflect a 90% gas filled clathrate structure as did the USGS assessments. The current totals from both the UA expert system (automated) and manual interpretation of resource maximums for gas hydrate were approximately 50% lower than the USGS maximum within the MPU area. This discrepancy may be caused by the USGS early general assessments using regional average values for unit porosity and reservoir thickness. It was understood that more work would be needed to understand the volumetric implications of lateral and vertical heterogeneities in the reservoirs.

Published estimations of free-gas within the MPU in the Sagavanirktok formation were not available prior to the UA resource assessment. Interestingly, the UA manual total in-place gas hydrate and free-gas of 2.53 TCF and automated total gas of 3.11 TCF brackets the USGS hydrate maximum of 2.73 TCF (Table 1). As recognized by both the USGS and UA work, the resource assigned to different pay units is somewhat problematic due to the wide spacing of the well data. Additional refinement/iterations are planned as the UA facies distribution and reservoir body dimensional modeling is completed. From a stratigraphic standpoint, it is possible that numerous fluvial reservoir sands that contain gas hydrate and/or free gas extend a considerable distance beyond the borehole in only 2 of 4 directions. However, lower resource volumes in these zones could be somewhat balanced by the presence of (1) more extensive resource-bearing multi-story deltaic and nearshore marine sands, (2) untapped resource-bearing fluvio-deltaic sands that exist between the wells, and (3) abundant faulting and fluid communication between wells, which may allow access to additional reservoir units not interpreted in the current low well density. Preliminary work on this issue was started in the MPU and explored within the AOI during Phase 1. Future activity may involve a more detailed approach to reservoir heterogeneity and the influence on volumetrics, potential well locations, and estimation/modeling of potential recovery. The structural and reservoir heterogeneity interpreted in this current analysis is likely to introduce an unknown and possibly significant amount of error and uncertainty into the modeling framework of gas hydrate dissociation and gas recovery and development scenarios.

The UA sequence stratigraphic method using UA automatic fluid predictor and confidence model (expert system #2, 25% confidence level) estimates gas hydrate and associated free gas resources from BIBPF down to Top Ugnu. A more accurate predictor (expert system #3) is presently under development and is planned for future MPU and AOI volumetrics. Like the manual assessment, expert system #3 also recognizes facies (e.g. coal-bearing zones) and considers reported or projected depths of the BHSZ, as derived by USGS and UAF studies.

The UA sequence stratigraphic method using maximum and minimum UA manual log analysis estimates gas hydrate and associated free gas resources over the interval from a most likely BIBPF pick down to the BHSZ. The BHSZ is determined from gridding empirical well interpretations from the UAF study (Westervelt, 2003) and constrained by USGS data where available. Uncertainty in reservoir salinity may complicate this analysis. Free gas calculations encompassed the BHSZ down to top Ugnu Formation, excluding the Staines Tongue equivalent interval under evaluation by USGS in Task 5.0. All interpreted coal zones were omitted. The coal contribution to potential background gas is under evaluation and looks initially to be negligible.

5.6.1.3 Miscellaneous Project Activities

- Met bi-weekly on development of fluid and lithology prediction expert system.
- Met monthly on neural network training and log review.
- Met weekly on current status of geologic mapping, volumetric analysis, coal gas, evaluation of sequence stratigraphic correlation.
- Met to discuss interpretation of seismic attributes, thesis and independent study reviews, and time-depth conversions.
- Held advisor meetings and reviewed documents related to graduate student work progress, theses, and independent studies.
- Held SSCIL meetings on volumetrics methodologies
- Discussed integration of upcoming seismic facies study with well-log facies work on volumetrics, completion of comparative volumetric analysis, manual gas hydrate/gas net-pay determinations, misleading coal gas contributions, etc.
- Held student (Hennes)/Advisor (Johnson) meetings to discuss progress, issues, edits, and structure of prepublication manuscript (under review at BPXA).
- Met to discuss recent progress, reinterpretation of some well-log picks for gas hydrate, coal, BIBPF, BHSZ, and resolving internal issues of time-depth tie.
 - Determined time-depth tie best fit for information originally provided to UA.
 - Discussed contents of data shared with UA by USGS, determined that BHSZ surface is required for comparative analyses.
 - Discussed USGS-provided synthetics: unclear if they are final synthetics used for USGS time-depth tie (plan to compare at USGS).
- Continued weekly maintenance of IT hardware.
 - Created backups and installed patches for all server and lab software.
 - Replaced dual CPUs on one workstation.
 - Swapped dual monitors and upcoming HDD.
 - Replaced motherboard on another workstation.
- Continued upgrades to Windows and Solaris machines
 - Applied standard patches and software updates.

- Solaris: ssl, ssh, weekly Solaris Recommended Patches
- Windows: daily updates of patches and anti-virus, petra patches
- Completed project management, related administration activities, data compilation, and submitted draft quarterly technical report.

5.6.1.4 Research Publications and Presentations

- April 2, 2004 University of Arizona Geodase Symposium: Andrew Hennes poster/talk on data processing, visualization/interpretation techniques, recent waveform analyses, results of fault throw, fault activity, and fault seal potential.
- Gandler, G., 2004, "Preliminary spatial analysis of hydrate occurrence with respect to faulting, Milne Point Unit, Arctic Alaska Senior Independent Study Project, 20p.
- Hennes, A.M., et. al, 2004, "Structural constraints on gas-hydrate formation and distribution in the Milne Point Unit, North Slope, Alaska " MS Thesis prepublication, in review, 50 p. (See below thesis conclusions in 4.6.2.1)
- Prepared the following extended abstracts of findings and activities related to geology and geophysical research in the MPU for submission to September AAPG Hedberg Conference, Vancouver, BC:
 - Bob Casavant, Andrew Hennes, Roy Johnson, and Tim Collett— Structural analysis of a proposed pull-apart basin: Implications for gas hydrate and associated free-gas emplacement,
 - Greg Gandler, Bob Casavant, Karl Glass and Andrew Hennes, Casey Hagbo, and Roy Johnson - Preliminary spatial analysis of faulting and gas hydrate occurrence, Milne Point Unit, Arctic Alaska
 - Scott Geauner, Justin Manual, Bob Casavant, Karl Glass and Ken Mallon—Well log normalization and comparative volumetric analyses of gas hydrate and free-gas resources, Central North Slope, Alaska
 - Andrew Hennes, Roy Johnson, and Bob Casavant—Seismic characterization of a shallow gas hydrate-bearing reservoir on the North Slope of Alaska,
 - Mary Poulton, Bob Casavant, Karl Glass, and Bo Zhao— Model testing of methane hydrate occurrence on the North Slope of Alaska with artificial neural networks

5.6.1.5 Work In-Progress

- Analyzing a seismic section across Milne Point from Simp32-14 to MPD-01
 - Identifying major intraformational unconformities and their relationship to current log-based sequence stratigraphic framework.
 - Identification of reflector terminations representing downlap, onlap and intraformational erosion will assist in future seismic facies mapping and neural network seismic classification schemes.
- Characterizing the transtensional structural architecture within MPU. Several talks on this morphotectonic study will be presented by the UA team at the Hedberg conference.
- Extending the sequence stratigraphic framework developed for MPU into the rest of the AOI following completion of comparative MPU volumetric task.
- Studying spatial analysis of coal-bearing units (and potential CBM contribution) to location of free-gas occurrence and location of intraformational unconformities within the lower sequences.

- Evaluating relevance to depositional reconstructions, reservoir continuity, seismic attributes, and volumetrics.
- Planning and preparing oral and poster presentations for AAPG Hedberg Conference.
- Studying tectonic controls on the BIBPF and BHSZ in the AOI to understand and predict structural level changes and reconcile local differences between USGS and UA estimations of horizon depth.
- Calibrating and integrating geologic maps with seismic interpretation to identify target areas for data acquisition in gas hydrate and associated free gas within and near MPU
- Preparing for smooth transition into possible Phase 2 of project and addressing UA business management concerns
 - Lead-time required for graduate student contracting is a significant concern
 - Will request Phase 1 no-cost extension to help mitigate
- Studying the architecture of the transtensional basin in relation to the regional NW structural hingeline described in early reports and investigated in Hennes et al. (2004)

5.6.1.6 Continuing Needs and Future Work

- Development of a new seismic-based sequence stratigraphic framework in the MPU that will be guided/trained by the current log-based sequence stratigraphic framework.
- This seismic framework will be used to guide development of a new seismic facies classification scheme and assessment of lateral and vertical continuity of sand bodies in the Sagavanirktok formation that may provide input into a seismic expert system or neural network.
- Development of spatial analysis of fault morphology relative to porosity, reservoir and non-reservoir facies development for prospect development.
- Development of a comprehensive set of geologic maps for all sequences across the AOI showing prioritized locations for potential future test wells and/or wells for further data collection opportunities.

5.6.2 Subtask 6.2: Seismic Attribute Characterization and Fault Analysis – UA

5.6.2.1 Products

- Prepared draft prepublication manuscript for MS degree requirements (Hennes).
 - Prepared and edited figures for prepublication manuscript.
 - Submitted draft manuscript to BPXA; on-hold pending technical review.
- Prepared draft poster presentation for Hedberg conference.
- Completed supervised waveform classification of hydrate units C, D and E across entire Milne Point Survey utilizing well-interpretation, gas hydrate vs. no gas hydrate.
 - Maps show a varied lateral distribution.
- Derived two modified algorithms for fault seal analysis based on original clay-smear-potential (CSP) algorithm (Yielding et al. 1997).
- Applied 2 new CSP algorithms and shale-gouge-ratio (SGR) algorithm to three gas-hydrate-bearing horizons in MPU.
- Correlated fault seal potential and waveform classification
 - Fault seal may have an effect on gas-hydrate distribution (i.e.: possible trapping mechanism of original free gas before conversion into gas hydrate form).

- Completed fault throw and fault growth analysis over MPU.
- Correlated active faults late in stratigraphic section with gas-hydrate occurrence in C, D, and E units.
 - Active faults may provide accommodation space for development of reservoir sands necessary to contain gas-hydrate and may have served as conduits for original migration of free gas.
- Copied and sent NWEileen 3D seismic survey (truncated at 950 ms and MPU boundary) and associated data and checkshots to Tim Collett (USGS) as per June 25, 2004 written request and contractual permission confirmation from Robert Hunter.
- Determined conclusions about the effect of structure on gas hydrate distribution. Initial emplacement and future production of gas hydrates is highly dependent on the complex nature of faults in the MPU. The role structure plays in determining gas hydrate distribution is summarized below, after Hennes (2004).

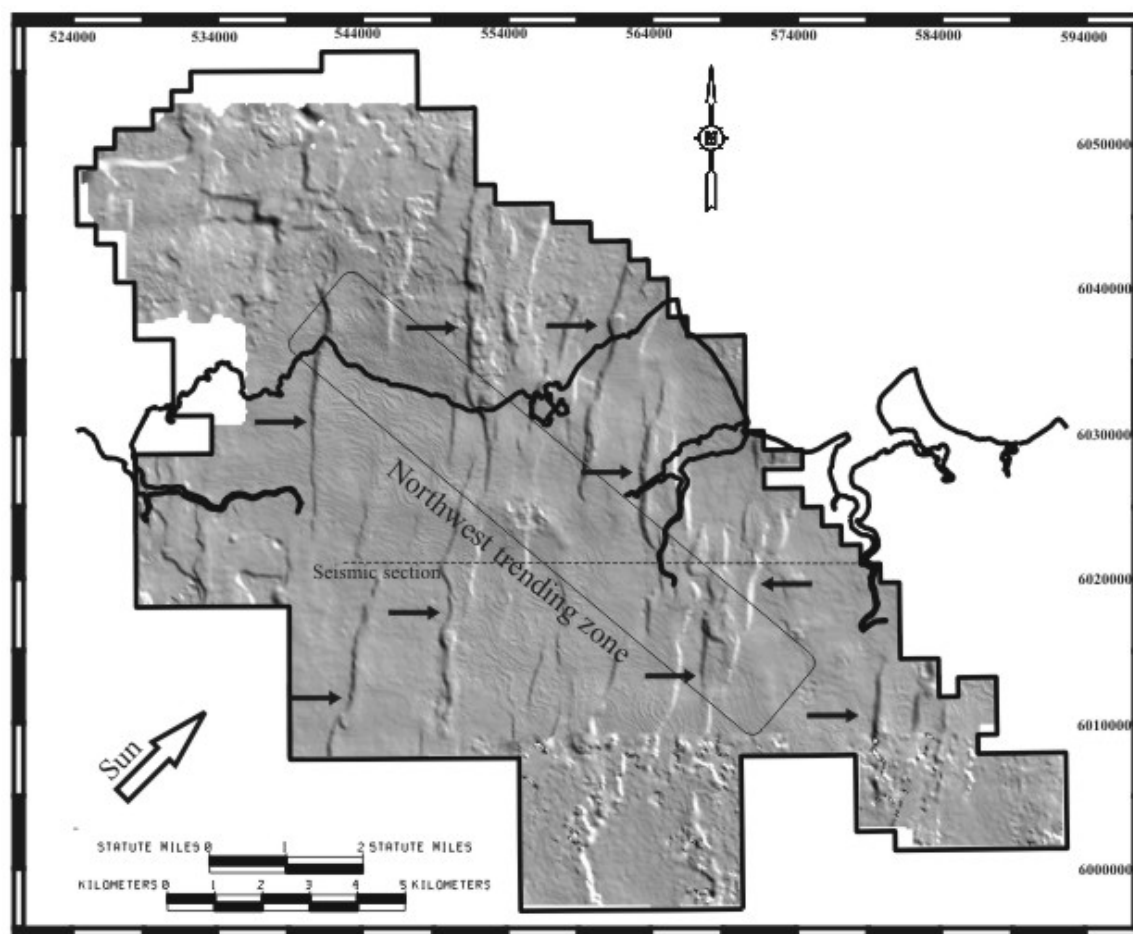


Figure 1: Shaded illumination map for the seismic horizon 34 surface. “Sun” direction is S45W with an altitude of 25 degrees. Note the strong north-northeast and more subtle northwest structural fabrics. Northwest trending zone referred to in text is indicated by the box. Arrows point to major “basin-bounding” faults that likely cut to current reservoir levels, interpreted by large throws, and through-going nature. Location of seismic cross-section (Figure 2) is shown by the dashed line.

- 1) The dominant structure in the shallow MPU (within the GHSZ) consists of steeply dipping normal faults that trend north–northeast with vertical offset ranging up to 400 ft (120m) as illustrated in figures 1-3. Throw values are used to calculate fault seal potential along horizons (Figure 2).

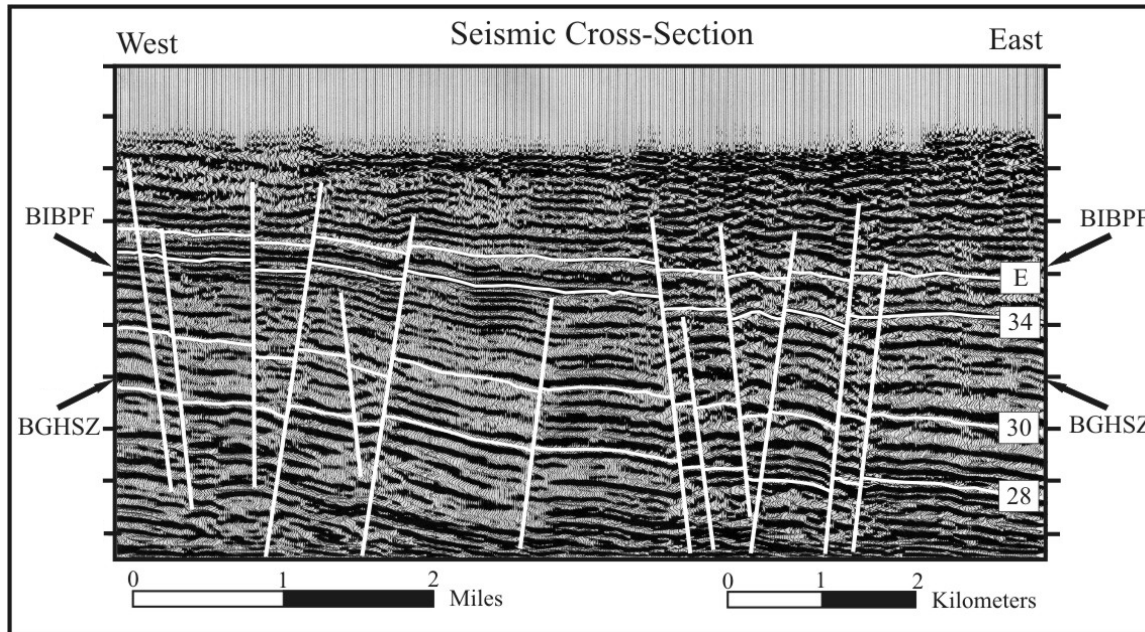
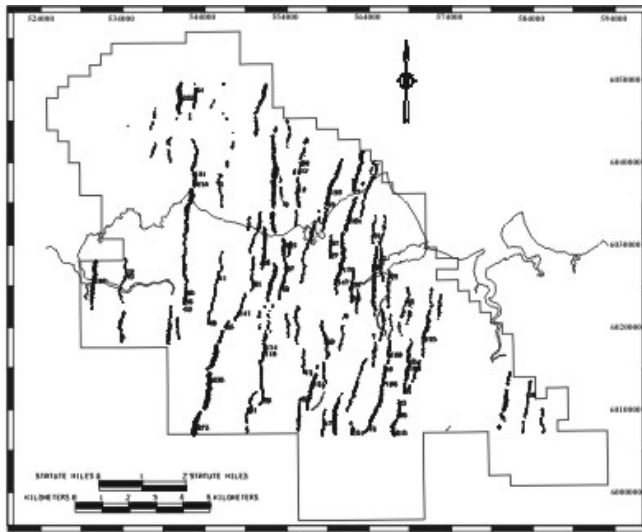


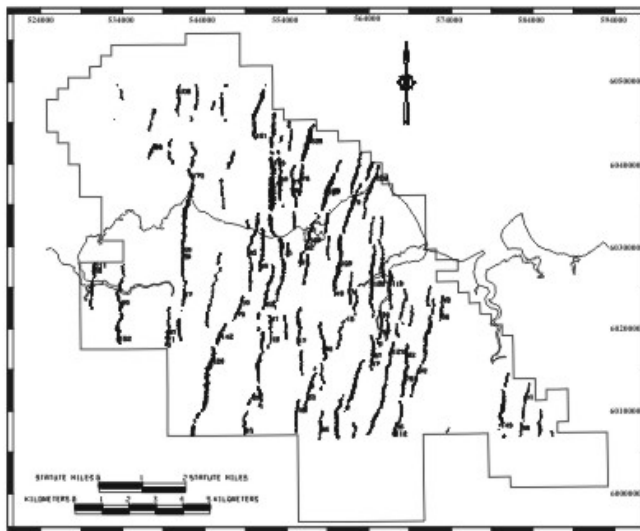
Figure 2: West to east seismic cross section (in milliseconds) of the wavelet processed Milne Point Survey; location is shown in Figure 1. Near vertical lines indicate seismically interpreted faults and near horizontal lines show four seismic horizons considered in this study: horizon 28, horizon 30, horizon 34, and Unit E. Approximate location of the base of the ice-bearing permafrost (BIBPF) and the base of the gas-hydrate stability field (BGHSZ) are shown with arrows.

- 2) In addition to the north–northeast trending structures, there is a subtle northwest-trending monoclinical structure that is directly above a large, production-level normal fault zone. Although no northwest-trending fault offsets are within seismic resolution in the shallow (<950 ms) data, this zone may consist of many small offset faults. This northwest trending zone is defined in shallow strata by a pronounced decrease in north–northeast-trending fault activity and is a dividing zone for two styles of shallow faulting and likely for gas hydrate distribution.
- 3) Interval fault growth calculations along all faults in the MPU show lateral and temporal variations in fault activity (figures 4-7 and Table 2). Fault activity generally shifts to the east with time.
- 4) Active faults are more prone to act as conduits for free gas, and also create accommodation space conducive to higher-energy, coarser-grained sedimentation. Both of these factors are favorable for accumulation of gas hydrate within reservoir sands. Seismic interpretation suggests gas hydrate distribution is concentrated in the eastern part of the MPU, which is consistent with the eastward temporal migration of fault activity.

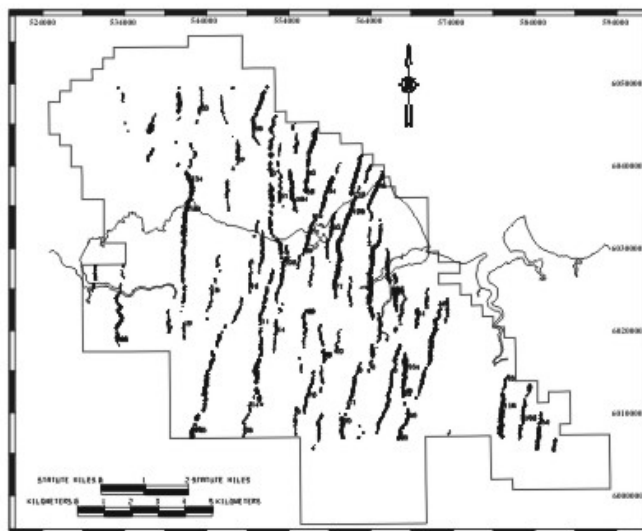


A

Figure 3. Fault throw (ft) calculated for all seismically interpreted faults in the MPU, along three stratigraphic intervals, horizon 28 (8A), horizon 30 (8B), and horizon 34 (8C). Width of faults corresponds to throw, the wider the fault, the larger the throw. Throw is annotated for various fault segments in feet. Note the change in lateral distributions with stratigraphic interval.



B



C

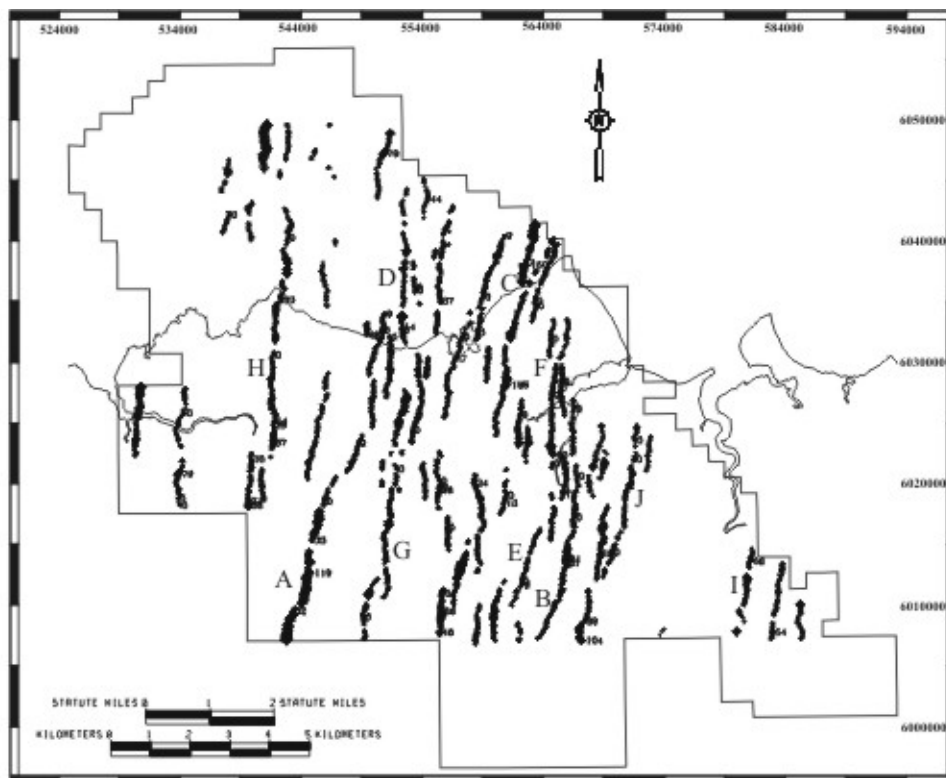


Figure 4. Fault growth for the stratigraphic interval between horizons 28 and 30. Thickest faults indicate highest growth values while thinner faults correlate to low growth values. Fault growth is annotated in feet for fault segments. Letter annotations refer to discussions of fault segments in Table 2. Fault growth is concentrated in the southwestern portion of the survey.

- 5) A modified algorithm for calculating clay smear potential (CSP_b) is more appropriate for exploration-type fault analysis. In the modified algorithm, clay smear is based on the following parameters: zone clay fraction, an assumption of evenly distributed thin shale beds through the faulted section, and fault throw.
- 6) Clay smear potential calculations in the MPU using the CSP_b algorithm produce relative values of fault seal potential for horizons that show lateral variations across the MPU. In general, faults with the highest seal potential are located northeast of the northwest-trending zone (Figure 8).
- 7) Direct seismic interpretation of thin gas hydrate-bearing intervals is complicated by a seismic tuning thickness close to gas hydrate-bearing reservoir thickness as well as by intermingled permafrost, which likely affects amplitudes. Supervised waveform classification on a wavelet processed, amplitude normalized 3-D seismic volume may mitigate these amplitude effects. Gas hydrate-similar waveforms, based on well-log interpretations, may delineate conservative estimates of gas hydrate distribution over USGS gas hydrate Units C, D, and E (figures 9-12).

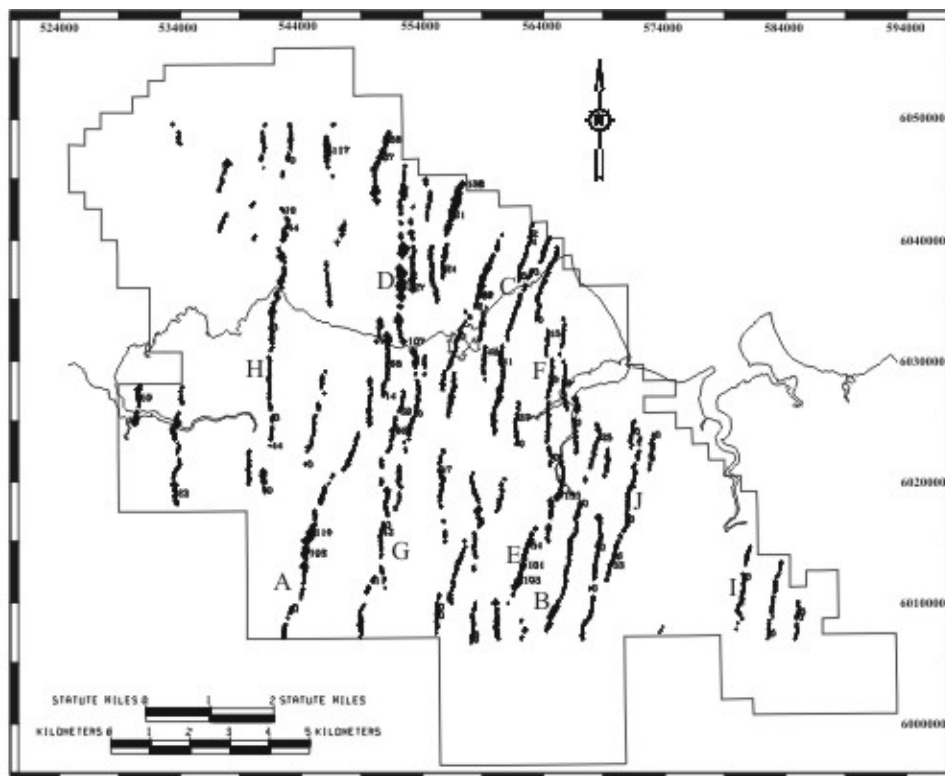


Figure 5. Fault growth for the stratigraphic interval between horizons 30 and 34. Thickest faults indicate highest growth values while thinner faults correlate to low growth values. Fault growth is annotated in feet for fault segments. Letter annotations refer to discussions of fault segments in Table 2. Fault growth is more distributed across the MPU than for interval 28-30.

- 8) Seismically interpreted gas hydrate distributions appear to be strongly controlled by north-northeast-trending faults, especially in the eastern MPU. This interpretation is consistent with trends observed in fault activity and fault seal potential. These results support a model in which thermogenic free gas began ~40 Mybp to migrate up active faults into the most permeable sand intervals, was subsequently trapped by sealing faults, and more recently (~2 Mybp) transformed into gas hydrate with regional depression of the geothermal gradient.
- 9) Several gas hydrate-bearing reservoirs are within hydraulic units defined in the eastern MPU, bounded by faults with high sealing potential, and represent prospects for potential production utilizing sublimation by depressurization.

5.6.2.2 Work in Progress

- Studying effects of permafrost on waveform classification.
- Incorporating revised MGE picks for BIBPF and gas hydrate stability base into seismic project.
- Continuing to revise supervised waveform classification based on gas hydrate and no gas hydrate waveforms as other interpretations are revised.
- Interpreting free gas near K-pad and Cascade.

- Tracking high-amplitude responses.
- Looking for up-dip extent into Milne Point 3D seismic survey.
- Creating amplitude scan on BGHSZ surface for free-gas interpretation.
 - Dependent upon receipt of improved surface from USGS or UA.
- Incorporating edits from BP and others into Hennes prepublication manuscript.
- Continuing work on poster for Hedberg conference.
- Cataloging work done to date and relevant Landmark files for smooth transition between Reflection Seismology students.
- Incoming Reflection Seismology student to visit USGS in Denver over summer in effort to help streamline communication between UA and USGS.

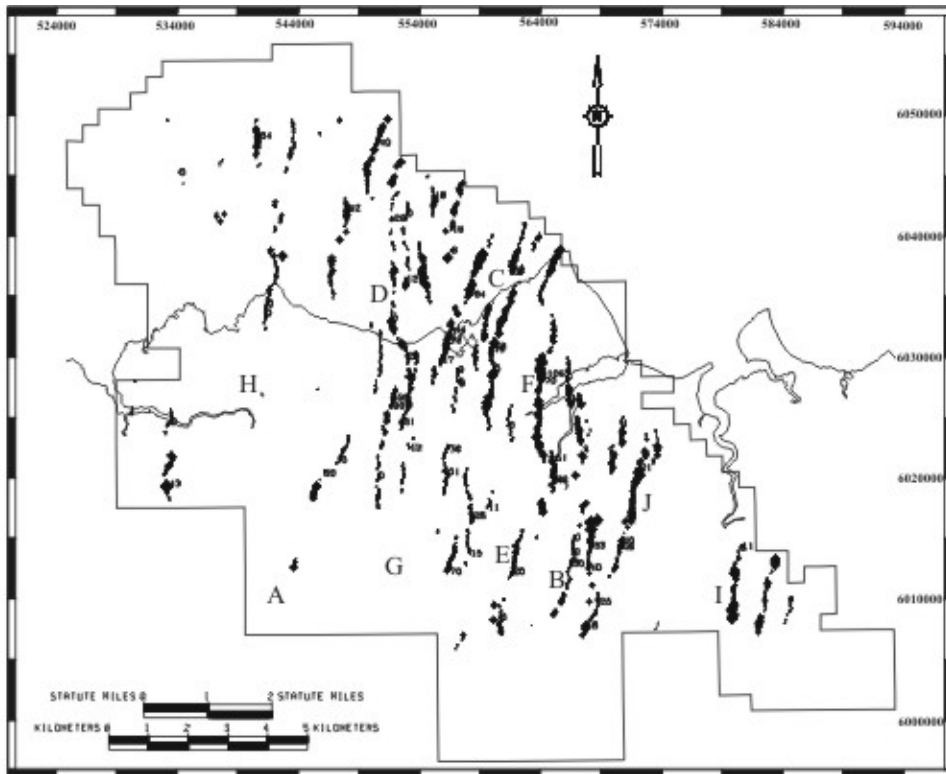


Figure 6. Fault growth for the stratigraphic interval between horizons 34 and E. Thickest faults indicate highest growth values while thinner faults correlate to low growth values. Fault growth is annotated in feet for fault segments. Letter annotations refer to discussions of fault segments in Table 2. Many faults tip out in this interval and growth is concentrated to the eastern and northeastern portions of the MPU.

Fault Activity		Interval 28-30 <i>(Figure 4)</i>		Interval 30-34 <i>(Figure 5)</i>		Interval 34-E <i>(Figure 6)</i>	
Interval Location		Deepest interval. Below GHSZ.		Middle interval. Straddles GHSZ.		Shallowest interval. Entirely in GHSZ.	
Fault Segment Activity	A	High	-	Moderate	-	None	
	B	Moderate	=	Moderate	-	Low	
	C	Moderate	-	Low	+	High	
	D	Low	+	High	-	Moderate	
	E	Low	+	Moderate	=	Moderate	
	F	Low	=	Low	+	High	
	G	Moderate	-	Low	-	None	
	H	Moderate	-	Low	-	None	
	I	Low	=	Low	+	High	
	J	Low	=	Low	+	High	
Comments		Most activity constrained on A in the SW.		Activity shifts NE up en echelon segments to D.		Activity concentrated on several faults NE of NW-trending zone.	
<p style="text-align: center;">Temporal shift in fault activity to the E-NE</p> <p style="text-align: center;">Activity concentrated on few faults Dispersed activity</p> <p style="text-align: center;">suggests change in near-surface stress regime</p>							

Table 2: Fault activity for three stratigraphic intervals (28-30, 30-34, 34-E) discussed in the text is detailed for fault segments: A, B, C, D, E, F, G, H, I, and J as seen in Figures 4, 5, and 6. Interval location refers to stratigraphic position in MPU. Fault segment activity is relative to each plot. Between each interval relative fault activity increases (+), decreases (-), or remains relatively constant (=). Comments refer to important features of the activity results discussed in the text.

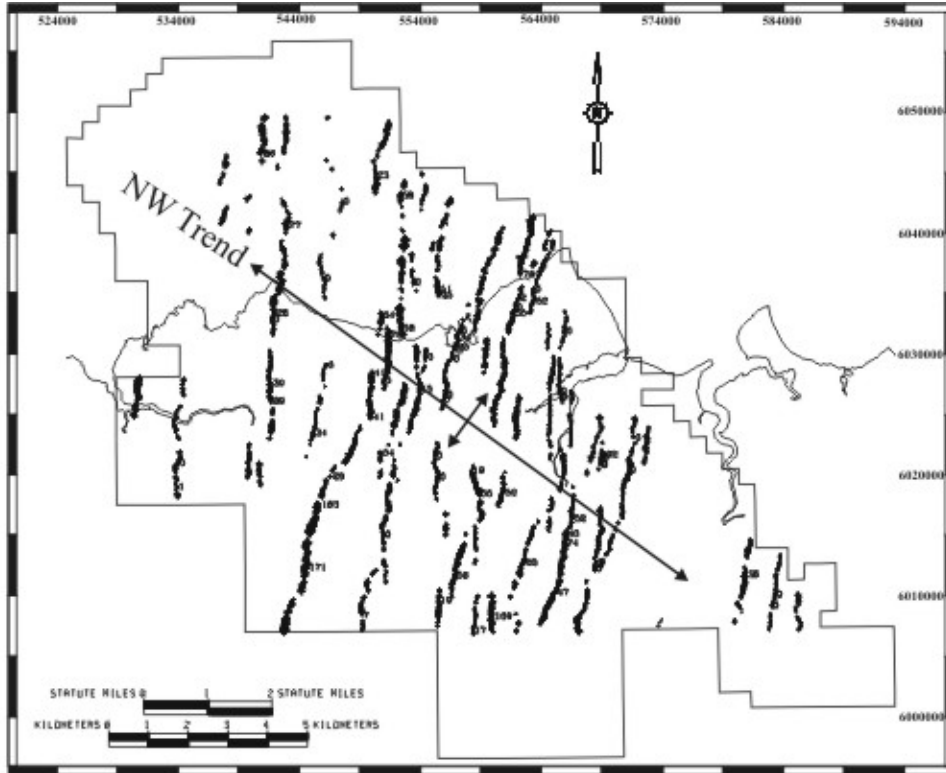
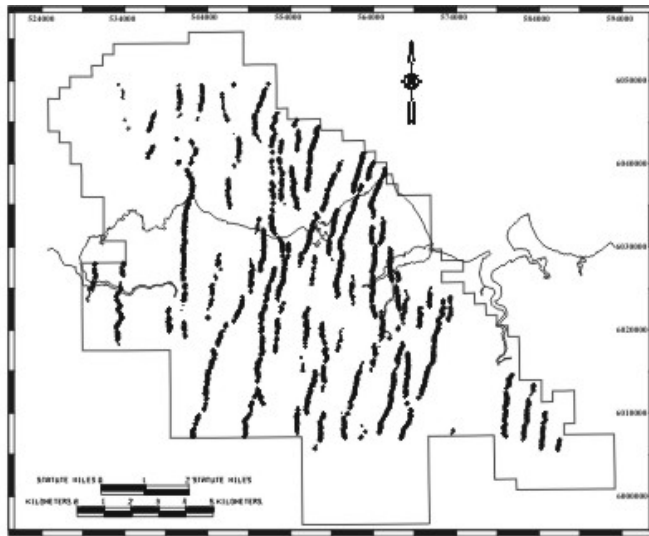


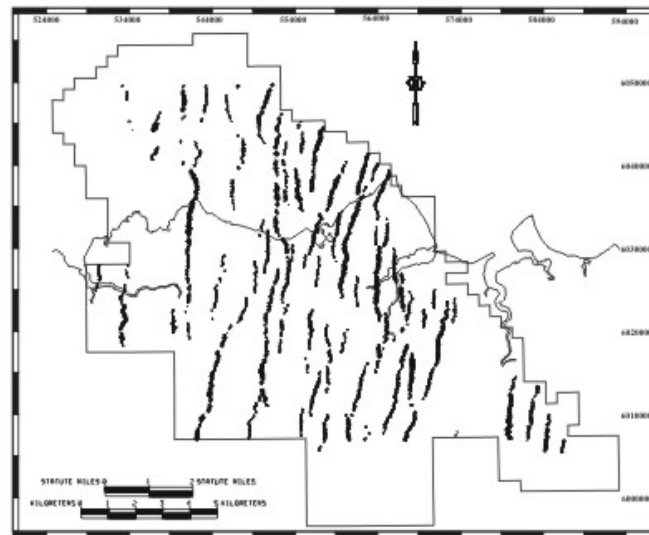
Figure 7. Fault growth for the stratigraphic interval between horizons 28 and 34, representing most of the GHSZ strata. Thickest faults indicate highest growth values while thinner faults correlate to low growth values. Fault growth is annotated in feet for fault segments. Lateral fault growth variations are compared in Figure 15. The northwest trend referred to in the text annotated as well as the direction orthogonal to this trend.

5.6.2.3 Future Work

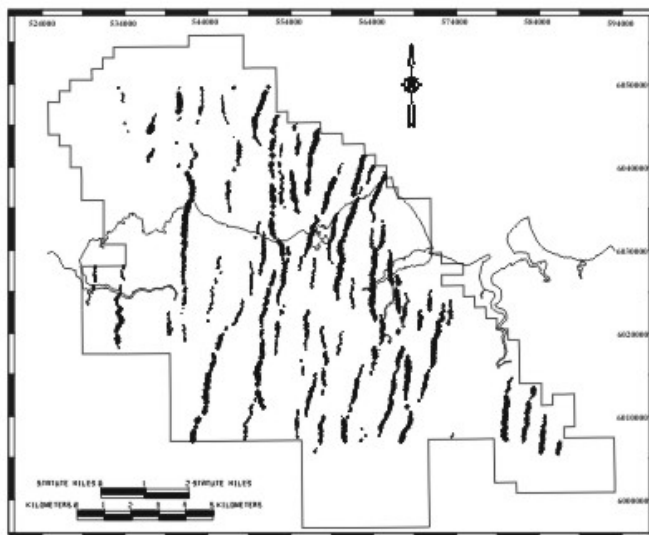
- Compare UA time-depth ties to USGS ties.
- Identify target areas for gas hydrate and perform highly detailed seismic interpretation, fault models, etc.
- Prepare for smooth transition into Phase 2 of project.
- Submit Hennes Prepublication to AAPG Bulletin.
- Participate in AAPG Hedberg Gas Hydrate Research Conference in September 2004.
- Complete processing on NW Eileen 3D survey to further increase Signal/Noise ratio.
- Interpret seismic horizons at top and bottom of hydrate-bearing intervals (if increased resolution allows) to yield better volumetric estimates.
- Continue search for associated free gas.
 - Rectify free-gas interpretations in Cascade well with NW Eileen 3D seismic survey
 - Track and tie this interpretation to Milne Point 3D survey.



A



B



C

Figure 8. Fault seal potential calculated for horizon 34 (Unit C gas hydrate) using three different methods. Thickness along a fault indicates the relative seal potential of the fault (thicker equals higher seal potential). Shale gouge ratio (SGR) results (A) show a homogenous distribution across the MPU, while clay smear potential (CSP) results show much lateral variation. CSPa results (B) and CSPb results (C) show similar lateral distribution. CSPb results are considered most the most realistic seal potential values for this study and are used in fault seal interpretations.

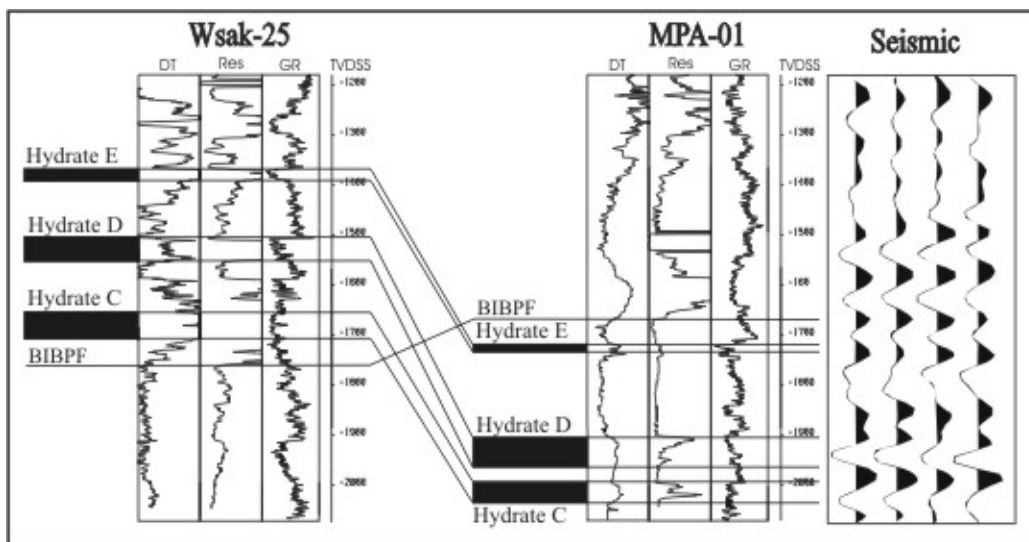


Figure 9. Well logs for wells Wsak-25 and MPA-01 (location in figure 10) including sonic (DT), deep resistivity (Res) and gamma ray (GR). Gas-hydrate inferences for three correlative units, gas-hydrate unit E, gas-hydrate unit D and gas-hydrate unit C (Collett, 1988), exhibit high velocities and high resistivities. Gamma-ray logs indicate that these gas hydrates occur in thin, sandy intervals. Note that the base of ice-bearing permafrost (BIBPF) crosscuts stratigraphy and may interfere with seismic response to gas hydrate. Seismic traces shown on right are scaled to the well logs, taken near the well bore of MPA-01, to show the qualitative resolution of the data and the waveform response to gas-hydrate-bearing intervals. Well units are total vertical depth sub-sea level (TVDSS).

- Obtain GIS information from North Slope, if possible, to correlate surface features to anomalous events in the 3D seismic data. Possible questions:
 1. Do lakes occur over gas chimney's?
 2. Do lakes thin permafrost, thus affecting shallow statics and time/depth conversion?
 3. Do lakes/rivers/surface features trend with faults?
 4. Did lakes/rivers affect acquisition and statics that may explain areas of anomalous seismic data?
- Obtain raw shot gathers (from BPXA) for additional processing, if available.
- Obtain cubes (from BPXA) for AVO analysis, if available.
- Obtain deeper data to complete more comprehensive fault analysis, if available.

5.6.3 Subtask 6.3: Petrophysical and Neural Network Attribute Analysis – UA

5.6.3.1 Products

- Worked iterations of the UA log-based expert system and associated algorithms that classify fluid saturations, estimate confidence levels, and predict coal occurrence.
 - Evaluated results and compared to manual-derived occurrences in wells (e.g. gas hydrate in NWEillen, Mallik well free-gas in MPK-38, Cascade-01, Kup. St. 1, WETW, etc).

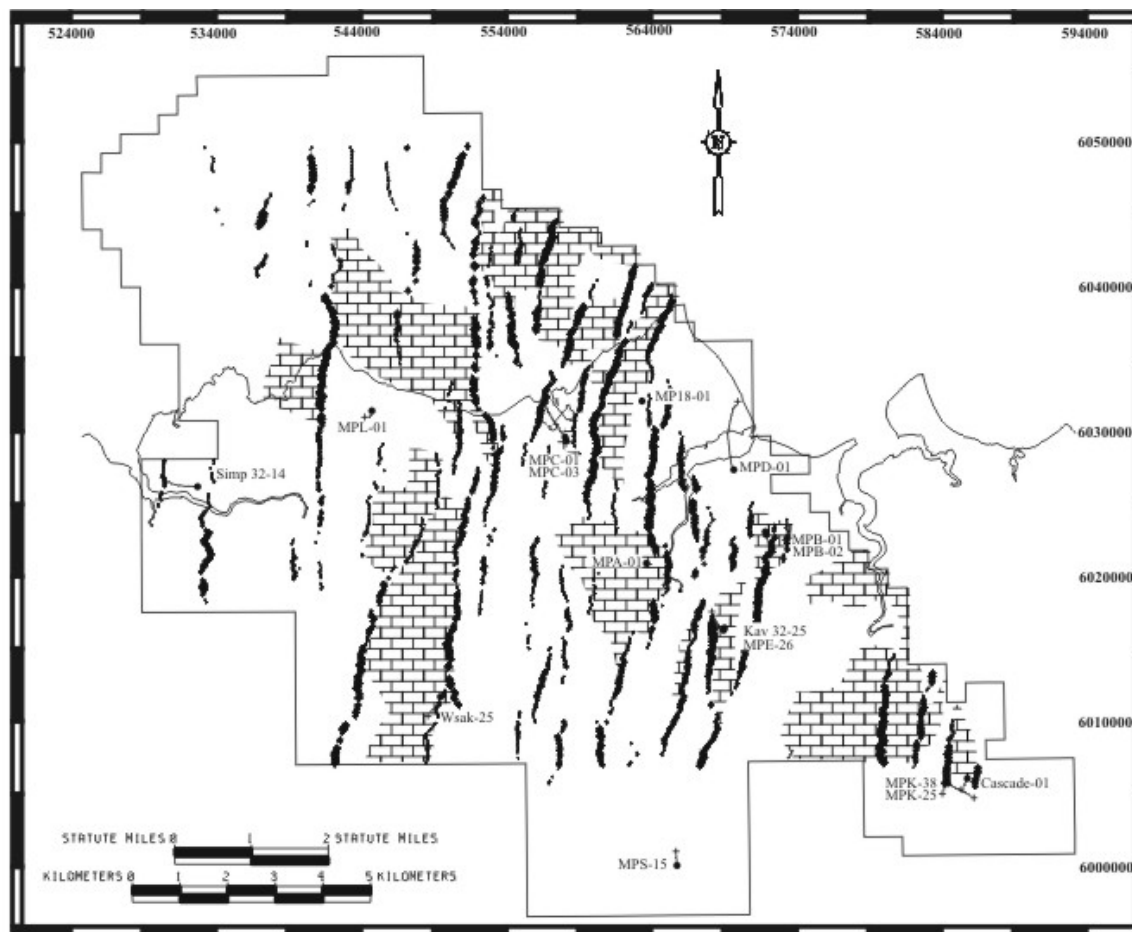


Figure 10. Results of supervised waveform classification along the Unit C gas-hydrate interval (Figure 9). Brick pattern indicates gas-hydrate-similar waveform classes based on well-log-interpreted occurrences. The blank areas indicate waveforms that are similar to those near non-hydrate-bearing wells and waveforms that did not fit into any class, based on the defined threshold values. Fault thickness indicates fault seal potential calculated for horizon 34 (Unit C) using the CSP_b method (thicker equals higher seal potential).

- Determined velocity and resistivity response for interpreted water-saturated zones.
 - Applied low-pass filters to curves to smooth out transitions.
- Completed auto-identification of coal-bearing units.
- Assessed influence of caliper log-derived borehole condition on expert system.
- Better explained fluid saturation confidence and probability.
- Determined limitations of USGS Lee equation method.
- Trained a neural network to predict gas hydrate, free gas, coal, clean sand, and water saturation components within reservoir sands from well log signatures.
 - Used only small samples from each well for training.
 - Currently using gamma, resistivity, and sonic logs for training.
 - Wells currently used to provide training examples are MPA01, MPB01, MPB02, NWEileen2, WSAK25, WSAK24, WSAK17, MPK38, 3K06, KupSt01, WETW and Cascade01.

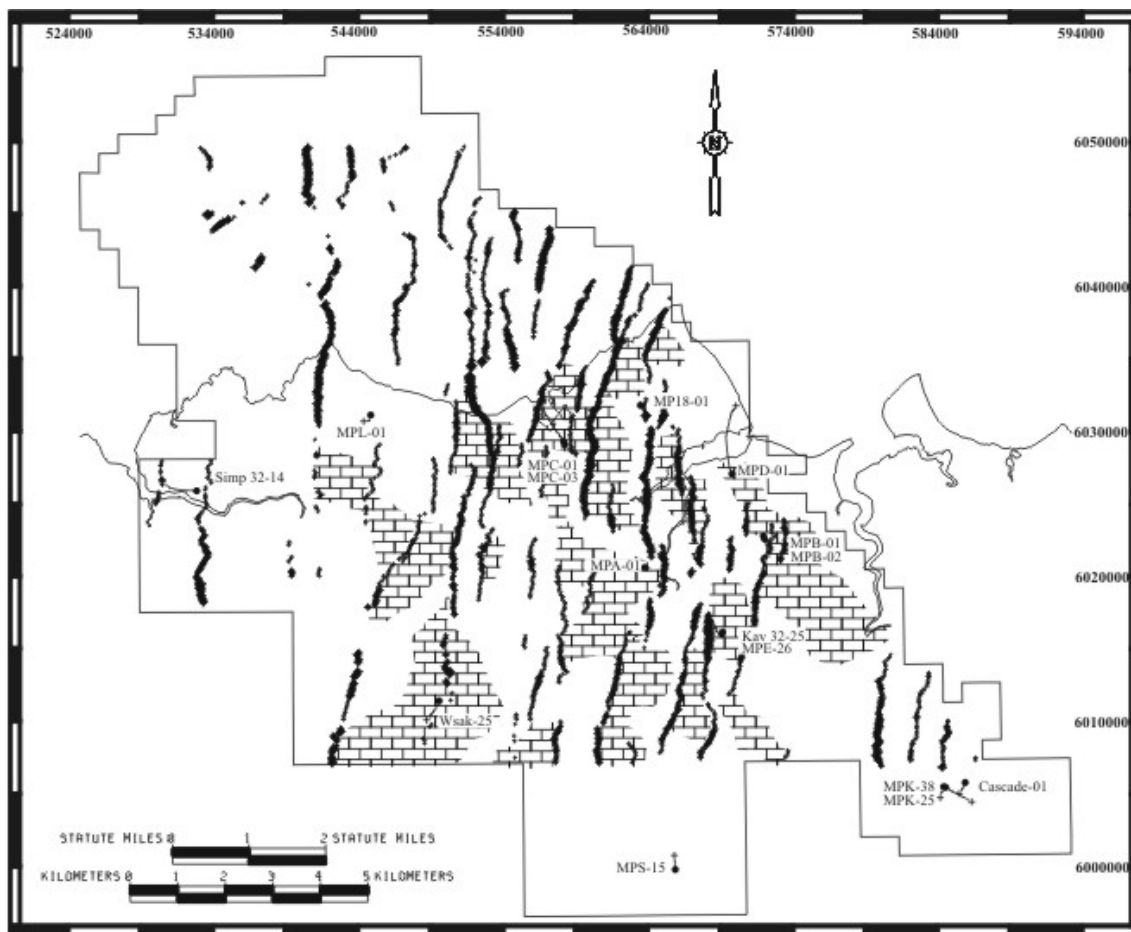


Figure 11. Results of supervised waveform classification along the Unit D gas-hydrate interval (Figure 9). Brick pattern indicates gas-hydrate-similar waveform classes based on well-log-interpreted occurrences. The blank areas indicate waveforms that are similar to those near non-hydrate-bearing wells and waveforms that did not fit into any class, based on the defined threshold values. Fault thickness indicates fault seal potential calculated for the Unit D horizon using the CSP_b method (thicker equals higher seal potential).

5.6.3.2 Work in Progress

- Refining the neural network to ensure good examples used for training.
- Analyzing automated fluid prediction in light of poor log sections and washouts.
- Investigating the potential contribution of in situ coalbed methane (CBM) to the gas component below the gas hydrate stability zone.
 - A volume typical of CMB contributions can be as much as 60 times that of a gas-filled reservoir sand.
 - A volume typical of gas produced from dissociation of gas hydrate can be as much as 160 times that of a gas-filled reservoir sand.

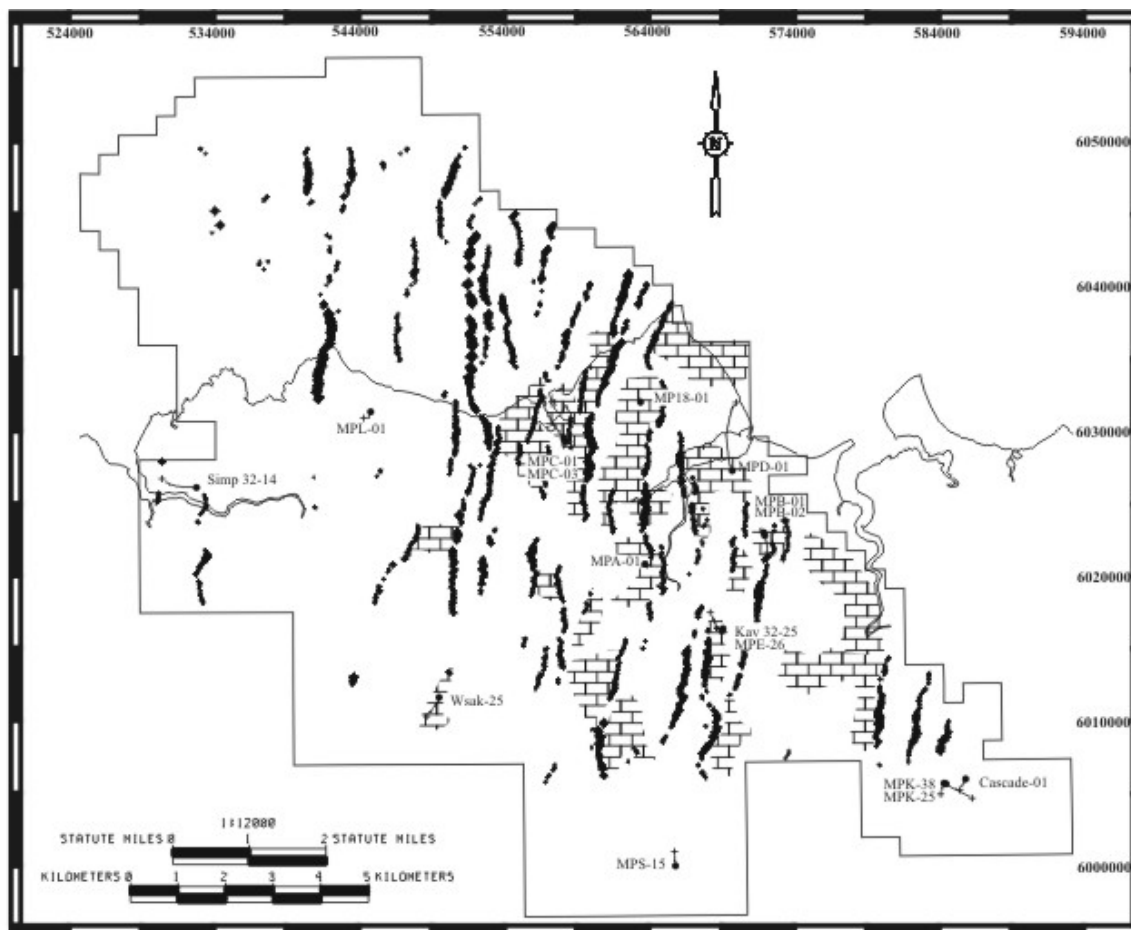


Figure 12. Results of supervised waveform classification along the Unit E gas-hydrate interval (Figure 9). Brick pattern indicates gas-hydrate-similar waveform classes based on well-log-interpreted occurrences. The blank areas indicate waveforms that are similar to those near non-hydrate-bearing wells and waveforms that did not fit into any class, based on the defined threshold values. Fault thickness indicates fault seal potential calculated for horizon E using the CSP_b method (thicker equals higher seal potential).

5.6.3.3 Future Work

- Test neural network with complete logs from all the wells in the study area when initial training results are satisfactory.
- Use neutron porosity and density logs (although less abundant) for training purposes to better distinguish coals from thin gas-bearing sands.
- Once training is completed, correlate the network results with the expert system results developed by Glass and Casavant.
 - Corroborate results from the two methods and determine if they provide a rapid way to identify potential pay zones in well logs.
 - Tie potential pay zones identified with a higher degree of confidence to the seismic data to improve interpretation of the seismic volume.
- Initiate log-based and seismic-base predictors for facies classification to begin in the fall.
- Evaluate method for identifying potential intra-permafrost gas hydrate zones due to disassociation of gas from gas hydrate during and after drilling operations.

5.7 TASK 7.0: Lab Studies for Drilling, Completion, and Production Support – UAF

University of Alaska Fairbanks

UAF Principle Investigator: Shirish Patil

UAF Co-Principle Investigator: Abhijit Dandekar

UAF Participating Scientists: David Ogbe, Godwin Chukwu and Santanu Khataniar

UAF Research Professional: Narender R Nanchary

UAF Graduate Students: *Jason Westervelt, Stephen Howe*, Namit Jaiswal, and Prasad Kerkar

UAF Undergraduate Student Assistant: Phillip Tsunemori

5.7.1 Subtask 7.1: Characterize Gas Hydrate Equilibrium

No further work was accomplished for this task during the reporting period.

Errata: The prior quarterly technical report #6 (January 2004 – March 2004) incorrectly attributed research to subtask 7.1 which should have been attributed to subtask 7.2, Relative Permeability studies.

5.7.2 Subtask 7.2: Relative Permeability Studies

5.7.2.1 Experiment Setup and Apparatus

The re-designed and modified experimental apparatus was used to first form synthetic gas hydrate and then measure relative permeability across these cores by the unsteady state method. Figure 13 is the schematic of the experimental setup to perform flow experiments either by re-circulating the fluids, or by flowing them through the core only once. Temperature of the core holder is maintained by circulating propylene glycol as coolant. The ISCO syringe pumps were used for saturating core with water, whereas top down gas injection was carried out using the gas cylinder under pressure. The re-circulator chiller was used to maintain the temperature of system. A backpressure regulator maintains a fixed downstream pressure to avoid gas hydrate dissociation. The dilute propylene glycol maintained confining pressure. The production of gas and water from the specimen as function of time is monitored using a mass flow meter and balance.



Figure 13: The experimental set-up picture constructed for forming gas hydrates and measuring relative permeability

5.7.2.2 Experimental Procedure

The gas-water relative permeability functions of two different partially hydrate saturated sediment (cores) systems have been studied. The measurements were conducted on both the Oklahoma 100 mesh sand as well as the re-saturated field sample from the Anadarko Hot Ice #1. The methane hydrate saturation, S_h in these samples was varied in the range of 5 to 30%. The effective permeability and relative permeability data for these two hydrate saturated cores are presented.

Cores were prepared by consolidating sand or mud samples obtained from the Anadarko Hot Ice #1 shallow non-gas hydrate-bearing cores. The dry weight of sand was measured and length of core inside the core holder was noted. The core is consolidated between the two distribution plugs. Overburden of around 150-200 psi was applied to maintain the high porosity of the core plug. The consolidated core is then flooded with water at low rates to completely remove air from the core. Approximately 10-15% pore volume of water is used to saturate the core plug.

5.7.2.2.1 Hydrate Formation in Core Holder

Gas hydrate formation and stability was a crucial and important aspect of this experiment. After trying several different techniques, the described technique was found to be successful in performing further displacement experiments. Saturated consolidated core was closed from both ends and overburden pressure was increased to approximately 1200 psig. This ensured the same initial pore volume. The valve leading to the upper distribution plug was opened to high pressure methane (approximately 900 psig), creating high pore pressure inside the core. After this, the ISCO pump was set to refill mode to collect a predetermined amount of water from the core. The amount of water collected determines the gas hydrate saturation in the core plug. Next, the pump was switched off and the temperature of core holder was reduced to approximately 1.5° C. The temperature ramping rate was around 5-6° C/hour. This temperature is just above ice formation temperature (around 30° F) at high pressures. This facilitated the gas hydrate formation (gas hydrate formation is a cold temperature reaction) and avoided ice formation. Apart from the above method, gas hydrate formation was also attempted using frost and sediment. This alternate method was not efficient and the time required for complete conversion was excessive. Moreover, the bulk gas hydrate formation was not initiated after some surface reaction in frost.

5.7.2.2.2 Single Phase Flooding

Gas and water flooding was carried out to measure the effective permeability for each gas hydrate saturation. This was an important step and required careful monitoring of gas flow rate. First, gas flooding was accomplished for a differential pressure of approximately 300 psi. The backpressure was around 540 psi and it provides a crucial role to prevent any dissociation of gas hydrates due to differential pressure.

Gas flooding was carried out to remove any free water during gas hydrate formation. Mobile water was collected in the vessel and monitored using electronic balance. The gas hydrate saturation value was determined using material balance for water (volume expansion for water to hydrate is 26%). The gas flooding was performed for around 5-8 hours. Due to permeability reduction the flow rate of gas was significantly small.

Water flooding was achieved at a constant flow rate (approximately 0.30 ml/minute) with backpressure of approximately 540 psi. Cold water (T= 5° C) was injected from the bottom of the core, displacing the excess and free gas in the core plug. Low temperature and water flow rate retarded the gas hydrate dissociation. Gas hydrate dissociation was closely monitored using a gas flow meter. A sudden increase in flow rate of gas from the core plug indicated the dissociation of gas hydrates in core plug. Water from the core plug accumulated in a collection vessel as shown in the schematic (Figure 14). Volume was monitored by electronic balance. The difference between the injected and collected water amount was used to calculate the porosity of the porous medium in the presence of gas hydrate.

5.7.2.2.3 The Displacement Experiment

After measuring the effectively permeability of the core to water, cold methane gas was injected at a constant differential pressure of 310 psi for primary drainage displacement. The injection continued for about 10 to 12 hours, at which time the flow of water becomes almost zero and the flow rate across the core had stabilized. The cold methane gas was also injected at a constant flow rate in some experiments and injection maintained for 10 to 12 hours, at which time the fractional flow of water becomes almost zero and the pressure drop across the core had stabilized.

In order to confirm that gas hydrates were not lost during the experiment in the core, the lower valve (Figure 14) was closed and the temperature of system was increased. The upper valve was opened to the methane cylinder and the volume change in the cylinder was monitored. As the temperature reaches approximately 8-9° C, there is a sudden increase in the volume of the cylinder at approximately 1200 minutes (Figure 15), indicating dissociation of gas hydrates. This reaction confirmed the presence of gas hydrate in the core during the displacement experiment. After completion of the experiment, the core holder was dismantled and the weight of sediment was measured. The increase in weight of sand from initial dry weight was adjusted for an irreducible water saturation value.

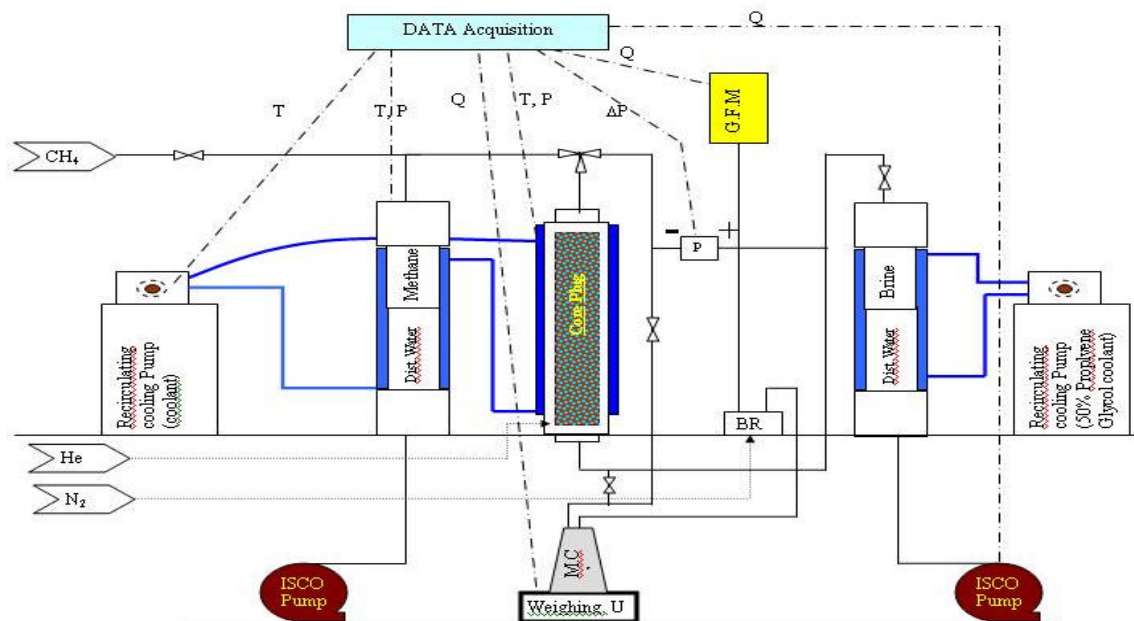


Figure 14: Schematic of laboratory apparatus for measuring relative permeability (Jan 2004).

5.7.2.3 Experimental Results

Gas hydrate can be created in a variety of ways in the laboratory. It can be formed in bulk or in a porous media. However, it is presently unclear which laboratory methods and facilities produce results that accurately simulate in-situ conditions, such that measured properties can be used to model geologic settings. Natural conditions may form gas hydrate more slowly than many laboratory techniques.

5.7.2.3.1 Gas Hydrate Formation Analysis

Gas hydrate formation and dissociation was monitored by the constant pressure (pore pressure) and constant volume (Methane cylinder) method and the results are presented in Figures 15-16. For the constant pressure (726 psia) case, the dissociation pressure was 7.5° C, similar to that reported by Westervelt (2004). Results confirmed that gas hydrate did form within the core holder.

The cell was cooled while maintaining constant pressure via a regulating valve. The temperature ramping for gas hydrate formation was around 4-5° C/hour and kept at 1° C for 6-10 hours. After gas hydrate formation was complete, the cell temperature was increased and the plateau in pressure/volume of methane cylinder reappeared due to gas hydrate dissociation. The changes were rapid, indicating rapid gas hydrate dissociation.

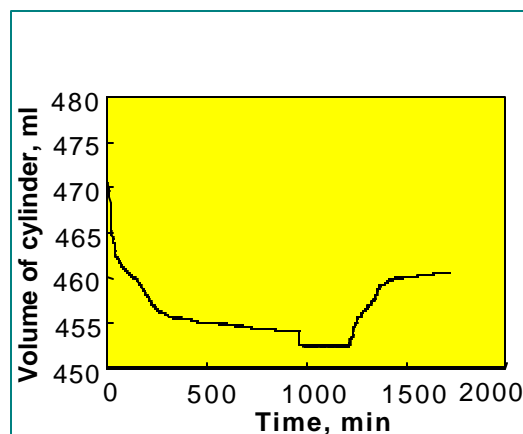


Figure 15: Volume change in methane cylinder (726 psi) confirms gas hydrate dissociation

5.7.2.3.2 Permeability Discussion

The effective permeability results were plotted for gas flow through gas hydrate-bearing porous media formation. The results were compared with Mehrad's (1989) work (Figure 17). Mehrad conducted his experiment in unconsolidated medium (without any confining pressure), resulting in a higher value for permeability.

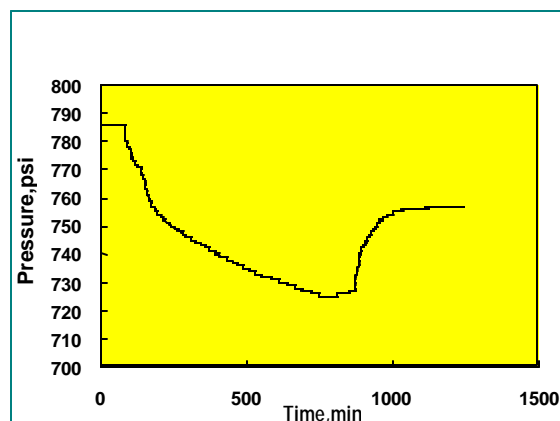


Figure 16: Pressure decline confirms gas hydrate formation.

The relative permeability was calculated using the JBN method for data reduction. Figure 18 displays relative permeability for various gas hydrate saturation values (irreducible water saturation of 0.12.).

Relative permeability and effective permeability for gas hydrates in porous media (coarse sand) was measured for three gas hydrate saturation values. For higher gas hydrate saturation values, there is a considerable change in relative permeability. This might be attributed to the distribution of gas hydrates in the core (i.e. for water flow there might be grain rearrangement in structure and an observed difference in relative permeability). There was no significant change in absolute permeability, probably due to a similar distribution of gas hydrates in the sand (likely cementing the core).

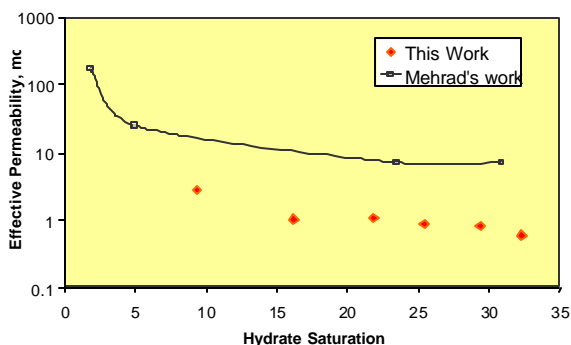


Figure 17: Effective permeability for various gas hydrate saturation values

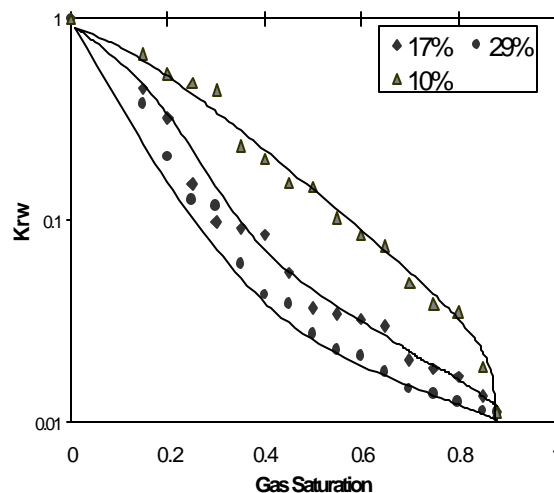


Figure 18: Relative permeability curves for various hydrate saturation values (S_h % = 10, 17, 29).

5.7.2.3.3 Quarterly Results

Several experiments were conducted in this quarter. Results indicate that key factors for successful synthesis of methane hydrate in porous media appear to be highly dependent on those aspects that influence the availability, mass transfer, and concentration of gas-hydrate forming species at the growth front. These factors include elevated pressure conditions, and a high surface-to-volume ratio of the reacting grains to minimize the thickness of the developing gas hydrate layer through which the reactants must pass. Low surface to volume ratio of porous media and insufficient rate of heat transfer may result in unstable gas hydrates, which may dissociate during water injection. Therefore, type of porous media and conditions used to form gas hydrate may play a crucial role in determining type of gas hydrate interaction with a porous media (pore filling, pore coating etc). Under certain circumstances, areas of localized lower pore pressure correspondingly affect physical properties. Typically, formation of natural gas hydrate within permafrost will decrease effective permeability more than formation of gas hydrate beneath permafrost. This decrease in effective permeability may enable differentiating areas that contain a combination of permafrost and gas hydrate from sub-permafrost gas hydrate.

Lab methods can derive different relative permeability results than those in porous media within natural field conditions and much variation exists in the properties of sediment (for our case Anadarko field samples) that contain natural gas hydrate. For example, in nature, efficient transport of free gas in faults can bypass surrounding sediments. Where a fault intersects a layer of coarse sand beneath a permeability barrier, the gas can spread horizontally to produce a hydrate horizon within the gas hydrate stability field. In the case of gas hydrate formation from

low fluxes of dissolved methane, growth habit and corresponding permeability reduction remain an open question (Nimblett and Ruppel, 2003). Results in this study are related to situations in which water in medium to coarse sediments is exposed to free methane in which gas hydrates can later form within the largest pore spaces. As a result there can be a non-uniform (or zonation) of gas hydrate saturation in the porous media, as shown in Figure 19. Moreover, in consolidated media sediments such growth habit can lead to rapid permeability reduction (compared to no gas hydrate saturation) and capillary sealing with respect to free gas. Thus, disseminated gas hydrates in a natural system can be self limiting for fluid flow.

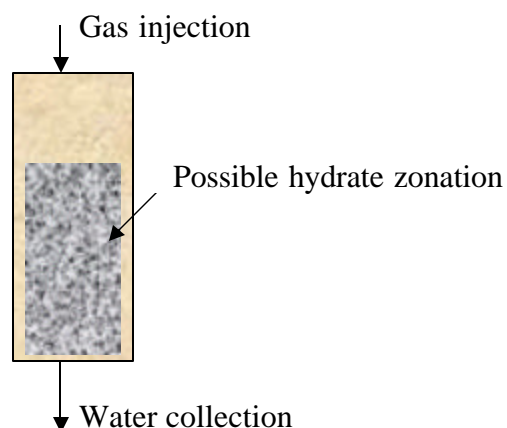


Figure 19: Possible gas hydrate zonation in the sample

The results presented in figures 20 and 21 show that the effective permeability of unconsolidated cores that are partially saturated with gas hydrates, generally tends to decline as gas hydrate saturation increases. The decreasing effective permeabilities, however, do not follow any particular decline or trend.

Thus, the effective permeability is not only a function of gas hydrate saturation, but also of the type of gas hydrate formation, grain structure and gas hydrate distribution within the porous media. Moreover, a small amount of clay sediment or a small change in water content can also significantly influence effective permeability. Every time the gas hydrate saturation increases, it may result in a new porous media with unique permeability characteristics.

Figures 20 and 21 show that the core samples have reduced effective gas permeability compared to effective water permeability. Similar observations were recently made by Kleinberg et al., 2003. The solid gas hydrates are not expected to move under any reasonable pressure gradient and gas hydrate can be thought of as an immobile phase, which offers additional resistance to fluid flow. Hence, effective permeability decreases as saturation increases. Growth of gas hydrates in the largest pore structures permits rearrangement of mineral grains and leaves connected water paths through the sediment. These are the conditions required for the growth of gas hydrate nodules and lenses. Water permeability is expected to be more than gas permeability, which was confirmed in this study. Moreover, the water injection and pressure gradient may cause some dissociation and perhaps rearrangement of gas hydrates, leading to gas production and also an increase in permeability for water compared to gas. During displacement, the possibility of the restructuring of gas hydrates cannot be ruled out, leading to significant reduction in effective permeability to gas.

The relative permeabilities of formations that characterize the flow of water and gas also depend crucially on how gas hydrate forms within the pore space of the sediment. The sample results for relative permeability measurement for the Anadarko fields sample are presented in Table 3 and in Figure 22. These experiments were carried out at low temperature (like field conditions) at

very low flow rates to preclude the possibility of extensive gas hydrate dissociation. Relative permeability values in this study vary over a wide range with gas hydrate saturation. It is well known that gas is non-wetting and is thus “pore filling” as opposed to “pore coating”. Therefore, another reason for the observed wide range may be as gas saturation increases (crossing some critical value) in presence of water and gas hydrates there is some possibility of nucleation of gas hydrates, which may result in a change in pore structure. At present, nucleation phenomenon of gas hydrates in presence of porous media is still topic of research.

However, in order to better understand the effect or impact of gas hydrate saturation on gas–water relative permeabilities, plots of gas hydrate saturation versus relative permeability for iso-gas saturation were also constructed. These results are shown in figures 22-26, which includes both the Oklahoma 100 mesh sand sample and the Anadarko field sample. As seen in figures 22 and 23, the water relative permeabilities demonstrate a rather well defined trend of decreasing relative permeability with increasing gas hydrate saturation. A similar trend is also seen for the gas relative permeability in the case of the Anadarko field sample, i.e. K_{rg} values decrease with increasing gas hydrate saturation. However, much data scatter is observed in the Oklahoma 100 mesh sand sample. The results plotted in figures 22-25 would be somewhat analogous to comparing the relative permeability characteristics of different porous media, with an additional phenomenon of gas hydrates offering further increased resistance and generally reducing the relative permeabilities. A possible explanation for this observed behavior of gas relative permeabilities as a function of gas hydrate saturation could be attributed to rock properties such as pore size distribution and wettability characteristics and also be attributed to the distribution of gas hydrate saturation within the pore space. However, considering the limited amount of data, at this stage, it is not possible to offer a sound theoretical explanation as to precisely why the scatter in K_{rg} as a function of gas hydrate saturation is seen only in the case of the Oklahoma sand sample. When additional samples and data are available, it may be possible to rule out some of the variables mentioned above.

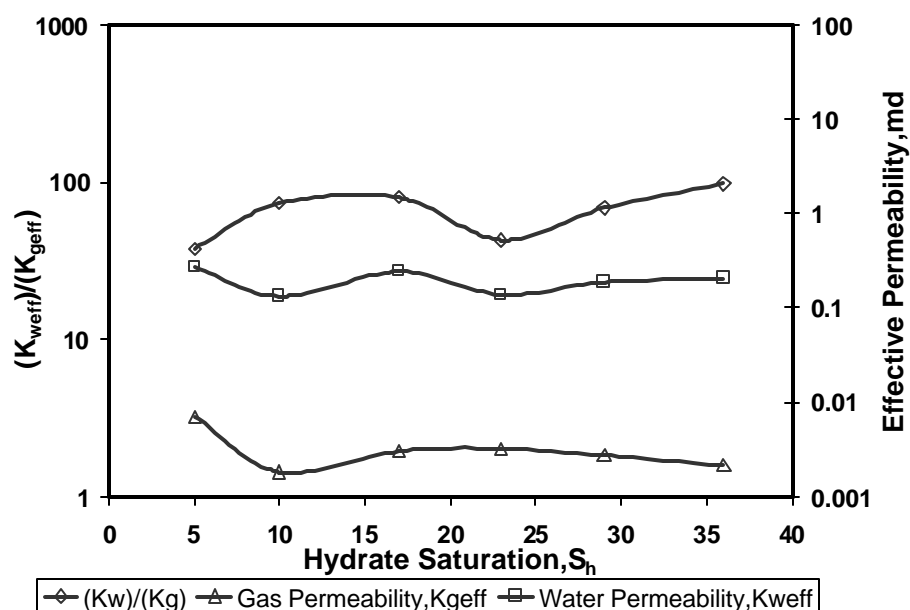


Figure 20: Ratio of effective permeability to gas and water for different hydrate saturation values for the Oklahoma 100 mesh sand samples

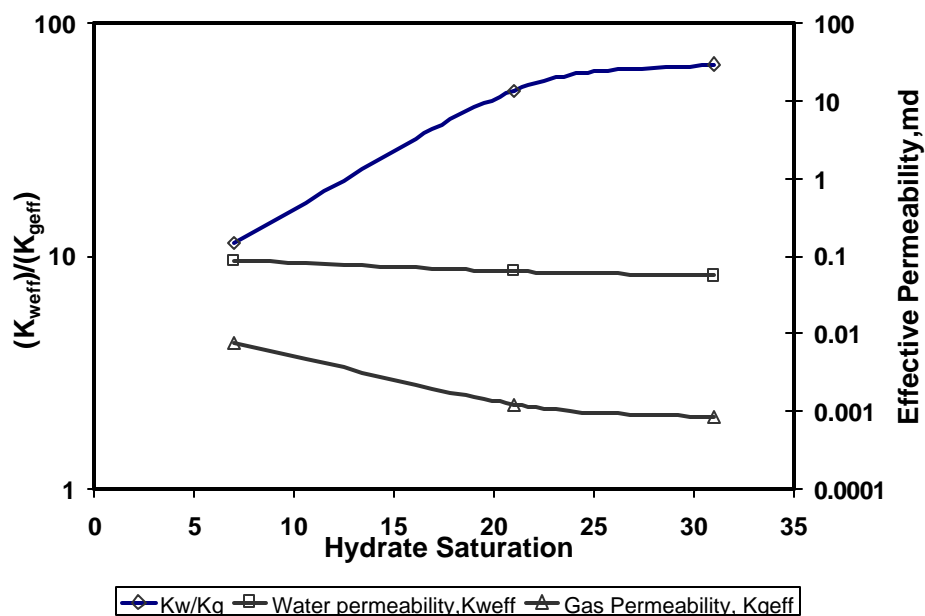


Figure 21: Ratio of effective permeability to gas and water for different hydrate saturation values for the Anadarko field samples

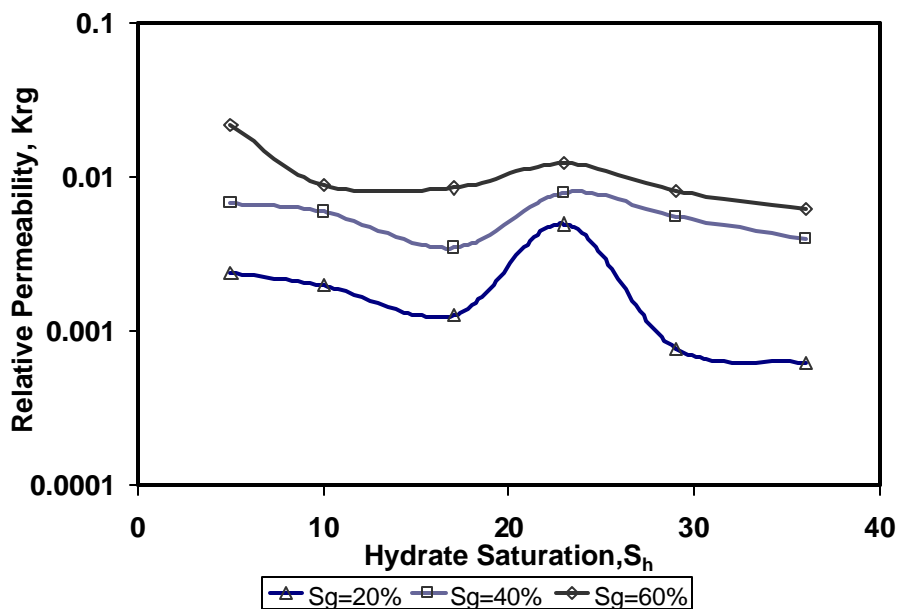


Figure 22: Gas relative permeability data at different hydrate saturation for Oklahoma 100 mesh sand sample.

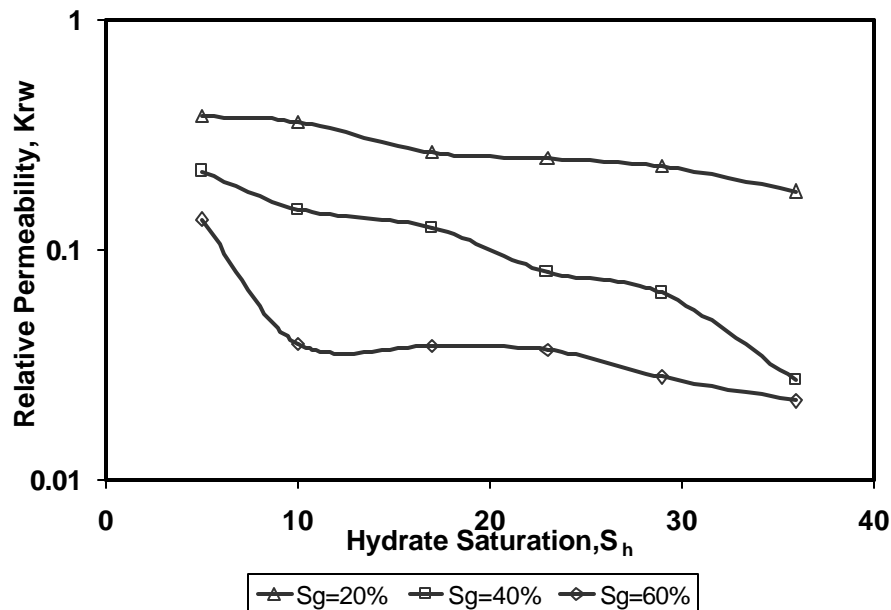


Figure 23: Water relative permeability data at different hydrate saturation values for Oklahoma 100 mesh sand sample.

Table 3: Basic data for gas-brine (2%) relative permeability measurements at 7 % hydrate saturation for Anadarko field sample.

Dimensions of core sample		
Length, in	5.5	
Diameter, in	1.5	
Differential pressure data for effective permeability		
	WATER	GAS
Inlet Press, P_i , psi	940	900
Outlet Press, P_o , psi	800	800
Confining Pressure, psi	1200	
Porosity and Permeability		
Porosity, Φ	0.119	
	Water	GAS
K_{eff} , md	0.0887	0.00742
K_{abs} , md	20.0	

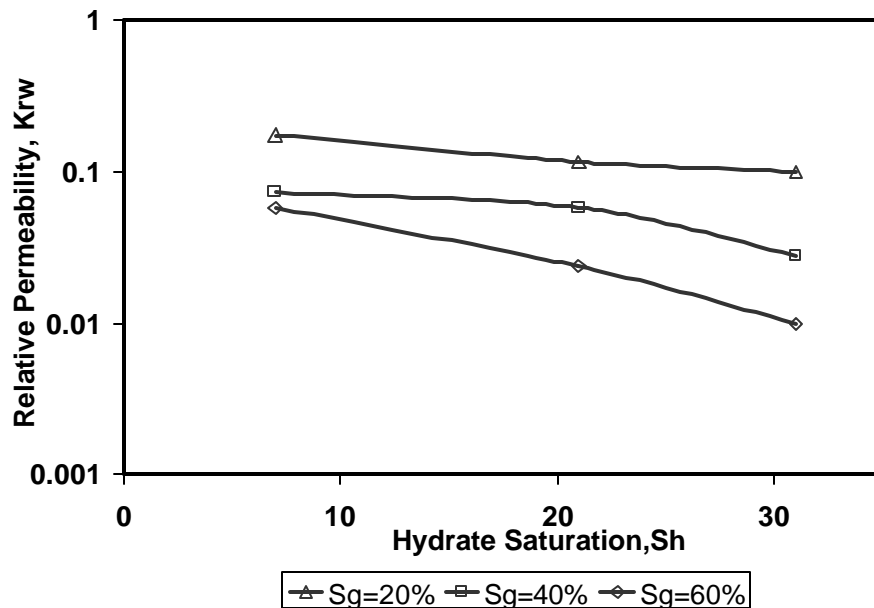


Figure 24: Brine (2%) relative permeability data at different hydrate saturation for Anadarko field sample.

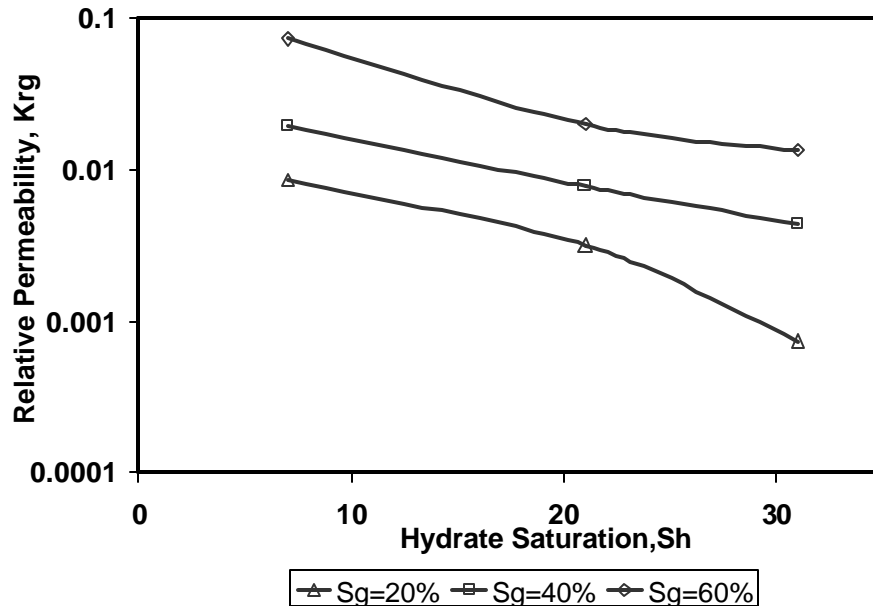


Figure 25: Gas relative permeability data at different hydrate saturation for Anadarko field samples.

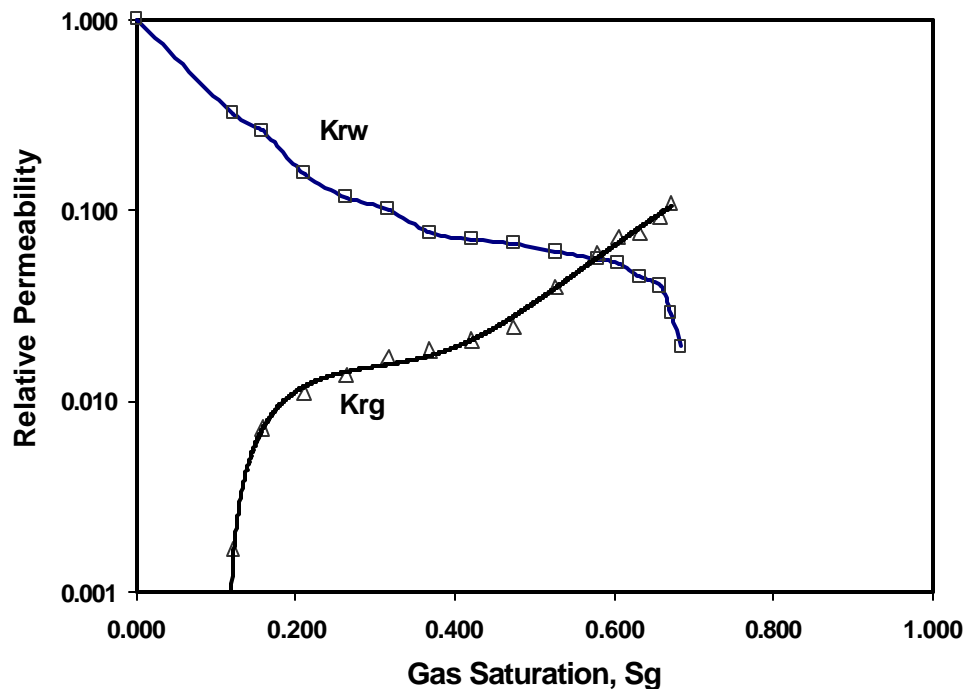


Figure 26: Gas-brine (2%) relative permeability data for Anadarko field sample.
Hydrate saturation $S_h = 7\%$

5.7.2.3.4 Conclusion

Based on the study conducted in this work, the following main conclusions can be drawn:

1. Gas hydrates were successfully formed by this new method within the core holder.
2. Relative permeability measurements were achieved on both the Oklahoma 100 mesh sand sample and shallow field samples obtained from the Anadarko Hot Ice # 1.
3. The type of gas hydrate growth influences the mechanism of formation and the gross morphology of gas hydrate occurrence. It not only depends on a number of sediment parameters, including grain size, porosity, and pore structure, but also parameters such as non-uniform dissociation, fluid parameters such as viscosity, and also the method of forming hydrates.
4. It is evident that the relative permeability inferred from unsteady-state core floods conducted in this study is a lumped parameter. This not only includes hydrate saturation, but also the effects of dissociation instabilities caused by fluid flow, fines migration due to gas production, and local compaction in porous media at low temperatures.
5. These relative permeability curves generated in the laboratory for sand samples and field samples could, to some extent, describe the field behavior of two phase flow in the presence of gas hydrates and could help design reservoir models to better simulate the dynamic flow behavior expected during gas production from gas hydrate-bearing reservoirs.

5.7.2.3.5 Future Work

1. The gas-water relative permeability data for gas hydrate systems, obtained in the first phase, is primarily for reconstituted sediment samples. However, we still lack realistic

gas-water relative permeability data for gas hydrate systems from actual field samples from the Sagavanirktok reservoir interval within MPU. Sediment samples from objective field areas are necessary to continue this analysis. Moreover, this is very crucial for the reservoir simulation work, as gas-water relative permeability data provides direct input to reservoir and fluid flow modeling.

2. Unfortunately, the dynamics of growth and dissociation of gas hydrates in presence of fluid flow are not yet fully known. Therefore, for the formation and distribution of gas hydrate within the pore structure of porous media, these relative permeability curves can be predicted by additional experimental measurements. Hence, there may be a need to conduct the laboratory displacements in a fully scaled model of the field-scale displacement to predict the functional relationship between permeability, porosity, pore structure discontinuities, tortuosity, and fluid parameters such as viscosity and dissociation in-stability.
3. Additional relative permeability tests should be performed at different temperature conditions, which would significantly contribute to our understanding of the relative permeability characteristics of gas hydrate-bearing petroleum systems.

5.8 TASK 8.0: Evaluation of Drilling Fluid and Assess Formation Damage

5.8.1 Subtask 8.1: Design Integrated Mud System for Effective Drilling, Completion and Production Operation

5.8.1.1.1 Task 8 Objectives

- Design fully integrated mud system for permafrost and gas hydrate bearing reservoirs.
- Determine mud contamination and formation damage risk.
- Evaluate mud chiller system such as one used in Mackenzie Delta program.

5.8.2 Task 8.2, Assess Formation Damage: Testing, Analysis and Interpretation

5.8.2.1 Background, Experiment Approach and Design

Limiting the extent of filtrate invasion is important. Invasion of filtrate with associated fine particles may create a zone of reduced permeability around the wellbore which may not respond to backflushing and may cause lower production rates. Filtrate that penetrates clay-bearing sections may cause swelling and subsequent sloughing into the wellbore. The depth of penetration of mud filtrate into the formation near the wellbore will affect the response of electrical logging tools. Correct interpretation of the logs and gas hydrate-bearing reservoirs require accurate knowledge regarding the extent of this mud filtrate invasion zone and any reduction of effective reservoir permeability in this zone.

Formation damage is commonly caused by the loss of mud filtrate through the borehole wall and its subsequent invasion of the formation. Formation damage mechanisms can be numerous and complex. The experiment approach to study formation damage is to investigate borehole filtration and its dependence upon physical parameters such as annular velocity, the constituents of drilling fluid, and reservoir samples.

Understanding dynamic filtration properties under borehole conditions is particularly important to ensure fewer drilling problems. Numerous investigators have studied the static and dynamic filtration of drilling fluids. Marx employed a dynamic filtration core holder to circulate mud and simulated the actual borehole conditions. Peden et. al. concluded that the dynamic filtrate loss was significantly affected by the annular velocity and the permeability of the rock. Interstitial velocity is another factor controlling fines release. Grusbeck and Collius; Gabriel and Inamdar identified and later Sharma et. al. confirmed a critical interstitial velocity above which fines will be mobilized and redeposited at pore throats.

In this investigation, an experimental apparatus has been designed and is under construction. A specially designed dynamic filtration cell will be used to study permeability impairment under dynamic flow conditions. Drilling mud will be circulated across the face of a core and the dynamic filtration rate can be measured. Permeability changes measured in this manner will help determine the depth of invasion of both the mud filtrate and the mud solids and the resulting permeability impairment. After mud circulation, reverse injection of methane gas can be performed. Return permeabilities will be measured.

5.8.2.2 Accomplishments and Challenges

- Designed and fabricated control panel which will hold all valves, back pressure regulators (BPR), multipoint pressure indicator, and the lines.
- Designed and fabricated compact core holder stand to prevent destabilization of the mud and coolant lines from the bottom of the core holder from the mounting and removal of core samples.
- Designed lines to ensure that drilling mud lines are 3/8" size whereas methane gas and overburden or BPR nitrogen or exhaust lines are of 1/4" and 1/8" size respectively.
- Planned use of compressed air cylinder as depicted in the layout from March 2004 quarterly report #6 for introducing the drilling mud from accumulator to recirculation unit and moving floating piston back to its original position at 25 psi.
- Designed the drilling fluid recirculation unit to require a continuous air supply at 80-100 psi to activate the solenoid valves, move the floating piston in the accumulator, and to change the cycle.
 - This use of air in accumulator leads to another fidget regarding the possibility of air being trapped in it and reducing its volume available for drilling mud over a period. To overcome this particular problem, a vacuum line was introduced from in-house supply.
- Plan to utilize one methane gas cylinder and 3 Nitrogen cylinders each of 2263 psi cylinder gas pressure to simulate overburden, and 2 BPR's.
 - These compressed gas cylinders are generally not useable until a pressure regulator is incorporated to reduce the gas pressure to a workable level that can be safely utilized in equipment and instruments. There are two basic types of regulators available. Single stage pressure regulators reduce the cylinder gas pressure to the delivery pressure in one (1) step. This one step pressure reduction results in a slight change in delivery gas pressure as the cylinder pressure decays. In most cases, the delivery pressure will rise. The single stage regulator is a satisfactory and cost effective selection if slight variations in delivery pressure

and/or periodic adjustments are not detrimental to the application. Double stage pressure regulators reduce the cylinder gas pressure to a working level in two (2) steps. The cylinder gas pressure is reduced by the first stage to a preset, intermediate level, which becomes the gas pressure at the second stage inlet. This allows the second stage to fine-tune the final delivery pressure. Thus, double stage regulators provide a constant delivery pressure unaffected by cylinder pressure decay.

- Since the nitrogen gas will not be consumed and is designed to hold the pressure in-line through BPR's and apply pressure on the core sleeve, the choice of pressure regulators for nitrogen gas cylinders was an obvious and cost effective single stage pressure regulator. However, the methane gas will be consumed and since the plan is to determine its' initial and return permeability or in leak off tests, there remains a requirement to maintain methane gas pressure at a constant value.
- In this investigation, maximum methane gas pressure that can be tested is around 1500 psi. However, due to safety issues associated with flammable gas like methane, double stage gas regulators with tank inlet pressure of 2263 psi and delivery pressure of 1500 psi maximum are not common. This issue was resolved by recognizing the two-stage regulator design, available from the leading company of valves, fittings and gauges. The effect of two-stage regulators will be achieved with two single stage methane gas regulators connected in series with 1/4"x 6" nipple. The check valves on methane and nitrogen lines will avoid the possibility of decrease in pressure at the later stage of the cylinder usage.
- Designed flexible methane and overburden lines going into the core holder to facilitate the removal and mounting of core samples.
 - Employed 1/4" flexible hose for methane and quick-connects with check valve to hold the gas pressure in upstream lines and avoid the necessity of evacuating methane and nitrogen from lines before mounting new core sample. However, planning for a more sophisticated assembly to solve one problem led to other concerns. Due to the compact design of the core holder, street elbows were used at male NPT connection for employing quick-connects.
- Planned to circulate the coolant, Thermal H5S, through the cooling jackets around dynamic filtration core holder and drilling fluid recirculation unit.
 - Retained a floating piston accumulator of volume 2.5 liter in-line to replenish the mud as necessary, since 3/8" lines have been used for drilling mud and there is a possibility of a significant volume of drilling mud to be flowed through those lines.
 - Wrapped 1/4" copper line for coolant around the accumulator to help simulate actual drilling conditions, i.e. maintaining temperature of drilling fluid around 2-10°C, constant in accumulator, core holder and recirculation system is critical and hence FP50-MC 230V/60Hz Julabo Refrigerated circulator with RS-232 interface will be utilized for this purpose. Two high pressure in-line temperature sensors have been fastened which will give signal to a CN612 Series Omega monitor.
- Placed differential pressure gauges in-line.
 - The positive pressure port of regulators is connected to the line and negative is kept open to the atmosphere as shown in the modified layout (Figure 27).

- The maximum differential pressure of these gauges was selected as a safer value of 2000 psi to avoid the rupture of the diaphragm.
- The bleed ports from the positive ends of the gauges were connected to the exhaust line with the valves to control.

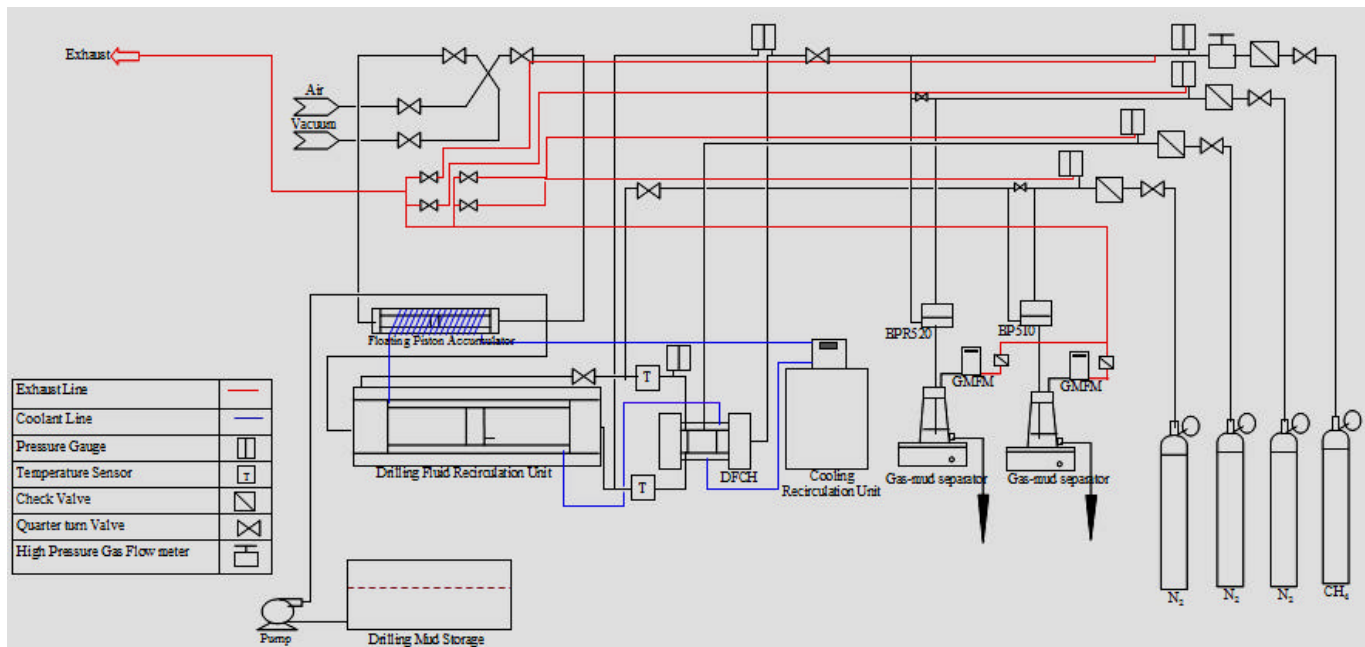


Figure 27: Modified Layout for assessing formation damage due to static, dynamic filtration and by leak-off tests

5.8.2.3 Future Work

The primary challenge in this investigation has been the timeframe and patience that is exercised in appreciating the specifications of recent available test equipment and ordering and procuring the proper equipment. Final procurement of few test accessories will include dynamic weighing units, Julabo refrigerated circulator, six 9-pin RS-232 cables and 3-phase, 230V power supply, drilling circulating pump and drilling fluid constituents. Additional work required will include:

- Comprehend software such as Winct AND Weighing, Smart RPS-2500 Temco Recirculation System, IO Terminal Communication Aalborg Version 1.03, CN 606/612 RS-232 Omega Temperature Monitor, Easy Temp.vi 2.0 Julabo.
- Test the experiment apparatus for leaks and attained pressure with water and nitrogen and calibrate the analytical tools.
- Perform critical velocity test to get flow rates, which can be applied without causing permeability reductions due to fines migration.
- Measure the return permeability with specific underbalance and overbalance pressure drops.
- Calibrate the results obtained with different approaches in an effort to quantify the significance of drilling fluid on potential formation damage.

5.9 TASK 9.0: Design Cement Program

No work on this task was performed during the reporting period. A related study to determine the efficacy of Argonne National Laboratory's Ceramcrete cement for completion operations was funded as discussed in Section 1.3. Ceramcrete may provide a viable alternative to current permafrost cements used in Alaska North Slope drilling operations.

5.10 TASK 10.0: Study Coring Technology

No work on this task was performed during the reporting period. Prior technical reports include this task.

5.11 TASKS 11.0 and 13.0: Reservoir Modeling and Project Commerciality and Progression Assessment – UAF, BP, LBNL, Ryder Scott

5.11.1 UAF Reservoir Model Accomplishments

As documented in previous technical reports, the industry-standard reservoir model CMG STARS was adapted to incorporate the description of the phase behavior of gas hydrate, heat flow, and compaction in the reservoir and the gas hydrate cap. CMG STARS allows input of our geologic description, calculation of well productivity, evaluation of well configurations, and investigation of various ways of dissociating the gas hydrates. Numerical studies were completed at UAF for gas recovery from a reasonable theoretical formation model containing gas hydrates (Figure 28). This UAF model assumes a 16 meter thick gas hydrate layer which extends from -905 meters to -921 meters, and is underlain by a 2 meter thick water saturated layer. The gas hydrate layer and aquifer is bounded by tight and relatively thick mud/silt formation that acts as a no-flow boundary above and below the gas hydrate-bearing reservoir. At the bottom of the gas hydrate layer, the pressure is 9 MPa and the temperature is 7.5 °C. The gas hydrate and water saturations in the gas hydrate-bearing interval are 0.6 and 0.4 respectively; and are 0 and 1 in other formations. Initial gas volume in place in the gas hydrate layer is about $5.7 \times 10^6 \text{ m}^3$ at STP. Three production principles were tested: depressurization, wellbore heating, and hot water/steam injection. For the depressurization production scheme, 54.4% of the total cumulative production was achieved after only 3 years of simulation. The temperature distribution after 3 years of simulation is shown in Figure 29. Significant gas production was achieved within a relatively tight gas hydrate layer for the production schemes of depressurization and well heating as shown in Figure 30. For the hot water injection, the four injection wells are set at the four corners of the model (Figure 31). The simulation runs were carried out with three different temperatures of 40, 60 and 80 °C. The advantage of this scheme is the combination of two most important mechanisms of dissociation, i.e., depressurization at the production well and thermal stimulation at the injection well. Temperature distribution and gas hydrate saturation profiles in the lowermost layer in the reservoir are shown in figures 32 and 33, respectively during hot water injection at 40°C. For the thermal stimulation production scheme, 81.3% and 90.4% of the total cumulative production was achieved after 3 years of simulation when hot water was injected at 40°C and 60°C, respectively (Figure 34). Figure 35 illustrates a comparison of all three-production schemes. The maximum EER of about 37.9 is obtained for the 40 °C water injection.

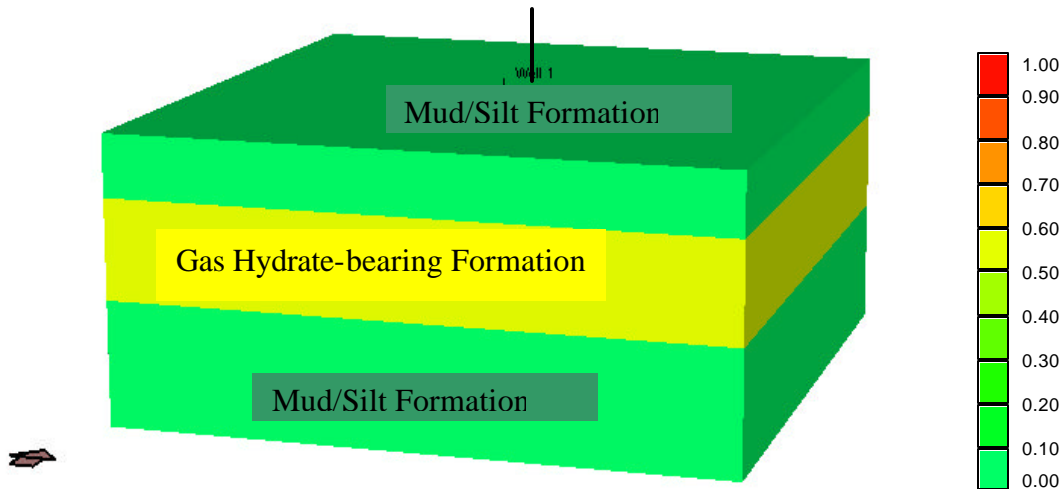


Figure 28: Hypothetical geologic model

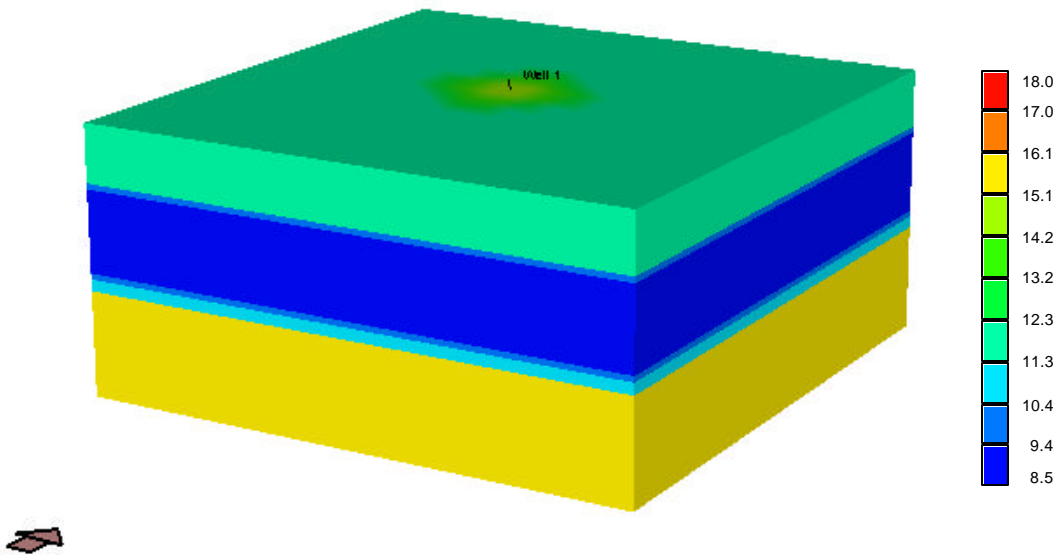


Figure 29: Temperature distribution after 3 years, depressurization case

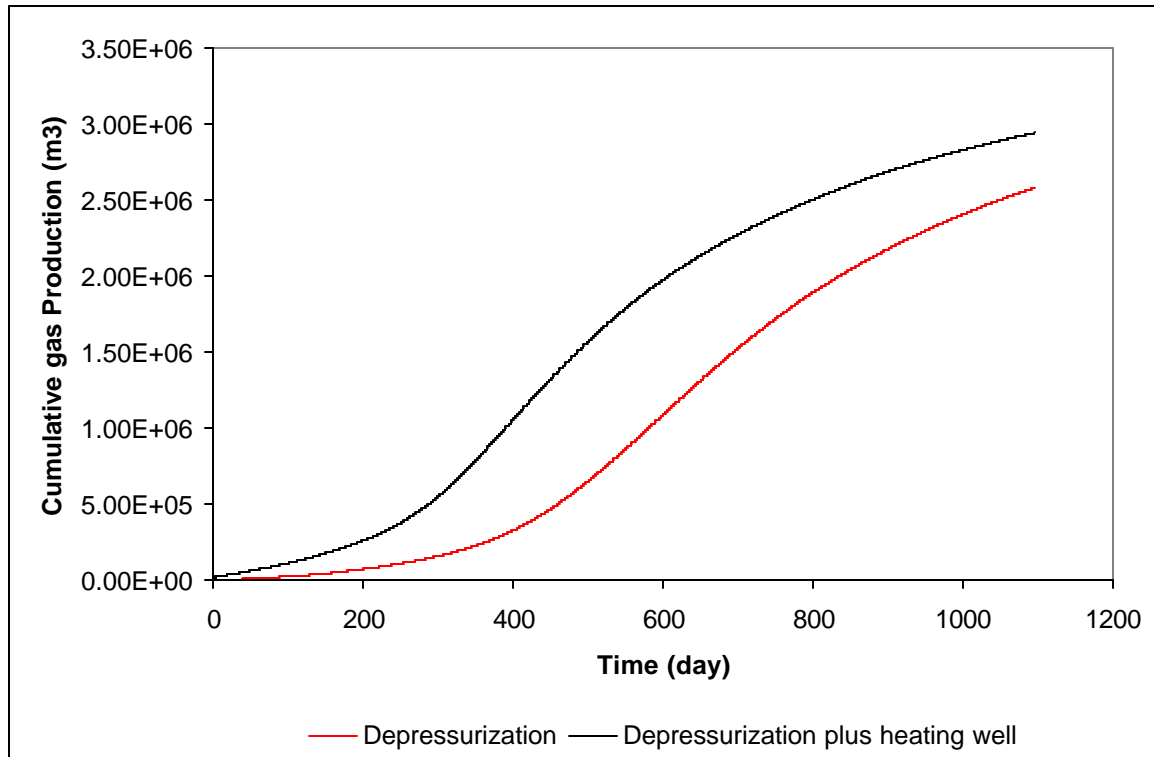


Figure 30: Cumulative gas produced vs. time (at low permeability, 15md)

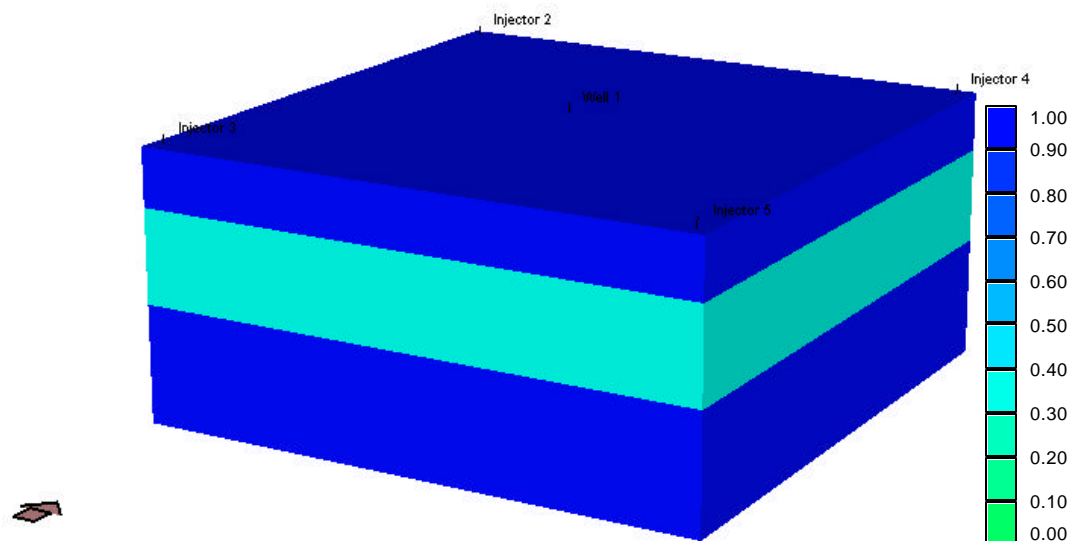


Figure 31: Location of injection, production wells, and initial distribution of water saturation.

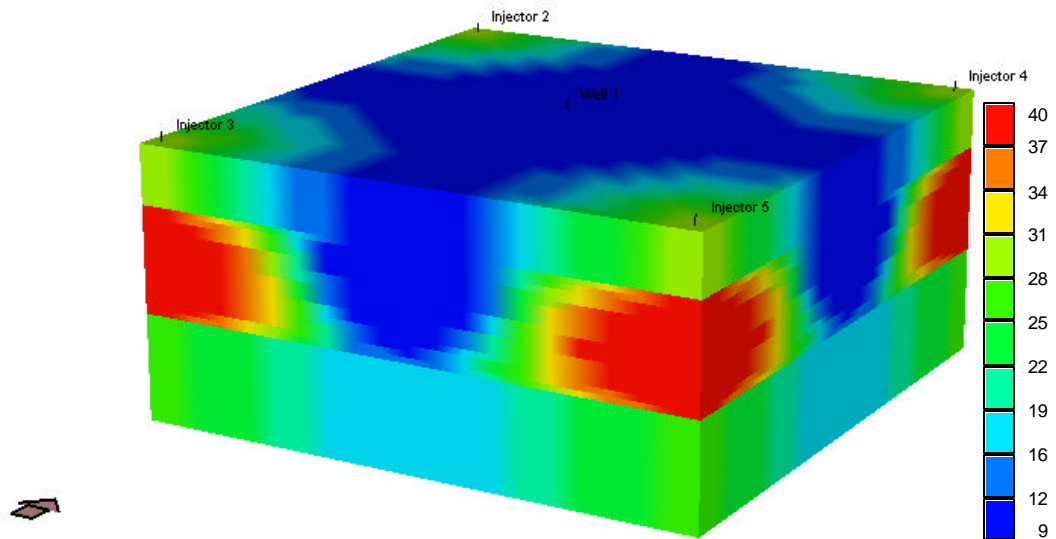


Figure 32: Temperature distribution after 3 years: depressurization and injection at 40 °C

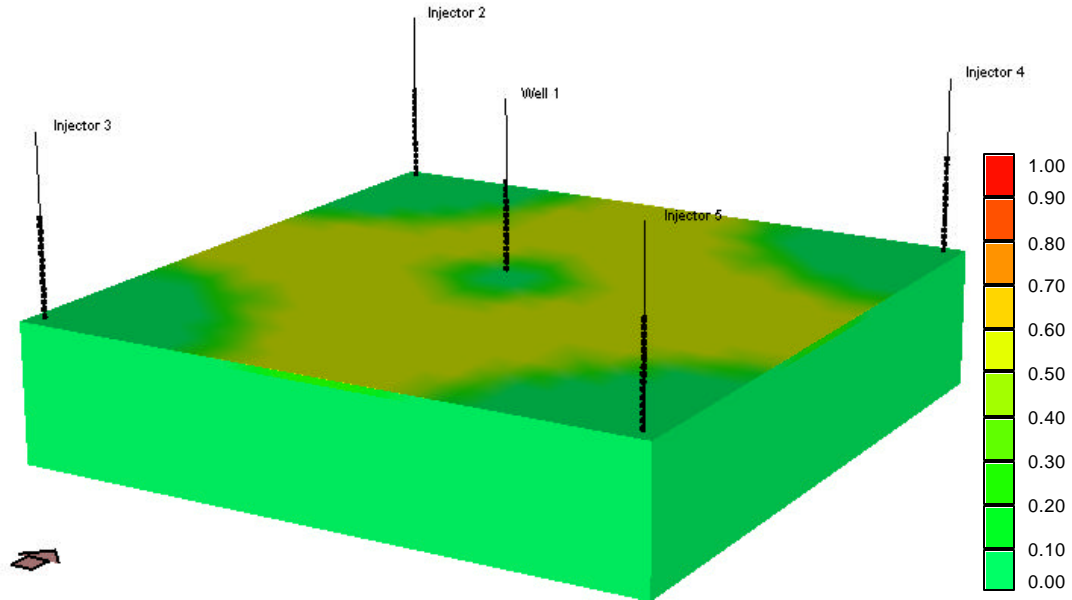


Figure 33: Gas hydrate-saturation profiles in the bottom gas hydrate-bearing layer during hot water injection after 9 months (Injection rate 20m³/day, water temperature = 40°C)

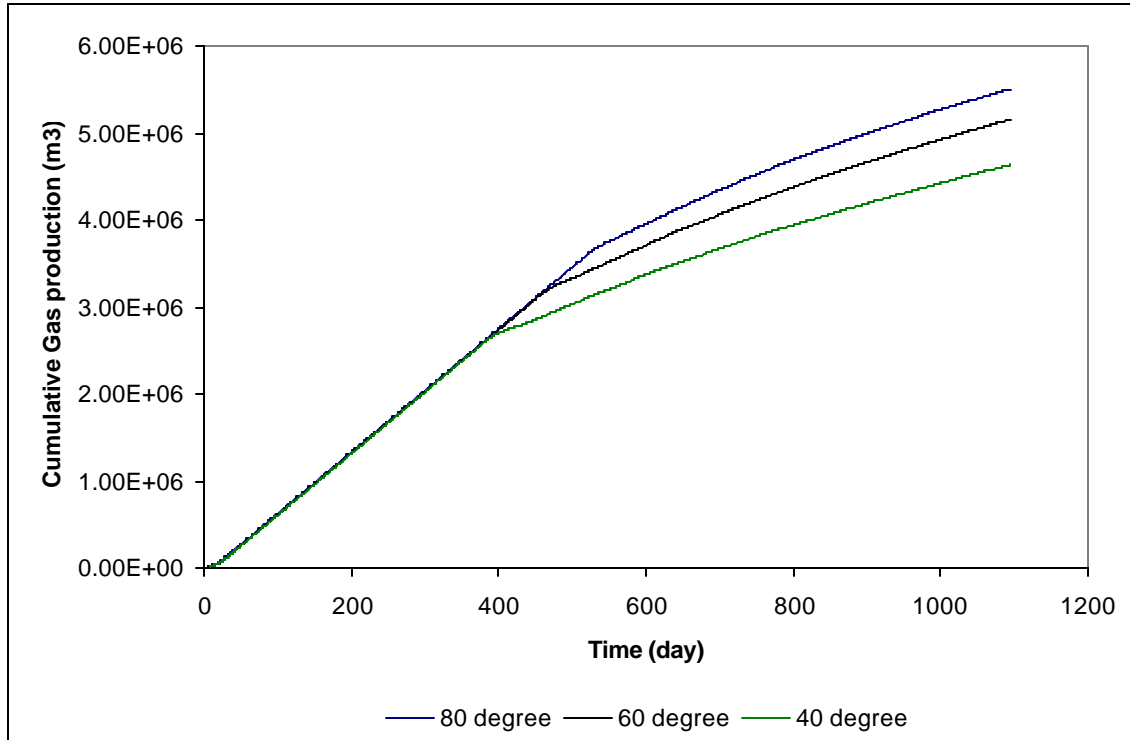


Figure 34: Cumulative gas produced vs. time (Hot water injection: Injection rate 20m³/day)

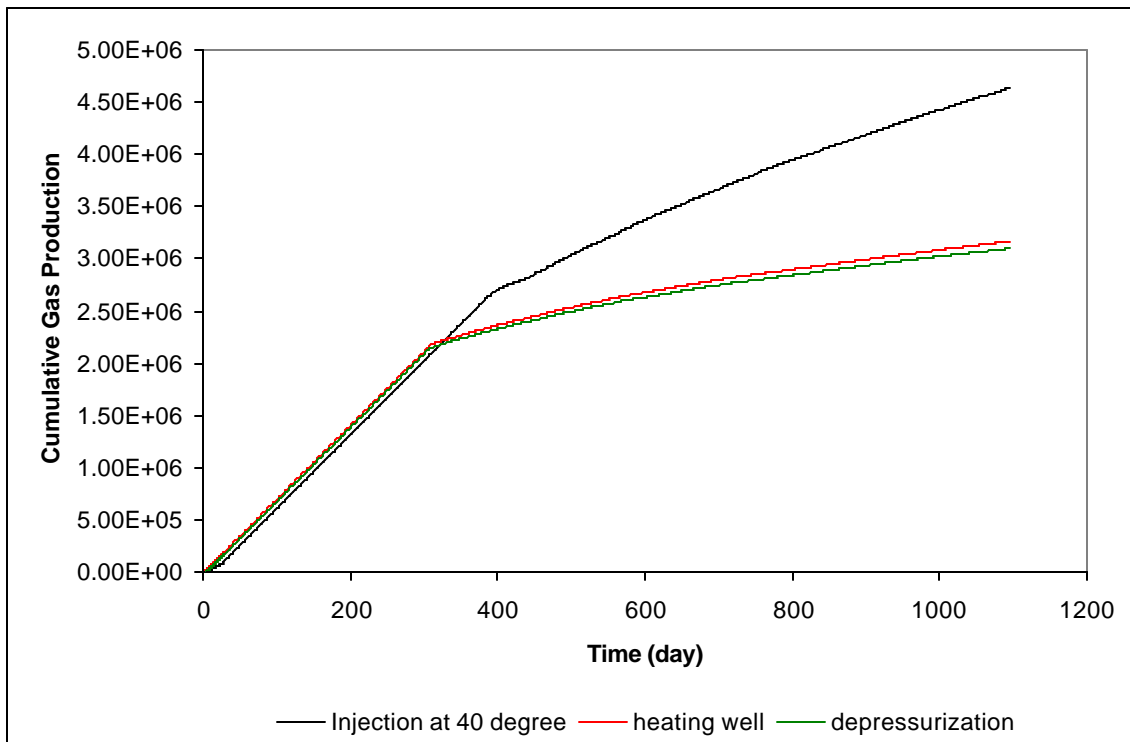


Figure 35: Comparison of all production schemes at 300 md reservoir permeability

5.11.1.1 UAF Reservoir Modeling Future Plans

- Compare a basic CMR STARS simulation to Lawrence Berkeley National Laboratory's June 2004 Beta release of *TOUGH-FX/Hydrate* simulator. A comparison of the physics of gas hydrate dissociation behavior between these 2 models may help improve the modeling capabilities. A *UAF* hydrate model can be revised and calibrated using modeling code from *LBNL*.

5.11.2 Ryder-Scott Company Reservoir Model Accomplishments

5.11.2.1 Production Test Screening Studies

In the second quarter, significant progress was made in moving state-of-the art geologic modeling work using a gas hydrate and free gas-bearing prospect description from Task 5.0 toward the downstream prospect evaluation stage. In an effort to meet Phase 2 progression decision timelines, while allowing for schedule slippage on reservoir engineering evaluation tools, several paths were pursued to move forward toward deliverables. Reservoir modeling work progressed using the commercially available reservoir simulation program CMG STARS and building on the foundational work accomplished by Hong and Darvish (2003) at the University of Calgary and by Howe (2004) at the University of Alaska Fairbanks. Several improvements and simplifications were made to the simulation deck to allow for rapid scenario testing while honoring the salient parameters in the gas hydrate decomposition by a depressurization process. Proper handling of an ice-phase is under consideration.

The results to date show that realistic reservoir descriptions can be modeled in commercial reservoir models as gas hydrate, gas, and water systems. CMG STARS can now provide realistic forecasts for Class I pressure dissociation cases that mirror similar descriptions in the academic research models that are under development. In addition, a further simplified modified material balance, moving front dissociation model was incorporated into ProCast to perform prospect screening. In all cases, the remaining uncertainties lie not in the detailed physics of the gas hydrate reactions, but in the macroscopic temperature, pressure and flow behaviors of specific reservoirs.

Modeling efforts by Hong (July 2003) at the University of Calgary and further validated by Howe (May 2004) laid the groundwork for describing the pressure and thermodynamic processes of gas hydrate dissociation by pressure reduction within CMG STARS. Several improvements to this work were accomplished by modifying the simulation technique to shorten the processing time without significantly affecting the results. Therefore, simulations achieved accommodate the limitations within the program as opposed to allowing the limitation in the program to affect the forward progress of the evaluation. The two significant changes in the raw simulation parameters supplied to STARS were the use of explicit "skin" layers to provide temperature boundary conditions both above and below the active grid cells. Both Hong (2003) and Howe (2004) noted that the single value of under/overburden temperature in STARS restricted their ability to initialize their variable depth models in temperature equilibrium. This shortcoming was solved by simply including high heat capacity, zero porosity layers both above and below

the grid. Addition of these layers allows greater flexibility in evaluating convective heat flux by including many layers in the heat mass layers.

The second limitation that specifically affected Howe (2004) was the arbitrary minimum temperature of 0°C or (32°F) within STARS. The developers of STARS hardwired this limitation into the code to reduce potentially erroneous forecasts for systems going below the freezing point of water. Unfortunately, the endothermic gas hydrate dissociation process can, in some cases, drive temperatures down to the water freezing point. If allowed to, grid cells will drop to about -1.5°C before a steady state heat flux causes the reservoir temperature to go asymptotic. When the STARS model attempts to solve a grid block temperature below 0°C, it resets it back to zero and continues iterating. This causes discontinuities in the forecast, but, surprisingly, did not affect the overall quality of the forecast; it just increased computation time significantly or locked-up the model on miniscule time steps. To avoid this problem, all temperatures in the grid were arbitrarily increased by 10° C and the reaction parameters were translated upward by 10° C as well. In this way, all the same physics are honored, but the program limitation is avoided (by about 10 degrees). Care was taken to mentally subtract 10° C from the results plots and outputs. This modification brought to light a current shortcoming in the STARS modeling parameters in which the water fusion reaction (formation of ice) is not yet handled. The lack of attention to this issue is understandable, given that until recently, the ability for the STARS to even run in an ice formation condition was not possible. Preliminary efforts to incorporate and understand an ice component and its effects are underway.

The last change was to evaluate the need to model the block model from Digert and Hunter (2003) description in 3 dimensions. This screening model was 138 X 20 X 10 cells as used in Howe (2004) and exhibited several dimensions of symmetry that could potentially be reduced. Figure 36 shows the results of this modeling. The blue and red lines represent the original model and a simplified strip model. The green line shows the simplified model with no heat flux from the outside layers, indicating the worst case of a gas dissociation process that slows to a trickle due to internal cooling.

Once the strip model validation effort and the ice component activities were in progress, attention was turned to using the validated component thermodynamic descriptions in conjunction with the reservoir descriptions and gas hydrate prospect evaluation within the Milne Point 3D seismic survey area provided by USGS (work in progress). This task should take the modeling effort to the point where it can be used to screen potential pilot areas and development scenarios within the Milne Point Unit area.

Depth and thickness grids for the Staines Tongue formation were exported by USGS and provided to Ryder Scott Company for incorporation into STARS. This effort primarily consisted of parsing the values from the ASCII text exports, converting them to the proper units and generating a second ASCII file that represents the data format expected by STARS. The same process was used to generate a temperature and pressure map of the study area with the temperature grid supplied by USGS and the pressure grid generated based off the depth and thickness maps where a typical hydrostatic pressure is applied to the center of each grid cell. The saturation grid to define gas hydrate-gas-water ternary saturations uses three input grids: the gas hydrate presence binary grid, the depth grid, and the base of ice or gas hydrate-bearing

permafrost grid, all supplied by USGS reservoir characterization studies in Task 5.0. Despite some issues related to the treatment of faults, figure 37 shows the initial saturation conditions view of the Milne point area where green represents gas hydrate, red represents free gas, and blue represents water. Figures 38 and 39 illustrate the initial temperature and pressure conditions.

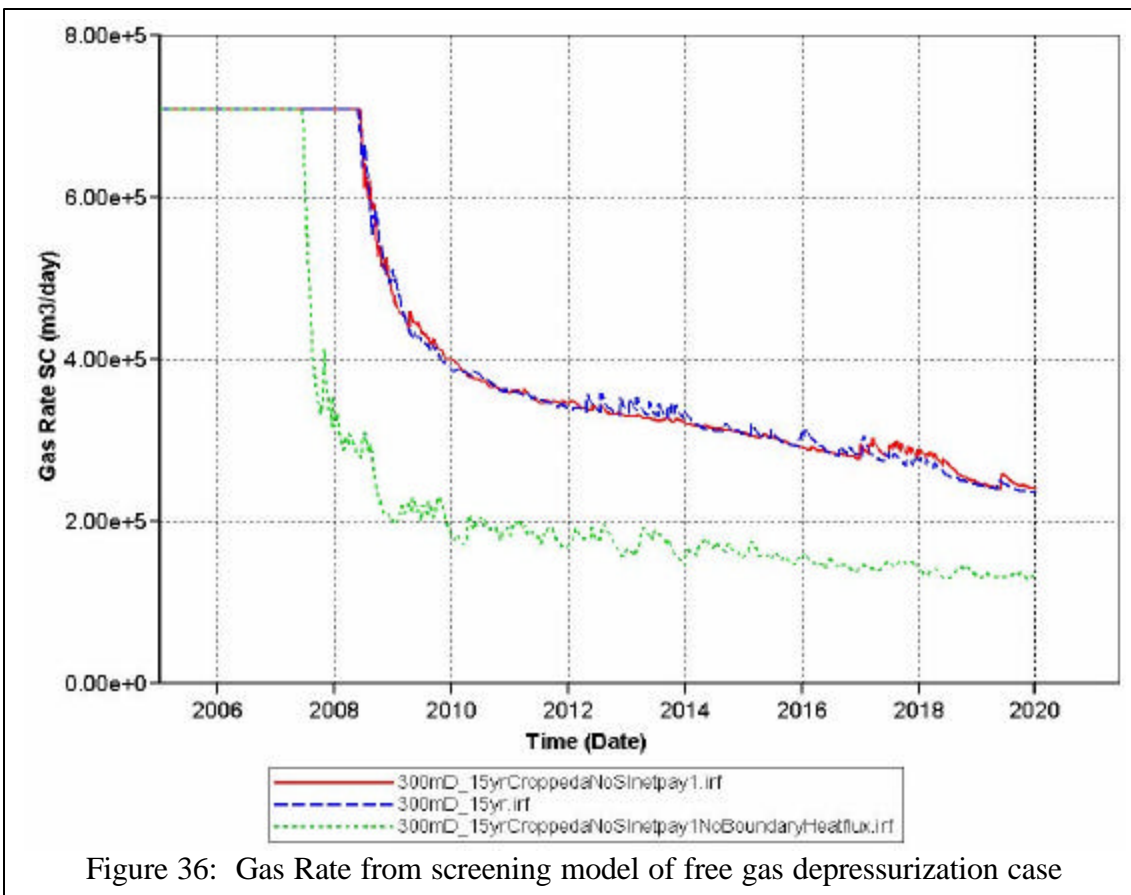
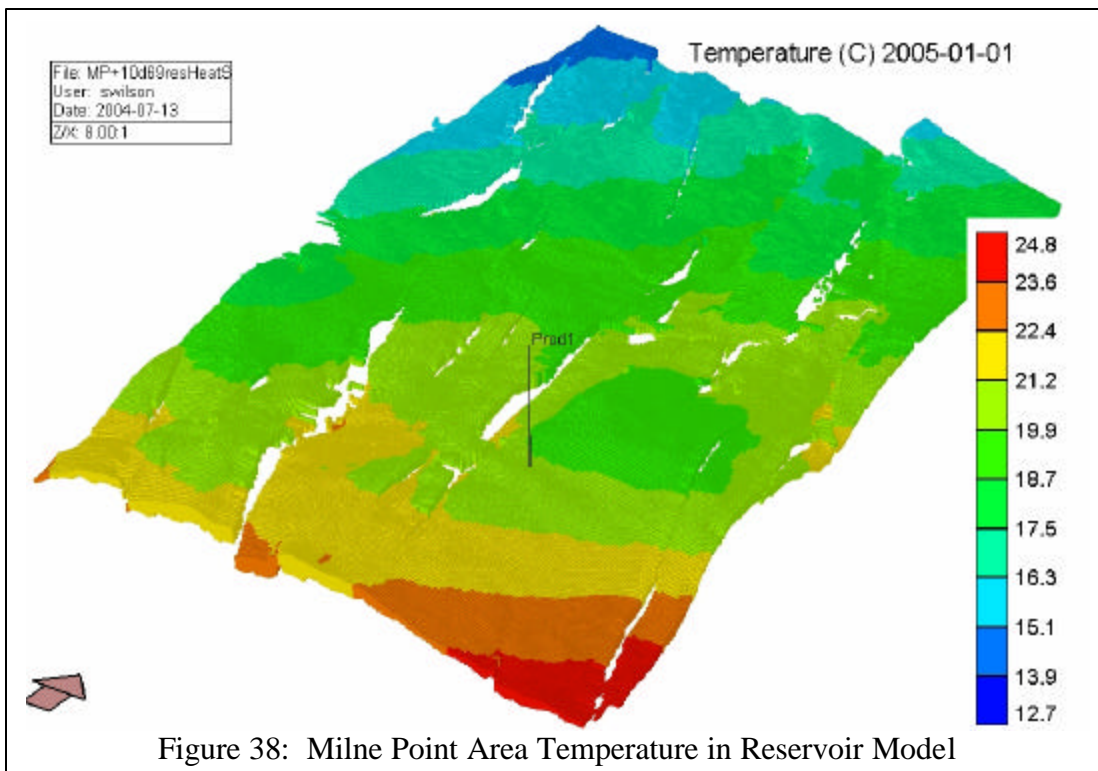
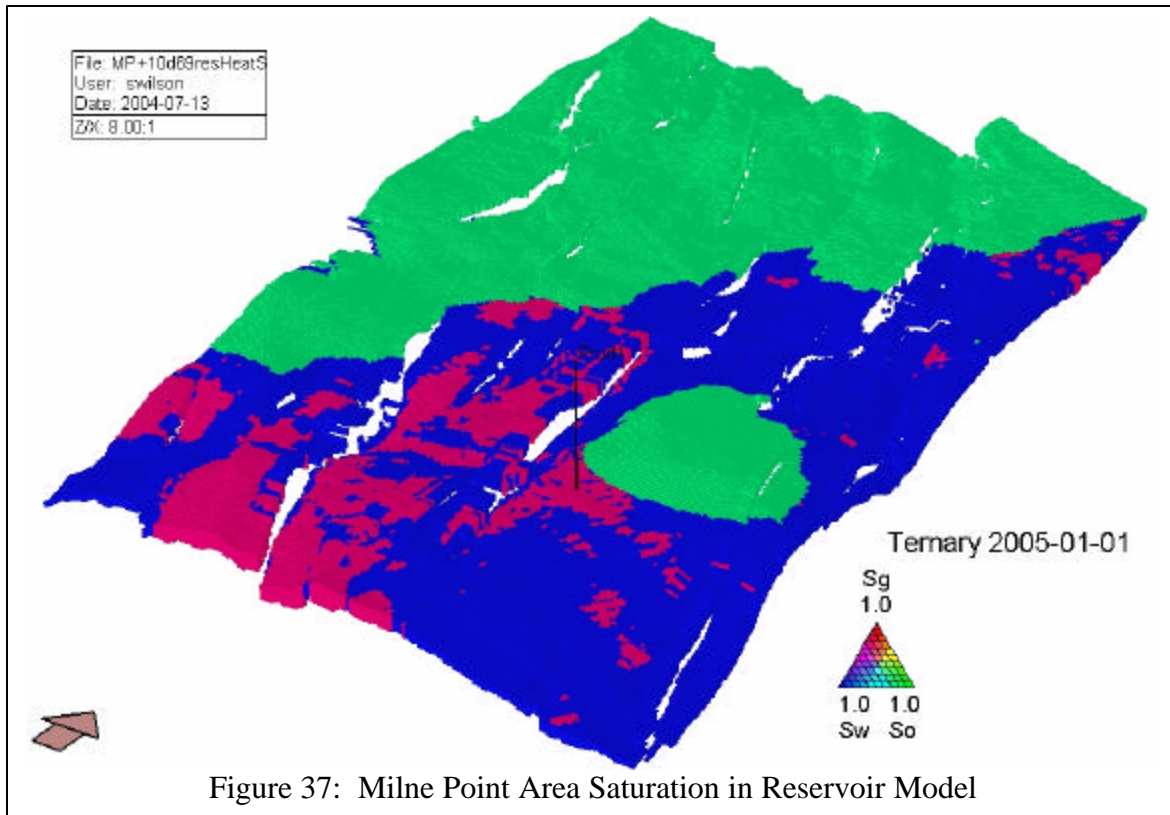


Figure 36: Gas Rate from screening model of free gas depressurization case

The most obvious candidate testing area for controlled gas depressurization is the small gas accumulation in the center of the model. This free gas is associated with an isolated gas hydrate accumulation formed by a fault-bounded portion of the Staines Tongue. A single 175 meter horizontal producer well is placed in this potentially high permeability layer and produced at rates up to 25 MMSCF/D. Within this initial model, the well is occasionally shut-in to evaluate model performance and to observe pressure and temperature recovery. To date, all behaviors are as expected in gas underlying gas hydrate pressure-induced dissociation systems. They are strongly influenced by vertical conductive heat flux (see Figure 40), pressure propagation through the gas hydrate mass (i.e. relative permeability to water or gas in gas hydrate), and the exposed surface area of the dissociation front to the reduced pressure. As long as the regional reduced pressure front contacts the gas hydrate-bearing strata within a reasonable time frame, producing well trajectories (horizontal vs. vertical), and rate of production are of minor consequence. For these reasons, a small gas accumulation could become a preferred initial potential testing site since smaller volumes of free gas would have to be handled before initiating gas dissociation from gas hydrate.



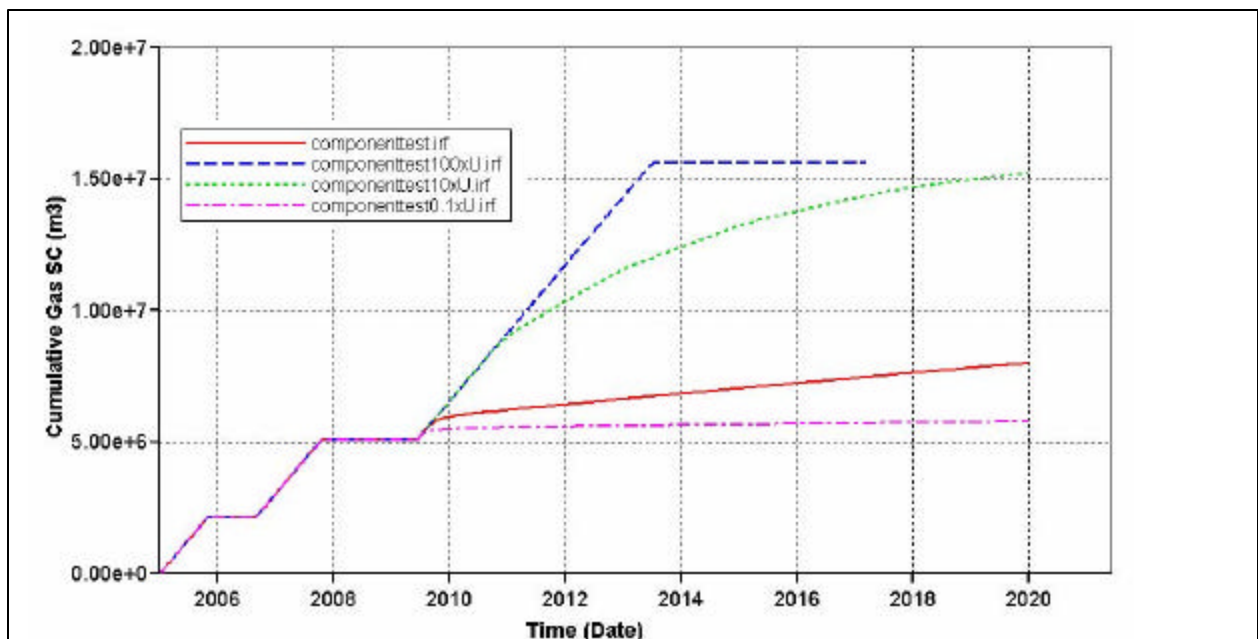
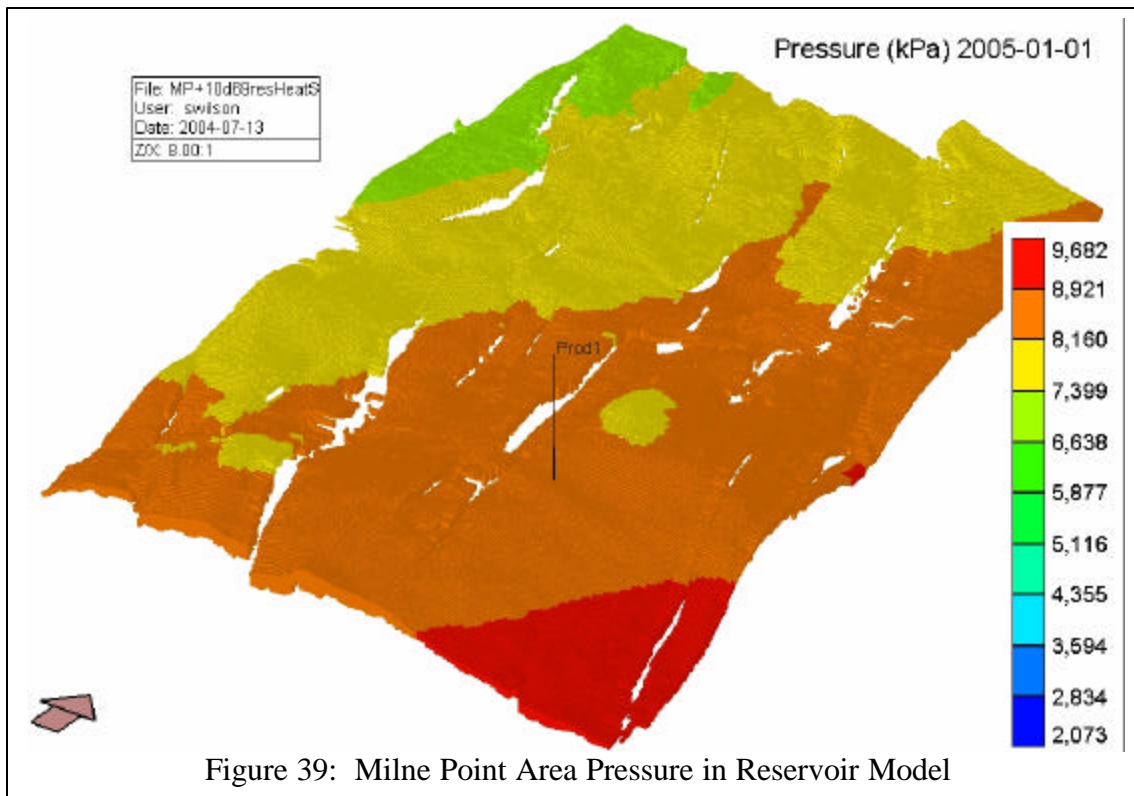


Figure 40: Sensitivity to conductive heat flux constant. Red base case is matched value from Mallik Simulation (provided by Collett).

Although only calibration runs have been completed to date, the results look reasonable and sufficient for screening purposes. Figure 41 illustrates the modeled time series showing temperature reduction and subsequent recovery in the gas hydrate mass near the producing well as gas from hydrate is dissociated via pressure depletion of the adjacent free gas. Figure 42 illustrates saturation changes through time during a 15 year gas production period.

5.11.2.2 Simplified Screening model development and testing.

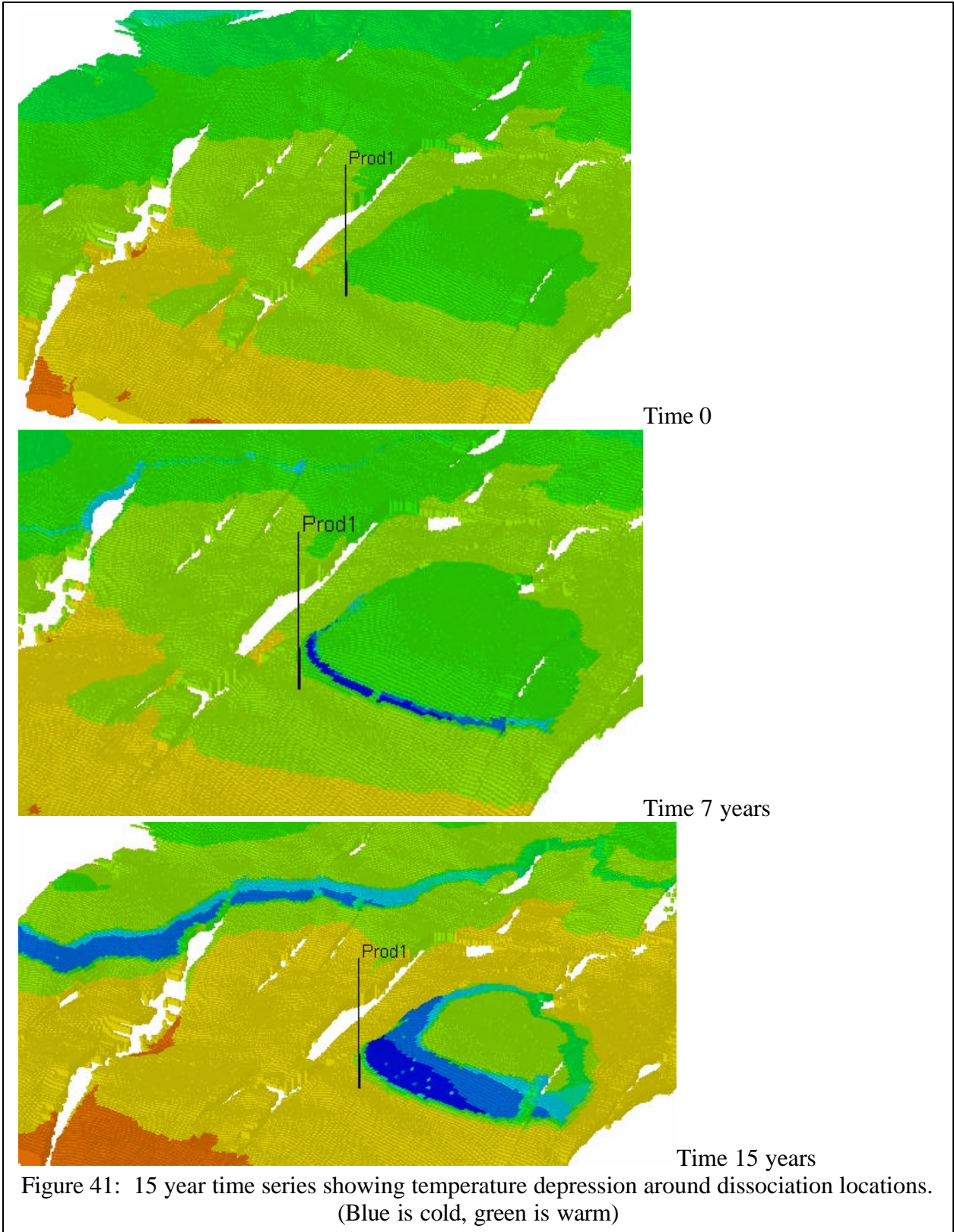
In an effort to enable rapid scenario testing, a material balance solution using a moving dissociation front model was developed and tested. The solution relies on determining an equilibrium pressure such that the simple gas material balance pressure (including dissociated hydrate gas) is equivalent to the pressure resulting from the volume of hydrate dissociating into gas and water during the same time step. Solving these two simple relationships simultaneously gives a single pressure that reflects both the pressure decrease caused by the removal of produced gas, and the pressure increase caused by gas hydrate dissociation. The reaction is assumed to occur over a specified effectively horizontal hydrate-gas surface at the base gas hydrate stability zone. As the predicted gas hydrate mass dissociates, this hydrate-gas surface retreats upward according to the material balance parameters of porosity, saturation and net exposed area in the gas hydrate-bearing areas.

Two terms were enabled to characterize the speed and quantity of dissociation which are similar in form to the Kim-Bishnoi terms used in smaller scale dissociation reactions. As proposed by Pooladi-Darvish (2004), fugacity was replaced by pressure as a simplification as well. The dimensions of the first defining constant is *mass/(area-pressure-time)* or in gravity independent oilfield units, *lbs/(ft²-psi-day)*. The second constant was required to capture time/distance dependent transient reaction decay, as the dissociation front moves farther from the isolated sink and the return gas path becomes more tortuous. This term is analogous to the diffusivity term used in transient Darcy formulations. The dimensions are *1/time* and *1/days* in oilfield units. It must be stressed that neither term is mathematically correlated to any of the theoretical gas hydrate dissociation parameters; just as the C and n factors in the well-accepted back-pressure equation

$$q = C(p_r^2 - p_{wf}^2)^n$$

are not correlated to their more rigorous Darcy counterparts.

The last feature of the formulation is a stepwise variation of surface area to depth. Since depth is tracked as the front retreats, it is trivial to apply differing surface areas in the gas hydrate dissociation equation. In this way a proxy for a complex reservoir description can be entered, without the overhead of a legitimate three dimensional model. Figure 43 shows the data entry panel used in ProCast to model this data. The program can be downloaded at www.ryderscott.com/download2/setupprocast.exe and installed with password Procast2004.



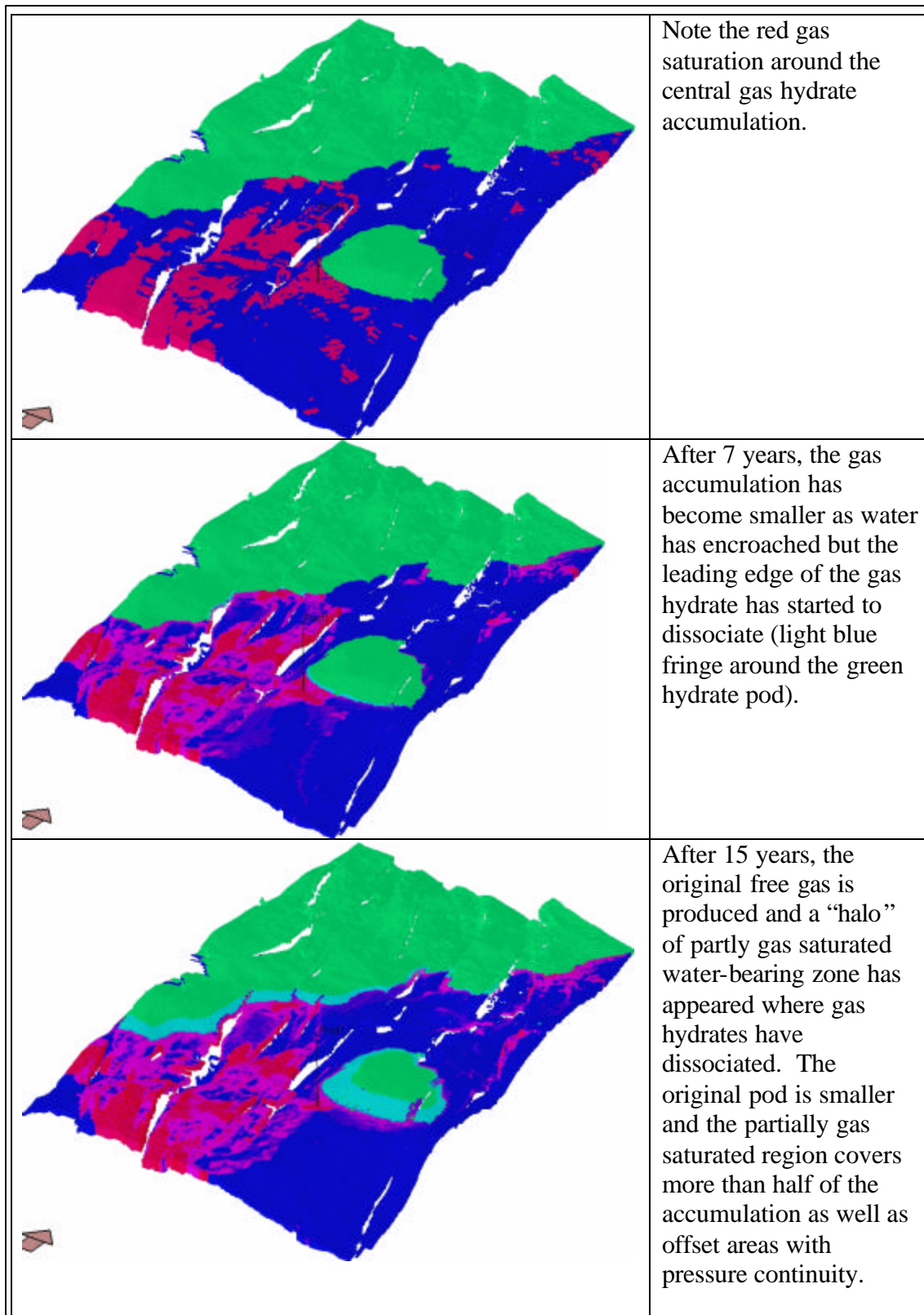


Figure 42: 15 year time series showing ternary saturation.
 (Dark blue is water, green is gas hydrate, red is free gas)

Gas Hydrate Dissociation

Hydrate Saturation: 70 %

Top of Hydrate: 1650 ft ss

Gas-Hydrate Contact: 2493 ft ss

Gas-Water Contact: 2953 ft ss

Reservoir Dip: 1.6 degrees

Net Thickness: 100 ft

Formation Width: 2500 ft

Formation Porosity: 25.1 %

Hydrate Pressure Decline: 0 %/year

Kim-Bishnoi Constants

Time Constant 1/days	Dissoc. Constant #/(ft ² -psi-day)
0.00105	1.5e-005

Horizontal Slice Distribution

% of average interface surface area	Depth (ss)
	TOS
10	1700
20	1800
20	1900
30	2000
10	2100
10	2493

Enter % between depths that represent the amount of gas contained in the structure from the prior depth entry to the next line

Buttons: Help, Cancel, OK

Figure 43: ProCast Data Entry Panel reflecting Hydrate terms

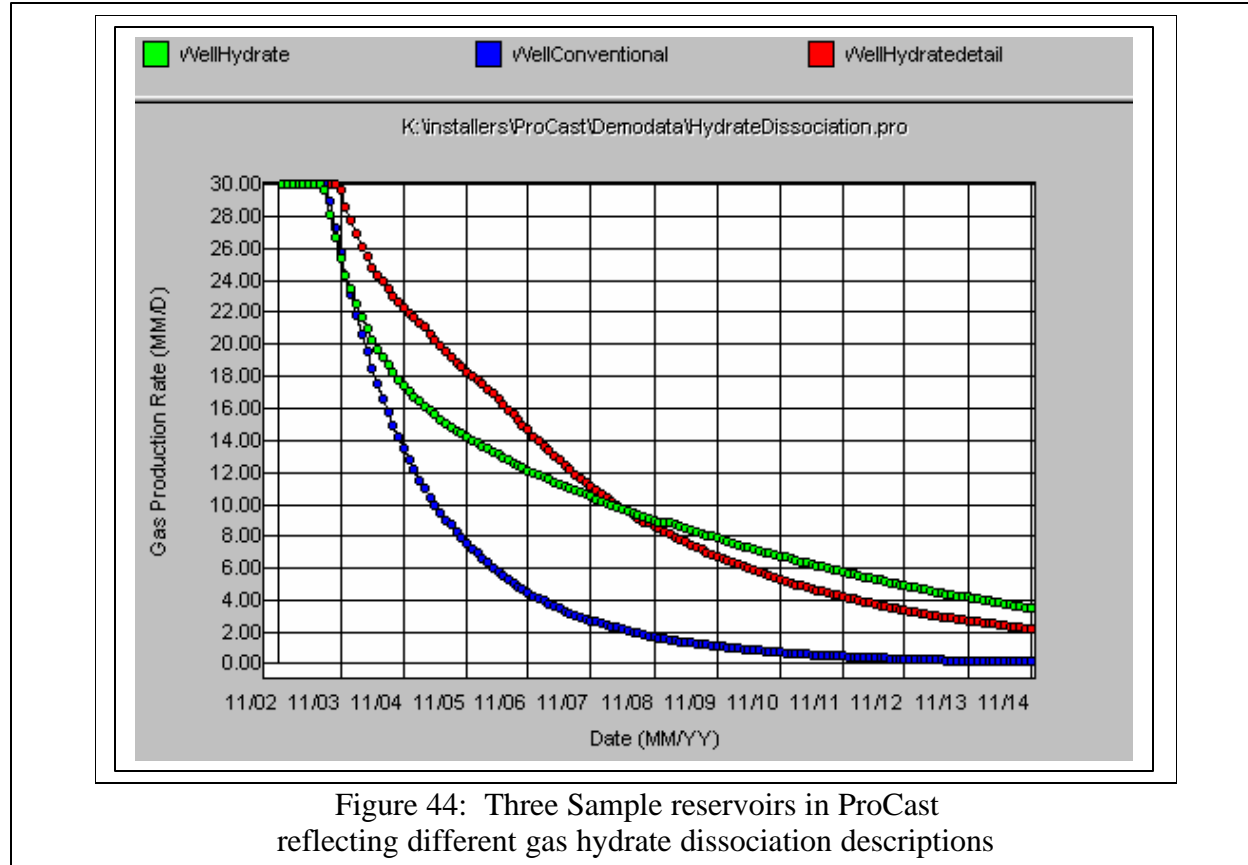
The limiting assumptions of this model are many:

1. No transient pressure behavior,
2. Steady-state temperature depression or time dependent dissociation decay caused by temperature depression,
3. No inhibitor modeling is handled,
4. No heat gain/loss is modeled explicitly, although it can be incorporated into the tuning parameters,
5. Gas-leg volumes are continuous and high permeability,
6. No compaction or permeability degradation of the reservoir occurs.

Although these assumptions limit the problems that can be modeled with this system, the amount of uncertainty in these same parameters in more rigorous models at this time is sufficiently large that the result from the simple model falls within the range of outcomes from the complex models.

A sample dataset testing these features was built and is stored in the samples directory of the install directory. This sample includes a conventional gas well, a simple hydrate dissociation

well with associated gas leg, and a complex hydrate dissociation reservoir with a varying dissociation surface as the front retreats. Figure 44 shows these three cases.



The expected workflow for use of this methodology would be to simulate a specific reservoir using a rigorous tool like TOUGHFX or STARS, match the response by tuning the two ProCast Hydrate Parameters from each reservoir, and run screening studies with ProCast to identify focus areas for further detailed work. This stand-alone model could also be used by those without access to the more complex models to screen their own prospects using the default parameters. Once field data is available, ProCast parameters can be matched directly to the field data.

5.12 TASK 12.0: Select Drilling Location and Candidate – BP, UA, USGS

Reservoir and fluid characterization studies in Task 6.0, investigation of seismic technologies in tasks 5.0 and 6.0, and reservoir and economic modeling studies in tasks 11.0 and 13.0 are helping to identify prospective areas within MPU for potential phase 2 gas hydrate data acquisition and/or production testing operations. The associated project study by USGS as funded primarily by the regional ANS BLM-USGS research has identified seismic attribute anomalies potentially associated with changes in pore fluid types (water, free gas, and gas hydrate) within reservoir (sand-prone) intervals. These studies will help BPXA determine whether or not to proceed into Phase 2 research.

6.0 CONCLUSION

Interim conclusions are presented at this stage in the research program. The first dedicated gas hydrate coring and production testing, NW Eileen State-02, was drilled in 1972 within the Eileen gas hydrate trend by Arco and Exxon. Since that time, ANS methane hydrates have been known primarily as a drilling hazard. Industry has only recently considered the resource potential of conventional ANS gas during industry and government efforts in working toward an ANS gas pipeline. Consideration of the resource potential of conventional ANS gas created the industry – government alignment necessary to reconsider the resource potential of the potentially huge (40 – 100 TCF in-place) unconventional ANS methane hydrate accumulations beneath or near existing production infrastructure. Studies show this in-place resource is compartmentalized both stratigraphically and structurally within the petroleum system.

The BPXA – DOE collaborative research project is designed to enable industry and government to make informed decisions regarding the resource potential of this ANS methane hydrate petroleum system through comprehensive regional shallow reservoir and fluid characterization utilizing 3D seismic data, implementation of methane hydrate experiments, and design of techniques to support potential methane hydrate drilling, completion, and production operations.

The potential commerciality of gas production from gas hydrate across a broad regional contact from adjacent free gas depressurization is demonstrated by the results of the collaborative BPXA-LBNL pre-Phase 1 scoping reservoir model and economics study (presented in the March 2003 Quarterly report and recent technical conferences) and corroborated by the results of the UAF and Ryder Scott Co. reservoir model research as presented in Section 5.9 of the December 2003 Quarterly report and herein. This collaborative research project will verify the size of the potential resource, determine the extent of reservoir/fluid compartmentalization, and validate potential production techniques.

7.0 PROJECT AND RELATED REFERENCES

7.1 General Project References

Casavant, R.R. and others, 2003, Geology of the Sagavanirktok and Gubik Formations, Milne Point Unit, North Slope, Alaska: Implications for neotectonics and methane gas hydrate resource development, AAPG Bulletin, in prep.

Casavant, R.R. and Gross, E., 2002, Basement Fault Blocks and Subthrust Basins? A Morphotectonic Investigation in the Central Foothills and Brooks Range, Alaska, at the SPE-AAPG: Western Region-Pacific Section Conference, Anchorage, Alaska, May 18-23, 2002.

Casavant, R.R. and Miller, S.R., 2002, Tectonic Geomorphic Characterization of a Transcurrent Fault Zone, Western Brooks Range, Alaska, at the SPE-AAPG: Western Region-Pacific Section Conference, Anchorage, Alaska, May 18-23, 2002.

Collett, T.S., 1993, "Natural Gas Hydrates of the Prudhoe Bay and Kuparuk River Area, North Slope, Alaska", The American Association of Petroleum Geologist Bulletin, Vol. 77, No. 5, May 1993, p. 793-812.

Collett, T.S., 2001, Natural-gas hydrates: resource of the twenty-first century? In M.W. Downey, J.C. Treet, and W.A. Morgan eds., *Petroleum Provinces of the Twenty-First Century: American Association of Petroleum Geologist Memoir 74*, p. 85-108.

Collett, T.S., 2001, MEMORANDUM: Preliminary analysis of the potential gas hydrate accumulations along the western margin of the Kuparuk River Unit, North Slope, Alaska (unpublished administrative report, December 6, 2001).

Collett et al., 2001, Modified version of a multi-well correlation section between the Cirque-2 and Reindeer Island-1 wells, depicting the occurrence of the Eileen and Tarn gas hydrate and associated free-gas accumulations (unpublished administrative report).

Collett et al., 2001, Modified version of a map that depicts the distribution of the Eileen and Tarn gas hydrate and associated free-gas accumulations (unpublished administrative report).

Collett, T.S., 2002, Methane hydrate issues – resource assessment, In the Proceedings of the Methane Hydrates Interagency R&D Conference, March 20-22, 2002, Washington, D.C., 30 p.

Collett, T.S., 2002, Energy resource potential of natural gas hydrates: *Bulletin American Association of Petroleum Geologists*, v. 86, no. 11, p. 1971-1992.

Collett, T.S., and Dallimore, S.R., 2002, Detailed analysis of gas hydrate induced drilling and production hazards, In the Proceedings of the Fourth International Conference on Gas Hydrates, April 19-23, 2002, Yokohama, Japan, 8 p.

Digert, S. and Hunter, R.B., 2003, Schematic 2 by 3 mile square reservoir block model containing gas hydrate, associated free gas, and water (Figure 2 from December, 2002 Quarterly and Year-End Technical Report, First Quarterly Report: October, 2002 – December, 2002, Cooperative Agreement Award Number DE-FC-01NT41332

Geauner, J.M., Manuel, J., and Casavant, R.R., 2003, Preliminary subsurface characterization and modeling of gas hydrate resources, North Slope, Alaska, , in: 2003 AAPG-SEG Student Expo Student Abstract Volume, Houston, Texas

Howe, Steven J., 2004, Production modeling and economic evaluation of a potential gas hydrate pilot production program on the North Slope of Alaska, MS Thesis, University of Alaska Fairbanks, 141 p.

Hunter, R.B., Casavant, R. R. Johnson, R.A., Poulton , M., Moridis, G.J., Wilson, S.J., Geauner, S. Manuel, J., Hagbo, C., Glass, C.E., Mallon, K.M., Patil, S.L., Dandekar, A., And Collett, T.S., 2004, Reservoir-fluid characterization and reservoir modeling of potential gas hydrate resource, Alaska North Slope, 2004 AAPG Annual Convention Abstracts with Program.

Hunter, R.B., Digert, S.A., Casavant, R.R., Johnson, R., Poulton, M., Glass, C., Mallon, K., Patil, S.L., Dandekar, A.Y., and Collett, T.S., 2003, “Resource Characterization and Quantification of Natural Gas-Hydrate and Associated Free-Gas Accumulations in the Prudhoe

Bay-Kuparuk River Area, North Slope of Alaska”, Poster Session at the AAPG Annual Meeting, Salt Lake City, Utah, May 11-14, 2003. Poster received EMD 2nd place, President’s Certificate for Excellence in Presentation (posters).

Hunter, R.B., Pelka, G.J., Digert, S.A., Casavant, R.R., Johnson, R., Poulton, M., Glass, C., Mallon, K., Patil, S.L., Chukwu, G.A., Dandekar, A.Y., Khataniar, S., Ogbe, D.O., and Collett, T.S., 2002, “Resource Characterization and Quantification of Natural Gas-Hydrate and Associated Free-Gas Accumulations in the Prudhoe Bay-Kuparuk River Area on the North Slope of Alaska”, presented at the Methane Hydrate Inter-Agency Conference of US Department of Energy, Washington DC, March 21-23, 2002.

Hunter, R.B., Pelka, G.J., Digert, S.A., Casavant, R.R., Johnson, R., Poulton, M., Glass, C., Mallon, K., Patil, S.L., Chukwu, G.A., Dandekar, A.Y., Khataniar, S., Ogbe, D.O., and Collett, T.S., 2002, “Resource Characterization and Quantification of Natural Gas-Hydrate and Associated Free-Gas Accumulations in the Prudhoe Bay-Kuparuk River Area on the North Slope of Alaska”, at the SPE-AAPG: Western Region-Pacific Section Conference, Anchorage, Alaska, May 18-23, 2002.

Hunter, R.B., et. al., 2004, Characterization of Alaska North Slope Gas Hydrate Resource Potential, Spring 2004 Fire in the Ice Newsletter, National Energy Technology Laboratory.

Jaiswal, Namit J., 2004, Measurement of gas-water relative permeabilities in hydrate systems, MS Thesis, University of Alaska Fairbanks, 100 p.

Lachenbruch, A.H., Galanis Jr., S.P., and Moses Jr., T.H., 1988 “A Thermal Cross Section for the Permafrost and Hydrate Stability Zones in the Kuparuk and Prudhoe Bay Oil Fields”, Geologic Studies in Alaska by the U.S. Geological Survey during 1987, p. 48-51.

Lee, M.W., 2002, Joint inversion of acoustic and resistivity data for the estimation of gas hydrate concentration: U.S. Geological Survey Bulletin 2190, 11 p.

Lewis, R.E., Collett, T.S., and Lee, M.W., 2001, Integrated well log montage for the Phillips Alaska Inc., Kuparuk River Unit (Tarn Pool) 2N-349 Well (unpublished administrative report).

Khataniar, S, Kamath, V.A., Omenihu, S.D., Patil, S.L., and Dandekar, A.Y., 2002, “Modeling and Economic Analysis of Gas Production from Hydrates by Depressurization Method”, The Canadian Journal of Chemical Engineering, Volume 80, February 2002.

Westervelt, Jason V., 2004, Determination of methane hydrate stability zones in the Prudhoe Bay, Kuparuk River, and Milne Point units on the North Slope of Alaska, MS Thesis, University of Alaska Fairbanks, 85 p.

Zhao, B., 2003, Classifying Seismic Attributes in the Milne Point Unit, North Slope of Alaska, MS Thesis, University of Arizona, 159 p.

7.2 Task 7, Gas Hydrate Phase Behavior and Relative Permeability References

ASTM, 2000, "Standard Test Method for Permeability of Granular Soils (constant head) D 2434-68", American Society for Testing and Materials, Annual Book of ASTM Standards, West Conshohocken, PA, 202-206.

Dvorkin, J., Helgerud, M.B., Waite, W.F., Kirby, S.H. and Nur, A., 2000, "Introduction to Physical Properties and Elasticity Models", in Natural Gas Hydrate in Oceanic and Permafrost Environments, edited by M.D. Max, pp 245-260, Kluwer, Dordrecht.

Gash, B.W., 1991, "Measurement of Rock Properties in Coal for Coalbed Methane Production", Paper 22909 presented at the 1991 SPE annual Technical conference and Exhibition, Dallas, October 6-9.

Johnson, E.F., Bossler, D.P., and Neumann, V.O., 1959, "Calculation of Relative Permeability from Displacement Experiments", Trans. AIME, 216, 370- 372.

Jones, S.C. and Roszelle, W.O., 1978, "Graphical Techniques for Determining Relative Permeability from Displacement Experiments", JPT, (May 1978), 807-817.

Joseph W. W. and Duane H.S., 2002, "Upper Limits on the Rates of Dissociation of Clathrate Hydrates to Ice and Free Gas", J. Phys. Chem. B., (May 2002), 106, 6298-6302.

Makogon, Y.F., Makogon, T.Y. and Holditch, S.A., 1998, "Several Aspects of the Kinetics and Morphology of Gas Hydrates", Proceedings of the International Symposium on Methane Hydrates: Resources in the Near Future?, Chiba City, Japan, 20-22, October 1998.

Masuda, Y., Ando, S., Ysukui, H., and Sato, K., 1997, "Effect of Permeability on Hydrate Decomposition in Porous Media", International Workshop on Gas Hydrate Studies, Tsukuba, Japan, Mar 4-6, 1997.

Mehrad, N., 1989, "Measurement of gas permeability in hydrate saturated unconsolidated cores", M.S thesis, University of Alaska Fairbanks.

Owens, W.W., Parrish, D.R., and Lamoreaux, W.E., 1956, "An Evaluation of Gas Drive Method for Determining Relative Permeability Relationships", Trans., AIME 207, 275-280.

Scheidegger, A.E., 1998, The Physics of Flow Through Porous Media, Macmillan, New York.

Sloan, E.D., 1998, Clathrate Hydrates of Natural Gases, Mercel Dekker, New York.

Spangenberg, W., 2001, "Modeling of the influence of gas hydrate content on the electrical properties of porous sediments", J of Geophys. Res B., 106, 6535-6549.

Stern, L.A., Kirby, S.H., Durham, W.B., Circone, S. and Waite, W.F., 2000, "Laboratory synthesis of pure methane hydrate suitable for measurement of physical properties and

decomposition behavior” in Natural Gas Hydrate in Oceanic and Permafrost Environments, edited by M.D. Max, pp 323-348, Kluwer, Dordrecht.

Tooth, J., Bodi, T., et al., 2000, “Analytical Techniques for Determination of Relative Permeability from Displacement Experiments”, Progress in Mining and Oilfield Chemistry, Vol-2, 91-100.

Westervelt, J.V., 2004. "Determination of methane hydrate stability zones in the Prudhoe Bay, Kuparuk River, and Milne Point units on the North Slope of Alaska". MS Thesis, University of Alaska Fairbanks, Fairbanks, AK

Wilder, J.W., Seshadri, K. and Smith, D.H., 2001, “Modeling Hydrate Formation in Media With Broad Pore Size Distributions”, Langmuir 17, 6729-6735.

Winters, W.J., Dillon, W.P., Pecher, I.A. and Mason, D.H., 2000, “GHASTLI-Determining physical properties of sediment containing natural and laboratory formed gas hydrate” in Natural Gas Hydrate in Oceanic and Permafrost Environments, edited by M.D. Max, pp 311-322, Kluwer, Dordrecht.

7.3 Task 8, Drilling Fluid Evaluation and Formation Damage References

Anselme, M.J., Reijnhout, M.J., Muijs, H.M., Klomp, 1993, U.C.; World Pat. WO 93/25798.

Belavadi, M.N., 1994, "Experimental Study of the Parameters Affecting Cutting Transportation in a Vertical Wellbore Annulus"; M.S.Thesis, UAF; Sept., 1994.

Bennion D.B., Thomas F.B., Bietz R.F., 1996, “Low permeability Gas Reservoirs: Problems, Opportunities and Solution for Drilling, Completion, Simulation and Production”; SPE 35577; May 1996.

Bennion D.B., Thomas F.B., Bietz R.F., 1996 “Formation Damage and Horizontal Wells- A Productivity Killer?” SPE 37138; International Conference on Horizontal Well Technology, Calgary; Nov. 1996.

Bennion D.B., Thomas F.B., Bietz R.F., 1995, “Underbalanced Drilling and Formation Damage- Is it a Total Solution?”; The Journal of Canadian Petroleum Tech.; Vol. 34 (9); Nov. 1995.

Bennion D.B., Thomas F.B., et al., 1995, “Advances in Laboratory Core Flow Evaluation to minimize Formation Damage Concerns with Vertical/Horizontal Drilling Application”; CAODC; Vol. 95 (105).

Bennion D.B., Thomas F.B., Jamaluddin, K.M., Ma T.; “Using Underbalanced Drilling to Reduce Invasive Formation Damage and Improve Well Productivity- An Update”; Petroleum Society of CIM; PTS 98-58.

Chadwick J., 1995, “Exploration in permafrost”; Mining Magazine; February, 1995.

Chen, W., Patil S.L., Kamath, V.A., Chukwu, G.A., 1998, "Role of Lecithin in Hydrate Formation/Stabilization in Drilling Fluids"; JNOC; October 20, 1998.

Chilingarian G.V., Vorabutr P., 1983, "Drilling and drilling fluids"; Elsevier; NY.

Cohen J.H., Williams T.E., 2002, "Hydrate Core Drilling Tests: Topical Report"; Maurer Technology Inc., Houston, Texas; November 2002.

Crowell, E.C., Bennion, D.B., Thomas, F.B., Bennion, D.W., 1992, "The Design & Use of Laboratory Tests to Reduce Formation Damage in Oil & Gas Reservoirs"; 13th Annual Conference of the Ontario Petroleum Institute.

Dallimore, S.R., Uchida, T., Collett, T.S., 1999, "Scientific Results from JAPEX/JNOC/GSC Mallik 2L-38 Gas Hydrate Research Well, Mackenzie Delta, Northwest Territories, Canada"; Geological Survey of Canada Bulletin 544; February, 1999.

Drill Cool Systems Canada Inc., www.drillcool.com.

Duncum, S.N., Edwards, A.R., Osborne, C.G., 1993, Eur. Pat. 536,950.

Francis P.A., Eigner M.R.P., et. al., 1995, "Visualization of Drilling-Induced Formation Damage Mechanisms using Reservoir Conditions Core Flood Testing"; paper SPE 30088 presented at the 1995 European Formation Damage Conference, The Hague, May 15-16.

Fu, S.B., Cenegy, L.M., Neff C.S., 2001, "A Summary of Successful Field Application of A Kinetic Hydrate Inhibitor"; SPE 65022.

Hammerschmidt E.G., 1934, Ind.Eng.Chem.; 26, 851.

Howard S.K., 1995, "Formate Brines for Drilling and Completion: State of the Art"; SPE 30498.

I.F.P. patents: Fr.Pats. 2,625,527; 2,625,547; 2,625,548; 2,694,213; 2,697,264; Eur. Pats. 594,579; 582,507323,775; 323307; US Pat. 5,244,878. Can.Pat. 2,036,084.

Jamaluddin A.K.M., Bennion D.B., et. al.; "Application of Heat Treatment to Enhance Permeability in Tight Gas Reservoirs"; Petroleum Society of CIM; Paper No. 98-01.

Kalogerakis N., Jamaluddin, et. al., 1993, "Effect of Surfactants on Hydrate Formation Kinetics"; SPE 25188.

Kamath V.A., Mutalik P.N., et. al., 1991, "Experimental Study of Brine Injection and Depressurization Methods for Dissociation of Gas Hydrate"; SPE Formation Evaluation; December 1991.

Kastube T.J., Dallimore S.R., et. al., 1999, "Gas Hydrate Investigation in Northern Canada"; JAPEX; Vol. 8; No. 5.

Kelland, M.A., Svartaas, T.M., Dybvik, L.A., 1994, "Control of Hydrate Formation by Surfactants and Polymers"; SPE 28506; p. 431-438.

Kotkoskie T.S., AL-Ubaidi B., et. al., 1990, "Inhibition of Gas Hydrates in Water-Based Drilling Mud"; SPE 20437.

Kutasov I.M., 1995, "Salted drilling mud helps prevent casing collapse in permafrost"; Oil & Gas Journal; July 31, 1995.

Marshal, D.S., Gray, R., Byrne, M.; 1997, "Development of a Recommended Practice for Formation Damage Testing"; SPE 38154; Presented at the 1997 SPE European Formation Damage Conference; Netherlands, 2-3 June 1997.

Maury V., Guenot A., 1995, "Practical Advantages of Mud Cooling Systems for Drilling"; SPE Drilling & Completion, March 1995.

Max M.D., 2000, "Natural Gas Hydrate in Oceanic & Permafrost Environments"; Kluwer Academic Publishers; Boston; 2000.

Muijs, H.M., Beers, N.C., et al., 1990, Can. Pat. 2,036,084.

Oort E.V., Friedheim J.M., Toups B., 1999, "Drilling faster with Water-Base Mud"; American Association of Drilling Engineers – Annual Technical Forum; Texas; March 30-31, 1999.

Paez, J.E., Blok, R., Vaziri, H., Islam M.R., 2001, "Problems in Hydrates: Mechanisms and Elimination Methods"; SPE 67322.

Pooladi-Darvish M., Hong, H., 2003, "A Numerical Study on Gas Production From Formations Containing Gas Hydrates"; Canadian International Petroleum Conference, Calgary, June 10-12, 2003.

Reijnhout, M.J., Kind, C.E., Klomp, 1993, U.C.; Eur. Pat. 526,929.

Robinson L.; 1977, "Mud equipment manual, Handbook 1: Introduction to drilling mud system"; Gulf Publishing Company; Houston

Sasaki K., Akibayashi S., Konno S., 1998, "Thermal and Rheological properties of Drilling Fluids and an Estimation of Heat Transfer Rate at Casing pipe"; JNOC-TRC, Japan; October 20-22, 1998.

Schofield T.R., Judis A., Yousif M., 1997, "Stabilization of In-Situ Hydrates Enhances Drilling Performance and Rig Safety"; SPE 32568 ; Drilling & Completion

Sira J.H., Patil S.L., Kamath V.A., 1990, "Study of Hydrate Dissociation by Methanol and Glycol Injection"; SPE 20770.

Sloan, E.D., 1994, World Pat. WO 94/12761.

Spence G.D., Hyndman R.D., 2001, "The challenge of Deep ocean Drilling for Natural Gas Hydrate"; Geoscience Canada; Vol.28 (4); December, 2001.

Sumrow Mike, 2002, "Synthetic-based muds reduce pollution discharge, improve drilling"; Oil & Gas Journal; Dec. 23, 2002.

Szczepanski R., Edmonds B., et. al., 1998, "Research provides clues to hydrate formation and drilling-hazard solutions"; Oil & Gas Journal; Vol. 96(10); Mar 9, 1998.

Toshiharu O., Yuriko M., et. al., 1998, "Kinetic Control of Methane Hydrates in Drilling Fluids"; JNOC-TRC; October 20-22, 1998.

Urdahl, O., Lund, A., Moerk, P., Nilsen, T.N., 1995 "Inhibition of Gas Hydrate Formation by means of Chemical Additives: Development of an Experimental Set-up for Characterization of Gas Hydrate Inhibitor Efficiency with respect to Flow Properties and Deposition"; Chem. Eng. Sci.; 50(5), 863.

Vincent M., Guenot Alain, 1995, "Practical Advantages of Mud Cooling System for Drilling"; SPE Drilling & Completion; March 1995.

Weidong C., Patil S.L., Kamath V.A., Chukwu G.A., 1998, "Role of Lecithin in Hydrate Formation/Stabilization in Drilling Fluids"; JNOC-TRC; October 20-22, 1998.

Yuliev, A.M.; Gazov, Delo, 1972, 10, 17-19, Russ.

Zakharov A.P., 1992, "Silicon-based additives improve mud Rheology"; Oil & Gas Journal; Aug. 10, 1992.

7.4 Task 10, Coring Technology References

Amann, H. et al., 2002, "First Successful Deep-Sea Operations of OMEGA-MAC, the Multiple Auto Corer, during the OTEGA-I campaign on Hydrate Ridge". Fachgebiet Maritime Technik. August 2002.

Carroll, John, 2002, "Natural Gas Hydrates: A Guide for Engineers". Gulf Professional Publishing. October 30, 2002.

Dickens, Gerald R. et al., 2000, "Detection of Methane Gas Hydrate in the Pressure Core Sampler (PCS): Volume-Pressure-Time Relations During Controlled Degassing Experiments". *Proc. of the Ocean Drilling Program*, Vol. 164.

Francis, T.J.G., 2001, "The HYACINTH project and pressure coring in the Ocean Drilling Program". Internal Document: Geotek, Ltd. July 2001.

Hohnberg, H.J. et al., 2003, "Pressurized Coring of Near-Surface Gas Hydrate Sediment on Hydrate Ridge: The Multiple Autoclave Corer, and First Results from Pressure Core X-Ray CT Scans". Geophysical Research Abstracts, Vol. 5. European Geophysical Society.

"HYACE", 2003, [www] <http://www.tu-berlin.de/fb10/MAT/hyace/description/describe.htm>. Accessed June 15th, 2003.

"Methane Hydrate Recovery", JNOC Website. [www] <http://www.mh21japan.gr.jp/english/mh/05kussaku.html#e>.

"Methane Hydrates: A US Department of Energy Website". www.fossil.energy.gov

"Natural Gas Demand". [www] www.naturalgas.org/business/demand.asp.

"Patent No. 6,214,804: The Pressure-Temperature Coring System". U.S. Patent Office. [www]<http://patft.uspto.gov/netacgi/nph-Parser?Sect1=PTO1&Sect2=HITOFF&d=PALL&p=1&u=/netahtml/srchnum.htm&r=1&f=G&l=50&s1=6,216,804.WKU.&OS=PN/6,216,804&RS=PN/6,216,804>. Viewed July 14, 2003

Rack, Frank R, "In-Situ Sampling and Characterization of Naturally Occurring Marine Hydrate Using the D/V JOIDES Resolution". Joint Oceanographic Institute, Cooperative Agreement DE-FC26-01NT41329.

Shukla, K., et al., 2002, "Overview on Hydrate Coring/Handling/Analysis". Westport Technology Center International. Prepared for DOE on December 12, 2002 under award No. DE-PS26-NT40869-1.

7.5 Task 11, 13: Reservoir and Economic Modeling References

Chuang Ji, Goodarz Ahmadi, Duane H. Smith. 2003; "Constant rate natural gas production from a well in a hydrate reservoir"; Energy Conversion and Management 44, 2403-2423.

Chuang Ji, Goodarz Ahmadi, Duane H. Smith, 2001, "Natural gas production from hydrate decomposition by depressurization"; Chemical eng. science 56, 5801-5814.

Stephen J Howe, 2004, Production modeling and economic evaluation of a potential gas hydrate pilot production program on the north slope of Alaska", MS Thesis, University of Alaska Fairbanks, Fairbanks, AK.

Howe, S.J., Nanchary, N.R., Patil S.L., Ogbe D.O., Chukwu G.A., Hunter R.B and Wilson S.J., "Production Modeling and Economic Evaluation of a Potential Gas Hydrate Pilot Production Program on the North Slope of Alaska", *Manuscript Under Preparation*.

Howe, S.J., Nanchary, N.R., Patil S.L., Ogbe D.O., Chukwu G.A., Hunter R.B and Wilson S.J., "Economic Analysis and Feasibility study of Gas Production from Alaska North Slope Gas Hydrate Resources", Submitted for Presentation at the AAPG Hedberg Conference in Vancouver in September 2004.

Jaiswal N.J presented on “Measurement of Relative Permeabilities for Gas-Hydrate Systems” and received third prize in International Thermal Operations and Heavy-Oil Symposium and SPE Regional Meeting Bakersfield, California, USA.

Jaiswal, N.J., Dandekar, A.Y., Patil, S.L. and Chukwu, G.C., “Measurement of Relative Permeability for Gas-Hydrate System”, at 54th Arctic Science Conference, 23rd Sept-2003.

Jaiswal N.J., Westervelt J.V., Patil S.L., Dandekar A.Y., Nanchary, N.R., Tsunemori P and Hunter R.B., “Phase Behavior and Relative Permeability of Gas-Water-Hydrate System”, Submitted for Presentation at the AAPG Hedberg Conference in Vancouver in September 2004.

McGuire, P.L., 1982, “Recovery of gas from hydrate deposits using conventional technology,” SPE/DOE 10832, *Proc. Unconventional Natural Gas Recovery Symposium Pittsburgh PA*, pp. 373-387, Society of Petroleum Engineers, Richardson Texas.

McGuire, Patrick L., 1982, “Methane hydrate gas production by thermal stimulation”; proceedings of the 4th Canadian Permafrost Conference, pp.356-362.

Moridis, G. J., 2002, “Numerical Studies of Gas Production from Methane Hydrates”. *Paper SPE 75691, presented at the SPE Gas Technology Symposium, Calgary, Alberta, Canada, 30 April – 2 May 2002b.*

Moridis, G.J. and Collett, T.S., 2004 in-press, “Gas Production from Class 1 Hydrate Accumulations”.

Moridis, G., Collett, T.S., Dallimore, S.R., Satoh, T., Hancock, S. and Weatherill, B., 2003, “Numerical simulation studies of gas production scenarios from hydrate accumulations at the Mallik site, Mackenzie Delta, Canada”. In, Mori, Y.S., Ed. Proceedings of the Fourth International Conference on Gas Hydrates, May 19-23, Yokohama, Japan, pp 239-244.

Nanchary, N.R., Patil S.L., Dandekar A.Y., “Numerical Simulation of Gas Production from Hydrate Reservoirs by Depressurization”, *Journal of Petroleum Science & Engineering* (Elsevier publication), *Under Review*.

Nanchary, N.R., Patil S.L., Dandekar A.Y and Hunter, R.B., “Numerical Modeling of Gas Hydrate Dissociation in Porous Media”, Submitted for Presentation at the AAPG Hedberg Conference in Vancouver in September 2004.

Swinkles, W.J.A.M. and Drenth, R.J.J., 1999, “Thermal Reservoir Stimulation Model of Prediction from Naturally Occurring Gas Hydrate Accumulations”, Society of Petroleum Engineers, SPE 56550, 13 p.

Tsunemori, Phillip, 2003, presented “Phase Behavior of Natural Gas from Gas Hydrates” and received first in International Thermal Operations and Heavy-Oil Symposium and SPE Regional Meeting Bakersfield, California, USA.

Tsyarkin, G.G. 1992, Appearance of two moving phase transition boundaries in the dissociation of gas hydrates in strata. Dokl. Ross. Akad. Nauk. 323. 52-57 (in Russian).

Yousif, M., H., Abass H., H., Selim, M., S., Sloan E.D., 1991, *Experimental and Theoretical Investigation of Methane-Gas-Hydrate Dissociation in Porous Media*, SPE Res. Eng. 18320, pages 69-76.

Tsyarkin, G.G. 1991, Effect of liquid phase mobility on gas hydrate dissociation in reservoirs. Izvestiya Akad. Nauk SSSR. Mekh. Zhidkosti i Gaza. 4: 105-114 (in Russian).

Westervelt J.V: MS Thesis: "Determination of methane hydrate stability zones in the Prudhoe Bay, Kuparuk River, and Milne Point units on the North Slope of Alaska".

7.6 Short Courses

"Natural Gas Hydrates", By Tim Collett (USGS) and Shirish Patil (UAF), A Short Course at the SPE-AAPG: Western Region-Pacific Section Conference, Anchorage, Alaska, May 18-23, 2002, Sponsored by Alaska Division of Geological and Geophysical Surveys and West Coast Petroleum Technology Transfer Council, Anchorage, Alaska.

8.0 LIST OF ACRONYMS AND ABBREVIATIONS

<u>Acronym</u>	<u>Denotation</u>
2D	Two Dimensional (seismic or reservoir data)
3D	Three Dimensional (seismic or reservoir data)
AAPG	American Association of Petroleum Geologists
AETDL	Alaska Energy Technology Development Laboratory
ANL	Argonne National Laboratory
ANN	Artificial Neural Network
ANS	Alaska North Slope
AOGCC	Alaska Oil and Gas Conservation Commission
AOI	Area of Interest
AVO	Amplitude versus Offset (seismic data analysis technique)
ASTM	American Society for Testing and Materials
BLM	U.S. Bureau of Land Management
BP	British Petroleum (commonly BP Exploration (Alaska), Inc.)
BPXA	BP Exploration (Alaska), Inc.
DOI	U.S. Department of Interior
DGGS	Alaska Division of Geological and Geophysical Surveys
DNR	Alaska Department of Natural Resources
EM	Electromagnetic (referencing potential in-situ thermal stimulation technology)
ERD	Extended Reach Drilling (commonly horizontal and/or multilateral drilling)
GEOS	UA Department of Geology and Geophysics
GOM	Gulf of Mexico (typically referring to Chevron Gas Hydrate project JIP)
GR	Gamma Ray (well log)
GTL	Gas to Liquid
GSA	Geophysical Society of Alaska
HP	Hewlett Packard
JBN	Johnson-Bossler-Naumann method (of gas-water relative permeabilities)
JIP	Joint Industry Participating (group/agreement), ex. Chevron GOM project
JNOC	Japan National Oil Corporation
JOGMEC	Japan Oil, Gas, and Metals National Corporation (reorganized from JNOC 1/04)

KRU	Kuparuk River Unit
LBNL	Lawrence Berkeley National Laboratory
LNG	Liquefied Natural Gas
MGE	UA Department of Mining and Geological Engineering
MPU	Milne Point Unit
NETL	National Energy Technology Laboratory
ONGC	Oil and Natural Gas Corporation Limited (India)
PBU	Prudhoe Bay Unit
PNNL	Pacific Northwest National Laboratory
Sag	Sagavanirktok formation
SPE	Society of Petroleum Engineers
TCF	Trillion Cubic Feet of Gas at Standard Conditions
TCM	Trillion Cubic Meters of Gas at Standard Conditions
UA	University of Arizona (or Arizona Board of Regents)
UAF	University of Alaska, Fairbanks
USGS	United States Geological Survey
USDOE	United States Department of Energy
VSP	Vertical Seismic Profile

9.0 APPENDICES

9.1 APPENDIX A: Project Task Schedules and Milestones

9.1.1 U.S. Department of Energy Milestone Log

Program/Project Title: DE-FC26-01NT41332: Resource Characterization and Quantification of Natural Gas-Hydrate and Associated Free-Gas Accumulations in the Prudhoe Bay - Kuparuk River Area on the North Slope of Alaska

Identification Number	Description	Planned Completion Date	Actual Completion Date	Comments
<i>Task 1.0</i>	Research Management Plan	12/02	12/02	Subcontracts Completed Research Management ongoing
<i>Task 2.0</i>	Provide Technical Data and Expertise	MPU: 12/02 PBU: * KRU: *	MPU: 12/02 PBU: * KRU: *	Ongoing, See Technical Progress Report Description
<i>Task 3.0</i>	Wells of Opportunity Data Acquisition	Ongoing to 12/03-10/04	Ongoing	Ongoing, See Technical Progress Report Description
<i>Task 4.0</i>	Research Collaboration Link	Ongoing to 12/03-10/04	Ongoing	Ongoing, See Technical Progress Report Description
Subtask 4.1	Research Continuity	Ongoing	Ongoing	

Task 5.0	Logging and Seismic Technology Advances	Ongoing to 12/03-10/04		Ongoing, See Technical Progress Report Description
Task 6.0	Reservoir and Fluids Characterization Study	10/04		Interim Results to also be presented
Subtask 6.1	Characterization and Visualization	10/04		Interim Results to also be presented
Subtask 6.2	Seismic Attributes and Calibration	10/04		Interim Results to also be presented
Subtask 6.3	Petrophysics and Artificial Neural Net	10/04		Interim Results to also be presented
Task 7.0	Laboratory Studies for Drilling, Completion, Production Support	6/04		
Subtask 7.1	Characterize Gas Hydrate Equilibrium	6/04		
Subtask 7.2	Measure Gas-Water Relative Permeabilities	6/04		
Task 8.0	Evaluate Drilling Fluids	6/04		
Subtask 8.1	Design Mud System	11/03		
Subtask 8.2	Assess Formation Damage	5/04		
Task 9.0	Design Cement Program	10/04		
Task 10.0	Study Coring Technology	2/04		
Task 11.0	Reservoir Modeling	10/04		Interim Results to also be presented
Task 12.0	Select Drilling Location and Candidate	10/04		
Task 13.0	Project Commerciality & Progression Assessment	10/04		Interim Results to also be presented

- Date estimate dependent upon industry partner agreement for seismic data release

9.1.2 U.S. Department of Energy Milestone Plan (DOE F4600.3)

